

Generalized Low-rank plus Sparse Tensor Estimation by Fast Riemannian Optimization

Jian-Feng Cai, Jingyang Li and Dong Xia*

Hong Kong University of Science and Technology

(April 15, 2022)

Abstract

We investigate a generalized framework to estimate a latent low-rank plus sparse tensor, where the low-rank tensor often captures the multi-way principal components and the sparse tensor accounts for potential model mis-specifications or heterogeneous signals that are unexplainable by the low-rank part. The framework flexibly covers both linear and generalized linear models, and can easily handle continuous or categorical variables. We propose a fast algorithm by integrating the Riemannian gradient descent and a novel gradient pruning procedure. Under suitable conditions, the algorithm converges linearly and can simultaneously estimate both the low-rank and sparse tensors. The statistical error bounds of final estimates are established in terms of the gradient of loss function. The error bounds are generally sharp under specific statistical models, e.g., the sub-Gaussian robust PCA and Bernoulli tensor model. Moreover, our method achieves non-trivial error bounds for heavy-tailed tensor PCA whenever the noise has a finite $2 + \varepsilon$ moment. We apply our method to analyze the international trade flow dataset and the statistician hypergraph co-authorship network, both yielding new and interesting findings.

1 Introduction

In recent years, massive *multi-way* datasets, often called *tensor* data, have routinely arisen in diverse fields. An m th-order tensor is a multilinear array with m ways, e.g., matrices are second order tensors. These multi-way structures often emerge when, to name a few, information features are collected from distinct domains (Bi et al., 2020; Liu et al., 2017; Han et al., 2020; Bi et al., 2018; Zhang et al., 2020b; Wang and Zeng, 2019), the multi-relational interactions or higher-order interactions of entities are present (Ke et al., 2019; Jing et al., 2020; Luo and Zhang, 2020; Wang and

*Jian-Feng Cai’s research was partially supported by Hong Kong RGC Grant GRF 16310620 and GRF 16309219. Dong Xia’s research was partially supported by Hong Kong RGC Grant ECS 26302019 and GRF 16303320, 16300121.

Li, 2020; Pensky and Zhang, 2019), or the higher-order moments of data are explored (Anandkumar et al., 2014; Sun et al., 2017; Hao et al., 2020). There is an increasing demand for effective methods to analyze large and complex tensorial datasets. Low-rank tensor models are a class of statistical models for describing and analyzing tensor datasets. At its core is the assumption that the observed data obeys a distribution that is characterized by a *latent* low-rank tensor \mathcal{T}^* . Oftentimes, analyzing tensor datasets boils down to estimating the low-rank \mathcal{T}^* . This procedure is usually referred to as the *low-rank tensor estimation*. Together with specifically designed algorithms, low-rank tensor methods have demonstrated encouraging performances on many real-world applications and datasets such as the spatial and temporal pattern analysis of human brain developments (Liu et al., 2017), community detection on multi-layer networks and hypergraph networks (Jing et al., 2020; Ke et al., 2019; Wang and Li, 2020), multi-dimensional recommender system (Bi et al., 2018), learning the hidden components of mixture models (Anandkumar et al., 2014), analysis of brain dynamic functional connectivity (Sun and Li, 2019), image denoising and recovery (Xia et al., 2021) and etc.

However, the exact low-rank assumption is stringent and sometimes untrue, making low-rank tensor methods vulnerable under model misspecification or in the existence of outliers or heterogeneous signals. While low-rank structure underscores the multi-way principal components, it fails to capture the dimension-specific outliers or heterogeneous signals that often carry distinctive and useful information. Consider the international trade flow dataset (see Section 8) that forms a third-order tensor by the dimensions countries \times countries \times commodities. On the one hand we observe that the low-rank structure is capable to reflect the shared similarities among countries such as their geographical locations and economic structures, but on the other hand the low-rank structure tends to disregard the heterogeneity in the trading flows of different countries. This vital heterogeneity often reveals distinctive trading patterns of certain commodities for some countries. Moreover, the heterogeneous signals are usually full-rank and strong that can deteriorate the estimates of the multi-way low-rank principal components. We indeed observe that by filtering out these outliers or heterogeneous signals, the resultant low-rank estimates become more insightful. It is therefore advantageous to decouple the low-rank signal and the heterogeneous one in the procedure of low-rank tensor estimation. Fortunately, these outliers or heterogeneous signals are usually representable by a *sparse* tensor, which, is identifiable in generalized low-rank tensor models under suitable conditions.

In this paper, we propose a generalized low-rank plus sparse tensor model to analyze tensorial datasets. Our fundamental assumption is that the observed data is sampled from a statistical model characterized by the latent tensor $\mathcal{T}^* + \mathcal{S}^*$. We assume \mathcal{T}^* to be low-rank capturing the multi-way principal components, and \mathcal{S}^* to be sparse (the precise definition of being “sparse” can be found in Section 2) addressing potential model mis-specifications, outliers or heterogeneous signals that are

unexplainable by the low-rank part. Our framework is very flexible which covers both linear and generalized linear models, and can easily handle both quantitative and categorical data. Compared with existing literature on low-rank tensor methods (Gu et al., 2014; Xia et al., 2021; Zhang and Xia, 2018; Yuan and Zhang, 2017; Sun et al., 2017; Hao et al., 2020; Xia, 2019), our framework and method are more robust, particularly when the latent tensor is only *approximately* low-rank or when the noise have heavy tails. A special case of our model, robust sub-Gaussian tensor PCA, was proposed in Gu et al. (2014). Their method was based on matrix unfolding and is thus statistically sub-optimal. The robust tensor PCA model studied by Zhou and Feng (2017) was based on low tubal-rank and their method is sub-optimal for treating low Tucker-rank tensors. The Bernoulli tensor model introduced in Wang and Li (2020); Yu and Liu (2016), which cannot handle sparse corruptions, is also a special case of our model. See Table 1 for the comparison with related works. Compared with the aforementioned works on robust tensor estimation, our model is more general covering a much wider spectrum of tensor-related applications and our method deals with nearly all kinds of tensor data – Poisson (if intensity is strong), Bernoulli, heavy-tailed data, to name but a few. For instance, to our best knowledge, we derive the first non-trivial convergence rate for heavy-tailed tensor PCA. Meanwhile, our method is robust to model mis-specification up to sparse corruptions. See numerical comparison results in Section 7. We note that the generalized low-rank plus sparse matrix model has been investigated by Zhang et al. (2018) and Robin et al. (2020). However, the estimating procedure is more involved for tensors, the technical proofs are more challenging, and treating tensors by matrix unfolding is generally statistically sub-optimal.

With a properly chosen loss function $\mathcal{L}(\cdot)$, our estimating procedure is formulated into an optimization framework, which aims at minimizing $\mathcal{L}(\mathcal{T} + \mathcal{S})$ subject to the low-rank and sparse constraints on \mathcal{T} and \mathcal{S} , respectively. We propose a new and fast algorithm to solve for the underlying tensors of interest. The algorithm is iterative and consists of two main ingredients: the *Riemannian gradient descent* and the *gradient pruning*. By viewing the low-rank solution as a point on the Riemannian manifold, we adopt Riemannian gradient descent to update the low-rank estimate. Basically, the Riemannian gradient is the projection of the *vanilla gradient* $\nabla \mathcal{L}$ onto the tangent space of a Riemannian manifold. Unlike the vanilla gradient that is usually full-rank, the Riemannian gradient is often low-rank which can significantly boost up the speed of updating the low-rank estimate. Provided with a reliable estimate of the low-rank tensor \mathcal{T}^* , the gradient pruning is a fast procedure to update our estimate of the sparse tensor \mathcal{S}^* . It is based on the belief that, under suitable conditions, if the current estimate $\hat{\mathcal{T}}$ is close to \mathcal{T}^* entry-wisely, the entries of the gradient $\nabla \mathcal{L}(\hat{\mathcal{T}})$ should have small magnitudes on the complement of the support of \mathcal{S}^* . Then it suffices to run a screening of the entries of $\nabla \mathcal{L}(\hat{\mathcal{T}})$, locate its entries with large magnitudes and choose $\hat{\mathcal{S}}$ to minimize the magnitudes of those entries of $\nabla \mathcal{L}(\hat{\mathcal{T}} + \hat{\mathcal{S}})$. The procedure looks like

pruning the gradient $\nabla \mathcal{L}(\widehat{\mathcal{T}})$ – thus the name gradient pruning. The algorithm alternates between Riemannian gradient descent and gradient pruning until reaching a locally optimal solution.

1.1 Our Contributions

We propose a novel and generalized framework to analyze tensor datasets. Our framework allows the latent tensor to be high-rank, as long as it is within the sparse perturbations of a low-rank tensor. The sparse tensor can account for potential mis-specifications of the exact low-rank tensor models, making our framework robust to outliers, heavy-tailed distributions, heterogeneous signals, etc. Meanwhile, our framework flexibly covers both linear and generalized linear models, and is applicable to both continuous and categorical variables. Details are summarize in Table 1.

Methods	Model	Sparse outlier	SG-RPCA error rate	Heavy-tailed PCA	Poisson RPCA
TBM Wang and Li (2020)	Binary	No	N/A	No	No
tubal-tRPCA Lu et al. (2016)	RPCA	Yes	Only noiseless	No	No
Convex Gu et al. (2014)	RPCA	Yes	$O(rd^{m-1} + \Omega^*)$	No	No
Projected GD Chen et al. (2019)	GLM	No	N/A	No	No
Jointly GD Han et al. (2020)	GLM	No	$O(mrd)$ when $ \Omega^* = 0$	No	No
RGrad (this paper)	GLM	Yes	$O(mrd + \Omega^*)$	Yes	Yes

Table 1: Comparison with related literature. Here, GLM stands for generalized linear model. For the sub-Gaussian robust PCA (SG-RPCA) error rate, we assume $d_j \asymp d, j \in [m]$ for simplicity. We remark that a strong Poisson intensity is required by RGrad. See Lemma 8.2 in the supplement.

We develop a new and fast algorithm which can simultaneously estimate both the low-rank and the sparse tensors. The algorithm is based on the integration of Riemannian gradient descent and a novel gradient pruning procedure. Our proposed method works for both linear and generalized linear models, adapts to additional sparse perturbations, and is reliable in the existence of stochastic noise. We prove, in a general framework, that our algorithm converges fast even with fixed step-sizes, and establish the statistical error bounds of final estimates. The error bounds are sharp and proportional to the intrinsic degrees of freedom under many specific statistical models.

To showcase the superiority of our methods, we consider applying our framework to interesting examples. The first application is on the sub-Gaussian robust tensor principal component analysis (SG-RPCA) where the observation is simply $\mathcal{T}^* + \mathcal{S}^*$ with additive sub-Gaussian noise. We show that our method can recover both \mathcal{T}^* and \mathcal{S}^* with sharp error bounds, and recover the support of \mathcal{S}^* under fairly weak conditions. The second example is on the tensor PCA when the noise has heavy tails. We show that our framework is naturally immune to the potential outliers caused by

the heavy-tailed noise, and demonstrate that our method achieves non-trivial error bounds as long as the noise have a finite $2 + \varepsilon$ moment. This bridges a fundamental gap in the understanding of tensor PCA since the existing methods are usually effective only under sub-Gaussian or sub-Exponential noise. We then apply our framework to learn the latent low-rank structure \mathcal{T}^* from a binary tensorial observation, assuming the Bernoulli tensor model with a general link function, e.g., the logistic and probit link. Compared with the existing literature, our method is robust and allows an arbitrary but sparse corruption. Finally, our method is applied to Poisson tensor RPCA under a strong intensity condition. To our best knowledge, our results are the first in these three applications. We also provide computationally fast methods to obtain good initializations.

Lastly, we employ our method to analyze two real-world datasets: the international commodity trade flow network (continuous variables) and the statistician hypergraph co-authorship network (binary variables). We observe that the low-rank plus sparse tensor framework yields intriguing and new findings that are unseen by the exact low-rank tensor methods. The sparse tensor can nicely capture informative patterns which are overlooked by the multi-way principal components.

1.2 Notations and Preliminaries of Tensor

We use calligraphic-font bold-face letters (e.g. $\mathcal{T}, \mathcal{X}, \mathcal{T}_1$) to denote tensors, bold-face capital letters (e.g. $\mathbf{T}, \mathbf{X}, \mathbf{T}_1$) for matrices, bold-face lower-case letters (e.g. $\mathbf{t}, \mathbf{x}, \mathbf{t}_1$) for vectors and blackboard bold-faced letters (e.g. $\mathbb{R}, \mathbb{M}, \mathbb{U}, \mathbb{T}$) for sets. We use square brackets with subscripts (e.g. $[\mathcal{T}]_{i_1, i_2, i_3}, [\mathbf{T}]_{i_1, i_2}, [\mathbf{t}]_{i_1}$) to represent corresponding entries of tensors, matrices and vectors, respectively. Denote $[\mathcal{T}]_{i_1, :, :}$ and $[\mathbf{T}]_{i_1, :}$ the i_1 -th frontal-face and i_1 -th row-vector of \mathcal{T} and \mathbf{T} , respectively. Denote $\|\cdot\|_F$ the Frobenius norm of matrices and tensors, and denote $\|\cdot\|_{\ell_p}$ the ℓ_p -norm of vectors or vectorized tensors for $0 \leq p \leq \infty$. Thus, $\|\mathbf{v}\|_{\ell_0}$ represents the number of non-zero entries of \mathbf{v} , and $\|\mathbf{v}\|_{\ell_\infty}$ denotes the largest magnitude of the entries of \mathbf{v} . The j -th canonical basis vector is written as \mathbf{e}_j whose actual dimension might vary at different appearances. We denote $C, C_1, C_2, c, c_1, c_2 \cdots$ some absolute constants whose actual values can change at different lines.

An m -th order tensor is an m -way array, e.g., $\mathcal{T} \in \mathbb{R}^{d_1 \times \cdots \times d_m}$ means that its j -th dimension has size d_j . Thus, \mathcal{T} has in total $d_1 \cdots d_m$ entries. The j -th matricization (also called unfolding) $\mathcal{M}_j(\cdot) : \mathbb{R}^{d_1 \times \cdots \times d_m} \mapsto \mathbb{R}^{d_j \times d_j^-}$ with $d_j^- = (d_1 \cdots d_m)/d_j$ is a linear mapping so that, for example if $m = 3$, $[\mathcal{M}_1(\mathcal{T})]_{i_1, (i_2-1)d_3+i_3} = [\mathcal{T}]_{i_1, i_2, i_3}$ for $\forall i_j \in [d_j]$. Then, the collection $\text{rank}(\mathcal{T}) := (\text{rank}(\mathcal{M}_1(\mathcal{T})), \dots, \text{rank}(\mathcal{M}_m(\mathcal{T})))^\top$ is called the multi-linear ranks or *Tucker ranks* of \mathcal{T} . Given a matrix $\mathbf{W}_j \in \mathbb{R}^{p_j \times d_j}$ for any $j \in [m]$, the multi-linear product, denoted by \times_j , between \mathcal{T} and \mathbf{W}_j is defined by $[\mathcal{T} \times_j \mathbf{W}_j]_{i_1, \dots, i_m} := \sum_{k=1}^{d_j} [\mathcal{T}]_{i_1, \dots, i_{j-1}, k, i_{j+1}, \dots, i_m} \cdot [\mathbf{W}_j]_{i_j, k}$, $\forall i_{j'} \in [d_{j'}]$ for $j' \neq j; \forall i_j \in [p_j]$. If \mathcal{T} has Tucker ranks $\mathbf{r} = (r_1, \dots, r_m)^\top$, there exist $\mathcal{C} \in \mathbb{R}^{r_1 \times \cdots \times r_m}$ and $\mathbf{U}_j \in \mathbb{R}^{d_j \times r_j}$ satisfying $\mathbf{U}_j^\top \mathbf{U}_j = \mathbf{I}_{r_j}$ for all $j \in [m]$ such that $\mathcal{T} = \mathcal{C} \cdot \llbracket \mathbf{U}_1, \dots, \mathbf{U}_m \rrbracket := \mathcal{C} \times_1 \mathbf{U}_1 \times_2 \cdots \times_m \mathbf{U}_m$. This is

referred to as the Tucker decomposition of a low-rank tensor. Tucker ranks and decomposition are well-defined. Readers are suggested to refer (Kolda and Bader, 2009) for more details and examples on tensor decomposition and tensor algebra.

2 General Low-rank plus Sparse Tensor Model

Suppose that we observe data \mathfrak{D} , which can be, for instance, simply a tensorial observation such as the binary adjacency tensor of a hypergraph network or multi-layer network (Ke et al., 2019; Jing et al., 2020; Luo and Zhang, 2020; Wang and Li, 2020; Jin, 2015; Ji and Jin, 2016); a real-valued tensor describing multi-dimensional observations (Han et al., 2020; Sun et al., 2017; Sun and Li, 2019; Liu et al., 2017); or a collection of pairs of tensor covariate and real-valued response (Hao et al., 2020; Zhang et al., 2020a; Xia et al., 2020; Raskutti et al., 2019; Chen et al., 2019). At the core of our model is the assumption that the observed \mathfrak{D} is sampled from a distribution characterized by a latent large tensor, denoted by $\mathcal{T}^* + \mathcal{S}^*$, where \mathcal{T}^* has small multi-linear ranks and \mathcal{S}^* is sparse. Unlike the exact low-rank tensor models, the additional sparse tensor \mathcal{S}^* can account for potential model mis-specifications and outliers. Consider that \mathcal{T}^* has multi-linear ranks $\mathbf{r} = (r_1, \dots, r_m)^\top$ with $r_j \ll d_j$ so that $\mathcal{T}^* \in \mathbb{M}_{\mathbf{r}}$ where $\mathbb{M}_{\mathbf{r}} := \{\mathcal{W} \in \mathbb{R}^{d_1 \times \dots \times d_m} : \text{rank}(\mathcal{M}_j(\mathcal{W})) \leq r_j, \forall j \in [m]\}$. As for the sparse tensor, we assume that each slice of \mathcal{S}^* has at most α -portion of entries being non-zero for some $\alpha \in (0, 1)$. We write $\mathcal{S}^* \in \mathbb{S}_\alpha$ where the latter is defined by $\mathbb{S}_\alpha := \{\mathcal{S} \in \mathbb{R}^{d_1 \times \dots \times d_m} : \|\mathbf{e}_i^\top \mathcal{M}_j(\mathcal{S})\|_{\ell_0} \leq \alpha d_j^-, \forall j \in [m], i \in [d_j]\}$, where \mathbf{e}_i denotes the i -th canonical basis vector whose dimension varies at different appearances.

When the low-rank tensor \mathcal{T}^* is also sparse, it is generally impossible to distinguish between \mathcal{T}^* and its sparse counterpart \mathcal{S}^* . To make \mathcal{T}^* and \mathcal{S}^* identifiable, we assume that \mathcal{T}^* satisfies the *spikiness condition* meaning that the information it carries spreads fairly across nearly all its entries. Put differently, the spikiness condition enforces \mathcal{T}^* to be dense – thus distinguishable from the sparse \mathcal{S}^* . This is a typical condition in robust matrix estimation (Candès et al., 2011; Chen et al., 2020) and tensor completion (Xia and Yuan, 2019; Xia et al., 2021; Cai et al., 2019). For exact low-rank tensor models where \mathcal{S}^* is absent, this assumption is generally not required. See Section 6 in the supplementary file for more details.

Assumption 1. Let $\mathcal{T}^* \in \mathbb{M}_{\mathbf{r}}$, and suppose there exists $\mu_1 > 0$ such that the following holds: $\text{Spiki}(\mathcal{T}^*) := (d^*)^{1/2} \|\mathcal{T}^*\|_{\ell_\infty} / \|\mathcal{T}^*\|_{\text{F}} \leq \mu_1$, where $d^* = d_1 \cdots d_m$.

We denote $\mathbb{U}_{\mathbf{r}, \mu_1} := \{\mathcal{T} \in \mathbb{M}_{\mathbf{r}} : \text{Spiki}(\mathcal{T}) \leq \mu_1\}$ the set of low-rank tensors with spikiness bounded by μ_1 .

Relation between spikiness condition and incoherence condition. Let $\mathcal{T}^* \in \mathbb{M}_{\mathbf{r}}$ admit a Tucker decomposition $\mathcal{T}^* = \mathcal{C}^* \cdot \llbracket \mathbf{U}_1^*, \dots, \mathbf{U}_m^* \rrbracket$ with $\mathcal{C}^* \in \mathbb{R}^{r_1 \times \dots \times r_m}$ and $\mathbf{U}_j^* \in \mathbb{R}^{d_j \times r_j}$ satisfying $\mathbf{U}_j^{*\top} \mathbf{U}_j^* =$

\mathbf{I}_{r_j} for all $j \in [m]$. Suppose that there exists $\mu_0 > 0$ so that $\mu(\mathcal{T}^*) := \max_{j \in [m]} \max_{i \in [d_j]} \|\mathbf{e}_i^\top \mathbf{U}_j^*\|_{\ell_2} \cdot (d_j/r_j)^{1/2} \leq \sqrt{\mu_0}$. Then, \mathcal{T}^* is said to satisfy the incoherence condition with constant μ_0 . The spikiness condition implies the incoherence condition *and vice versa*. See Lemma 13.5.

After observing data \mathfrak{D} , our goal is to estimate the underlying $(\mathcal{T}^*, \mathcal{S}^*) \in (\mathbb{U}_{\mathbf{r}, \mu_1}, \mathbb{S}_\alpha)$. Often-times, the problem is formulated as an optimization program equipped with a properly chosen loss function. More specifically, let $\mathfrak{L}(\cdot) := \mathfrak{L}_{\mathfrak{D}}(\cdot) : \mathbb{R}^{d_1 \times \dots \times d_m} \mapsto \mathbb{R}$ be a smooth (see Assumption 2) loss function whose actual form depends on the particular applications. The estimators of $(\mathcal{T}^*, \mathcal{S}^*)$ are then defined by $(\hat{\mathcal{T}}_\gamma, \hat{\mathcal{S}}_\gamma) := \arg \min_{\mathcal{T} \in \mathbb{U}_{\mathbf{r}, \mu_1}, \mathcal{S} \in \mathbb{S}_{\gamma\alpha}} \mathfrak{L}(\mathcal{T} + \mathcal{S})$, where $\gamma > 1$ is a tuning parameter determining the desired sparsity level of $\hat{\mathcal{S}}_\gamma$. For ease of exposition, we tentatively assume that the true ranks are known. In real-world applications, \mathbf{r}, α can be selected by a BIC-type criterion (3.3). See Section 7 for more details. This generalized framework covers many interesting and important examples as special cases. These examples are investigated more closely in Section 5.

Example 2.1. (*Tensor robust principal component analysis*) For tensor RPCA, the data observed is simply a tensor $\mathcal{A} \in \mathbb{R}^{d_1 \times \dots \times d_m}$. The basic assumption of tensor PCA is the existence of a low-rank tensor \mathcal{T}^* , called the “signal”, planted inside of \mathcal{A} . See, e.g. (Zhang and Xia, 2018; Richard and Montanari, 2014) and references therein. The exact low-rank condition on the “signal” is sometimes stringent. Tensor robust PCA (Lu et al., 2016; Robin et al., 2020) relaxes this condition by assuming that the “signal” is the sum of a low-rank tensor \mathcal{T}^* and a sparse tensor \mathcal{S}^* . With additional additive stochastic noise, the Sub-Gaussian RPCA (SG-RPCA) model assumes $\mathcal{A} = \mathcal{T}^* + \mathcal{S}^* + \mathcal{Z}$ with $(\mathcal{T}^*, \mathcal{S}^*) \in (\mathbb{U}_{\mathbf{r}, \mu_1}, \mathbb{S}_\alpha)$ and \mathcal{Z} being a noise tensor having i.i.d. random centered sub-Gaussian entries. We reserve RPCA exclusively for SG-RPCA in the subsequent chapters. Given \mathcal{A} , the goal is to estimate \mathcal{T}^* and \mathcal{S}^* . A suitable loss function is $\mathfrak{L}(\mathcal{T} + \mathcal{S}) := \frac{1}{2} \|\mathcal{T} + \mathcal{S} - \mathcal{A}\|_{\text{F}}^2$, which measures the goodness-of-fit by $\mathcal{T} + \mathcal{S}$ to data. The estimator $(\hat{\mathcal{T}}_\gamma, \hat{\mathcal{S}}_\gamma)$ is thus defined by

$$(\hat{\mathcal{T}}_\gamma, \hat{\mathcal{S}}_\gamma) := \arg \min_{\mathcal{T} \in \mathbb{U}_{\mathbf{r}, \mu_1}, \mathcal{S} \in \mathbb{S}_{\gamma\alpha}} \frac{1}{2} \|\mathcal{T} + \mathcal{S} - \mathcal{A}\|_{\text{F}}^2. \quad (2.1)$$

Example 2.2. (*Learning low-rank structure from binary tensor*) In many applications, the observed data \mathcal{A} is merely a binary tensor. Examples include the adjacency tensor in multi-layer networks (Jing et al., 2020; Paul and Chen, 2020), brain structural connectivity networks (Wang et al., 2019; Wang and Li, 2020) and etc. Following the Bernoulli tensor model proposed in (Wang and Li, 2020) or generalizing the 1-bit matrix completion model (Davenport et al., 2014), we assume that there exist $(\mathcal{T}^*, \mathcal{S}^*) \in (\mathbb{U}_{\mathbf{r}, \mu_1}, \mathbb{S}_\alpha)$ satisfying $[\mathcal{A}]_\omega \stackrel{\text{ind.}}{\sim} \text{Bernoulli}(p([\mathcal{T}^* + \mathcal{S}^*]_\omega))$, $\forall \omega \in [d_1] \times \dots \times [d_m]$, where $p(\cdot) : \mathbb{R} \mapsto [0, 1]$ is a suitable inverse link function. Popular choices of $p(\cdot)$ include the logistic link $p(x) = (1 + e^{-x/\sigma})^{-1}$ and probit link $p(x) = 1 - \Phi(-x/\sigma)$ where $\sigma > 0$ is a scaling parameter. We note that, due to potential symmetry in networks, the entry independence statement might only hold for a subset of its entries (e.g., upper-triangular entries in a single-layer undirected network).

Compared with the exact low-rank Bernoulli tensor model (Wang and Li, 2020), ours is more robust to model mis-specifications and outliers. For any pair $(\mathcal{T}, \mathcal{S}) \in (\mathbb{U}_{\mathbf{r}, \mu_1}, \mathbb{S}_{\gamma\alpha})$, a suitable loss function is the negative log-likelihood. By maximizing the log-likelihood, we define

$$(\hat{\mathcal{T}}_\gamma, \hat{\mathcal{S}}_\gamma) := \arg \min_{\mathcal{T} \in \mathbb{U}_{\mathbf{r}, \mu_1}, \mathcal{S} \in \mathbb{S}_{\gamma\alpha}} - \sum_{\omega} ([\mathcal{A}]_{\omega} \log p([\mathcal{T} + \mathcal{S}]_{\omega}) + (1 - [\mathcal{A}]_{\omega}) \log (1 - p([\mathcal{T} + \mathcal{S}]_{\omega}))). \quad (2.2)$$

3 Estimating by Non-convex Optimization

Suppose that a pair¹ of initializations near the ground truth is provided. Our estimating procedure adopts a gradient-based iterative algorithm to search for a local minimum of the loss. Since the problem is a constrained optimization, the major difficulty is on the enforcement of constraints during gradient descent updates. To ensure low-rankness, we apply the Riemannian gradient descent algorithm that is fast and simple to implement. Meanwhile, we enforce the sparsity constraint via a gradient-based pruning algorithm.

3.1 Riemannian Gradient Descent

Provided with $(\hat{\mathcal{T}}_l, \hat{\mathcal{S}}_l)$ at the l -th iteration, the *vanilla* gradient of the loss function is $\mathcal{G}_l = \nabla \mathcal{L}(\hat{\mathcal{T}}_l + \hat{\mathcal{S}}_l)$. The naive gradient descent updates the low-rank part to $\hat{\mathcal{T}}_l - \beta \mathcal{G}_l$ with a carefully chosen stepsize $\beta > 0$, and then projects it back into the set $\mathbb{M}_{\mathbf{r}}$. This procedure is sometimes referred to as the projected gradient descent (PGD) (Chen et al., 2019). Oftentimes, the gradient \mathcal{G}_l has full ranks and thus the subsequent low-rank projection is computationally expensive. Observe that $\hat{\mathcal{T}}_l$ is an element in the smooth manifold $\mathbb{M}_{\mathbf{r}}$. Meanwhile, due to the smoothness of loss function, it is well recognized that the optimization problem can be solved by Riemannian optimization (Edelman et al., 1998; Kressner et al., 2014) on the respective smooth manifold. Therefore, instead of using the vanilla gradient \mathcal{G}_l , it suffices to take the *Riemannian gradient*, which corresponds to the steepest descent of the loss but is restricted to the tangent space of $\mathbb{M}_{\mathbf{r}}$ at the point $\hat{\mathcal{T}}_l$. The Riemannian gradient is low-rank rendering amazing computational speed-up. See numerical comparison in Section 7.

An essential ingredient of Riemannian gradient descent is to project the vanilla gradient onto the tangent space of $\mathbb{M}_{\mathbf{r}}$. Let \mathbb{T}_l denote the tangent space of $\mathbb{M}_{\mathbf{r}}$ at $\hat{\mathcal{T}}_l$. Suppose that $\hat{\mathcal{T}}_l$ admits a Tucker decomposition $\hat{\mathcal{T}}_l = \hat{\mathcal{C}}_l \cdot [\hat{\mathbf{U}}_{l,1}, \dots, \hat{\mathbf{U}}_{l,m}]$. The tangent space \mathbb{T}_l (Cai et al., 2020) has an explicit form written as $\mathbb{T}_l = \{\mathcal{D}_l \times_{i \in [m]} \hat{\mathbf{U}}_{l,i} + \sum_{i=1}^m \hat{\mathcal{C}}_l \times_{j \in [m] \setminus i} \hat{\mathbf{U}}_{l,j} \times_i \mathbf{W}_i : \mathcal{D}_l \in \mathbb{R}^{\mathbf{r}}, \mathbf{W}_i \in \mathbb{R}^{d_i \times r_i}, \mathbf{W}_i^{\top} \hat{\mathbf{U}}_{l,i} = \mathbf{0}\}$. Clearly, all elements in \mathbb{T}_l has their multi-linear ranks upper bounded by $2\mathbf{r}$. Given the vanilla

¹We will show, in Section 4, that obtaining a good initialization for \mathcal{S} is, under suitable conditions, easy once a good initialization for \mathcal{T} is available.

gradient \mathcal{G}_l , its projection onto \mathbb{T}_l is defined by $\mathcal{P}_{\mathbb{T}_l}(\mathcal{G}_l) := \arg \min_{\mathcal{X} \in \mathbb{T}_l} \|\mathcal{G}_l - \mathcal{X}\|_{\mathbb{F}}^2$. The summands in \mathbb{T}_l are all orthogonal to each other, allowing fast computation for $\mathcal{P}_{\mathbb{T}_l}(\mathcal{G}_l)$.

By choosing a suitable stepsize $\beta > 0$, the update by Riemannian gradient descent yields $\mathcal{W}_l := \hat{\mathcal{T}}_l - \beta \mathcal{P}_{\mathbb{T}_l}(\mathcal{G}_l)$. But \mathcal{W}_l may fail to be an element in $\mathbb{M}_{\mathbf{r}}$. To enforce the low-rank constraint, another key step in Riemannian optimization is the so-called *retraction*, which projects a general tensor \mathcal{W}_l back to the smooth manifold $\mathbb{M}_{\mathbf{r}}$. This procedure amounts to a low-rank approximation of the tensor \mathcal{W}_l . In addition, we also need to enforce the spikiness (or incoherent) condition on the low-rank estimate. Towards that end, we first truncate \mathcal{W}_l entry-wisely by $\zeta_{l+1}/2$ for some easily chosen threshold ζ_{l+1} and obtain $\widetilde{\mathcal{W}}_l$, and then retract the truncated tensor $\widetilde{\mathcal{W}}_l$ back to the manifold $\mathbb{M}_{\mathbf{r}}$. We show that a low-rank approximation of $\widetilde{\mathcal{W}}_l$ by a simple higher order singular value decomposition (HOSVD) guarantees the convergence of Riemannian gradient descent algorithm. More specifically, for all $j \in [m]$, compute $\mathbf{V}_{l,j}$ which is the top- r_j left singular vectors of $\mathcal{M}_j(\widetilde{\mathcal{W}}_l)$. The HOSVD approximation of $\widetilde{\mathcal{W}}_l$ with multi-linear ranks \mathbf{r} is obtained by $\mathcal{H}_{\mathbf{r}}^{\text{HO}}(\widetilde{\mathcal{W}}_l) := (\widetilde{\mathcal{W}}_l \times_{j=1}^m \mathbf{V}_{l,j}^\top) \cdot \llbracket \mathbf{V}_{l,1}, \dots, \mathbf{V}_{l,m} \rrbracket$. Basically, retraction by HOSVD is the generalization of low-rank matrix approximation by singular value thresholding, although HOSVD is generally not the optimal low-rank approximation of $\widetilde{\mathcal{W}}_l$. See, e.g. (Zhang and Xia, 2018; Xia and Zhou, 2019; Liu et al., 2017; Richard and Montanari, 2014) for more explanations. Now put these two steps together and we define a trimming operator $\text{Trim}_{\zeta, \mathbf{r}}$.

$$\text{Trim}_{\zeta, \mathbf{r}}(\mathcal{W}) := \mathcal{H}_{\mathbf{r}}^{\text{HO}}(\widetilde{\mathcal{W}}), \quad \text{where } [\widetilde{\mathcal{W}}]_\omega = \begin{cases} (\zeta/2) \cdot \text{Sign}([\mathcal{W}]_\omega), & \text{if } |[\mathcal{W}]_\omega| > \zeta/2 \\ [\mathcal{W}]_\omega, & \text{otherwise} \end{cases} \quad (3.1)$$

Equipped by the retraction and the entry-wise truncation, the Riemannian gradient descent algorithm updates the low-rank estimate by $\hat{\mathcal{T}}_{l+1} = \text{Trim}_{\zeta_{l+1}, \mathbf{r}}(\mathcal{W}_l)$, with a properly chosen ζ_{l+1} .

3.2 Gradient Pruning

The next step is to update the estimate of sparse tensor \mathcal{S}^* . Provided with the updated $\hat{\mathcal{T}}_l$ at the l -th iteration, an ideal estimator of the sparse tensor \mathcal{S}^* is to find $\arg \min_{\mathcal{S} \in \mathbb{S}_{\gamma_\alpha}} \mathcal{L}(\hat{\mathcal{T}}_l + \mathcal{S})$. Solving this problem is NP-hard for a general loss function. Interestingly, if the loss function is entry-wise meaning that $\mathcal{L}(\mathcal{T}) = \sum_{\omega} \mathfrak{l}_{\omega}([\mathcal{T}]_{\omega})$ where $\mathfrak{l}_{\omega}(\cdot) : \mathbb{R} \mapsto \mathbb{R}$ for each $\omega \in [d_1] \times \dots \times [d_m]$, the computation of sparse estimate becomes tractable. More exactly, given a tensor $\mathcal{G} \in \mathbb{R}^{d_1 \times \dots \times d_m}$, we denote $|\mathcal{G}|^{(n)}$ the value of its n -th largest entry in absolute value for $\forall n \in [d_1 \dots d_m]$. Thus, $|\mathcal{G}|^{(1)}$ denotes its largest entry in absolute value. The *level- α active indices* of \mathcal{G} is defined by $\text{Level-}\alpha \text{ AInd}(\mathcal{G}) := \{\omega = (i_1, \dots, i_m) : |[\mathcal{G}]_{\omega}| \geq \max_{j \in [m]} |\mathbf{e}_{i_j}^\top \mathcal{M}_j(\mathcal{G})|^{(\lfloor \alpha d_j^- \rfloor)}\}$. By definition, the *level- α active indices* of \mathcal{G} are those entries whose absolute value is no smaller than the $(1 - \alpha)$ -th percentile in absolute value on each of its corresponding slices. Clearly, for any $\mathcal{S} \in \mathbb{S}_{\alpha}$, the support

of \mathcal{S} belongs to the $\text{Level-}\alpha \text{ Alnd}(\mathcal{S})$.

We compute the vanilla gradient $\hat{\mathcal{G}}_l = \nabla \mathcal{L}(\hat{\mathcal{T}}_l)$ so that $[\hat{\mathcal{G}}_l]_\omega = \ell'_\omega([\hat{\mathcal{T}}_l]_\omega)$ and find $\mathbb{J} = \text{Level-}\alpha \text{ Alnd}(\hat{\mathcal{G}}_l)$. The indices in \mathbb{J} have the greatest potential in decreasing the value of loss function. The gradient pruning algorithm sets $[\hat{\mathcal{S}}_l]_\omega = 0$ if $\omega \notin \mathbb{J}$. On the other hand, for $\omega \in \mathbb{J}$, ideally, the entry $[\hat{\mathcal{S}}_l]_\omega$ is chosen to vanish the gradient in that $\ell'_\omega([\hat{\mathcal{T}}_l]_\omega + [\hat{\mathcal{S}}_l]_\omega) = 0$. However, for functions with always-positive gradient (e.g. e^x), it is impossible to vanish the gradient. Generally, we choose a pruning parameter $k_{\text{pr}} > 0$ and set

$$[\hat{\mathcal{S}}_l]_\omega := \arg \min_{s: |s + [\hat{\mathcal{T}}_l]_\omega| \leq k_{\text{pr}}} |\ell'_\omega([\hat{\mathcal{T}}_l]_\omega + s)|, \quad \forall \omega \in \mathbb{J}. \quad (3.2)$$

Basically, eq. (3.2) chooses $[\hat{\mathcal{S}}_l]_\omega$ from the closed interval $[-k_{\text{pr}} - [\hat{\mathcal{T}}_l]_\omega, k_{\text{pr}} - [\hat{\mathcal{T}}_l]_\omega]$ to minimize the gradient. For a properly selected loss function $\ell_\omega(\cdot)$, searching for the solution $[\hat{\mathcal{S}}_l]_\omega$ is usually fast. Moreover, for entry-wise square loss, the pruning parameter k_{pr} can be ∞ and $[\hat{\mathcal{S}}_l]_\omega$ has a closed-form solution. See Section 5 for more details. The procedure of gradient pruning is summarized in Algorithm 1.

Algorithm 1 Gradient Pruning for Sparse Estimate

Input: $\hat{\mathcal{T}}_l$ and parameters $\gamma > 1, \alpha, k_{\text{pr}} > 0$

Calculate the gradient $\hat{\mathcal{G}}_l = \nabla \mathcal{L}(\hat{\mathcal{T}}_l)$ and find $\mathbb{J} = \text{Level-}\gamma\alpha \text{ Alnd}(\hat{\mathcal{G}}_l)$

for $\omega \in [d_1] \times \cdots \times [d_m]$ **do**

$$[\hat{\mathcal{S}}_l]_\omega = \begin{cases} \text{by (3.2),} & \text{if } \omega \in \mathbb{J} \\ 0, & \text{if } \omega \notin \mathbb{J} \end{cases}$$

end for

Output: $\hat{\mathcal{S}}_l$

Final algorithm. Putting together the Riemannian gradient descent and the gradient pruning algorithm, we propose the following Algorithm 2. The algorithm alternately updates the low-rank estimate and the sparse estimate. We emphasize that the notations α and μ_1 in Algorithm 2 do not have to be exactly the model parameters α and μ_1 . In theory, we only require them to be larger than the true model parameters α and μ_1 , respectively. See Section 7 for more details.

Rank, sparsity and algorithmic parameters selection. For applications where the true ranks are small, we can simply run Algorithm 2 for multiple times with distinct choices of these ranks and decide the best ones according to certain criterion, e.g., interpretability if no ground truth (Jing et al., 2020; Fan et al., 2021) or the mis-clustering rate if ground truth is available (Ke et al., 2019; Zhou et al., 2013; Wang and Li, 2020). Sometimes, it suffices to take the singular values of the matricizations and decide the cut-off point by the famous *scree plot* (Cattell, 1966). For generalized

Algorithm 2 Riemannian Gradient Descent and Gradient Pruning

Initialization: $\hat{\mathcal{T}}_0 \in \mathbb{M}_{\mathbf{r}}$, stepsize β and parameters $\alpha, \gamma, \mu_1, k_{\text{pr}} > 0$
Apply Algorithm 1 with input $\hat{\mathcal{T}}_0$ and parameters $\alpha, \gamma, k_{\text{pr}}$ to obtain $\hat{\mathcal{S}}_0$
for $l = 0, 1, \dots, l_{\max} - 1$ **do**
 $\mathcal{G}_l = \nabla \mathcal{L}(\hat{\mathcal{T}}_l + \hat{\mathcal{S}}_l)$
 $\mathcal{W}_l = \hat{\mathcal{T}}_l - \beta \mathcal{P}_{\mathbb{T}_l} \mathcal{G}_l$
 $\zeta_{l+1} = \frac{16}{7} \mu_1 \frac{\|\mathcal{W}_l\|_{\text{F}}}{\sqrt{d^*}}$
 $\hat{\mathcal{T}}_{l+1} = \text{Trim}_{\zeta_{l+1}, \mathbf{r}}(\mathcal{W}_l)$
 Apply Algorithm 1 with input $\hat{\mathcal{T}}_{l+1}$ and parameters $\alpha, \gamma, k_{\text{pr}}$ to obtain $\hat{\mathcal{S}}_{l+1}$
end for
Output: $\hat{\mathcal{T}}_{l_{\max}}$ and $\hat{\mathcal{S}}_{l_{\max}}$

linear models, selecting the best \mathbf{r} and α is challenging. Nevertheless, we suggest to minimize the following BIC-type criterion:

$$\text{BIC}(\mathbf{r}, \alpha) := (\|\hat{\mathcal{S}}_{\mathbf{r}, \alpha}\|_{\ell_0} + \sum_{i=1}^m r_i d_i) \cdot \ln(d^*) - 2 \ln(\hat{L}_{\mathbf{r}, \alpha}) \quad (3.3)$$

where $\hat{\mathcal{S}}_{\mathbf{r}, \alpha}$ is the estimated sparse tensor and $\hat{L}_{\mathbf{r}, \alpha}$ denotes the respective value of likelihood function, i.e., $-2 \ln(\hat{L}_{\mathbf{r}, \alpha}) = d^* \log(\|\mathcal{A} - \hat{\mathcal{S}}_{\mathbf{r}, \alpha} - \hat{\mathcal{T}}_{\mathbf{r}, \alpha}\|_{\text{F}}^2)$ for Example 2.1 (assuming Gaussian noise with unknown variance) and $-\ln(\hat{L}_{\mathbf{r}, \alpha})$ is the RHS of (2.2) for Example 2.2. Criterion (3.3) works reasonably well for Example 2.1 and 2.2, and yields interesting outcomes on international commodity trade flows data. We also propose practical guideline on choosing the algorithmic parameters γ, μ_1 and k_{pr} . See Section 7 and the supplement for more details.

4 General Convergence and Statistical Guarantees

In this section, we investigate the local convergence of Algorithm 2 in a general framework, and characterize the error of final estimates in terms of the gradient of loss function. Their applications on more specific examples are collected in Section 5. Our theory relies crucially on the regularity of loss function. Recall that Algorithm 2 involves: routine 1. Riemannian gradient descent for the low-rank estimate; and routine 2. gradient pruning for the sparse estimate. It turns out that these two routines generally require different regularity conditions on the loss function, although these conditions can be equivalent in special cases (e.g. see Section 5.1). Recall that $\gamma > 1$ is the tuning parameter in Algorithm 2 which *only* plays a role in $\gamma\alpha$, i.e., the desired sparsity.

Assumption 2. (Needed for Low-rank Estimate) *There exist $b_l, b_u > 0$ such that $\mathcal{L}(\cdot)$ is b_l -strongly*

convex and b_u -smooth in a subset $\mathbb{B}_2^* \subset \{\mathcal{T} + \mathcal{S} : \mathcal{T} \in \mathbb{M}_r, \mathcal{S} \in \mathbb{S}_{\gamma\alpha}\}$ meaning that

$$\langle \mathcal{X} - (\mathcal{T}^* + \mathcal{S}^*), \nabla \mathcal{L}(\mathcal{X}) - \nabla \mathcal{L}(\mathcal{T}^* + \mathcal{S}^*) \rangle \geq b_l \|\mathcal{X} - \mathcal{T}^* - \mathcal{S}^*\|_F^2 \quad (4.1)$$

$$\|\nabla \mathcal{L}(\mathcal{X}) - \nabla \mathcal{L}(\mathcal{T}^* + \mathcal{S}^*)\|_F \leq b_u \|\mathcal{X} - \mathcal{T}^* - \mathcal{S}^*\|_F \quad (4.2)$$

for all $\mathcal{X} \in \mathbb{B}_2^*$. Note that b_l and b_u may depend on \mathbb{B}_2^* .

Note that the explicit form of subset \mathbb{B}_2^* in Assumption 2 is usually determined by the actual problems (see examples in Section 5). For the main theorem in this section (Theorem 4.1), we consider \mathbb{B}_2^* to be a small neighbour around the truth $\mathcal{T}^* + \mathcal{S}^*$. In this case, Assumption 2 requires the loss function to be *locally* strongly convex and smooth.

Assumption 3. (Needed for Sparse Estimate) Suppose that \mathcal{L} is an entry-wise loss meaning $\mathcal{L}(\mathcal{T}) = \sum_{\omega} \mathfrak{l}_{\omega}([\mathcal{T}]_{\omega})$ where $\mathfrak{l}_{\omega}(\cdot) : \mathbb{R} \mapsto \mathbb{R}$ for any $\omega \in [d_1] \times \cdots \times [d_m]$. There exist a subset $\mathbb{B}_{\infty}^* \subset \{\mathcal{T} + \mathcal{S} : \mathcal{T} \in \mathbb{M}_r, \mathcal{S} \in \mathbb{S}_{\gamma\alpha}\}$ and $b_l, b_u > 0$ such that

$$\langle [\mathcal{X}]_{\omega} - [\mathcal{Z}]_{\omega}, \nabla \mathfrak{l}_{\omega}([\mathcal{X}]_{\omega}) - \nabla \mathfrak{l}_{\omega}([\mathcal{Z}]_{\omega}) \rangle \geq b_l |[\mathcal{X} - \mathcal{Z}]_{\omega}|^2 \quad (4.3)$$

$$|\nabla \mathfrak{l}_{\omega}([\mathcal{X}]_{\omega}) - \nabla \mathfrak{l}_{\omega}([\mathcal{Z}]_{\omega})| \leq b_u |[\mathcal{X} - \mathcal{Z}]_{\omega}| \quad (4.4)$$

for $\forall \omega \in [d_1] \times \cdots \times [d_m]$ and any $\mathcal{X}, \mathcal{Z} \in \mathbb{B}_{\infty}^*$. Similarly, b_l and b_u may depend on \mathbb{B}_{∞}^* .

The gradient pruning Algorithm 1 operates on entries of the gradients. Intuitively, entry-wise loss not only simplifies the computation but also helps characterize the performance of gradient pruning algorithm. If the sparse component is absent in our model, i.e. the underlying tensor is exactly low-rank, Assumption 3 will be unnecessary. See Section 6 in the supplement for more details. Notice that the same parameters b_l, b_u are both used in Assumption 2 and Assumption 3. This slightly abuse of notations is for the ease of exposition. These parameters are not necessarily equal.

For an entry-wise loss, condition (4.3) and (4.4) imply the condition (4.1) and (4.2), respectively. Therefore, Assumption 2 can be a by-product of Assumption 3, if we ignore the possible differences between the two neighbours \mathbb{B}_2^* and \mathbb{B}_{∞}^* . In this way, these two assumptions can be merged into one single assumption. However, we state them separately for several purposes. First, they highlight the differences of theoretical requirements between Riemannian gradient descent and gradient pruning algorithms. Second, the neighbours in these assumptions (\mathbb{B}_2^* and \mathbb{B}_{∞}^*) can be drastically different. Third, keeping them separate eases subsequent applications for special cases (e.g., for exact low-rank estimate in Section 6).

The signal strength $\underline{\lambda}$ is defined by $\underline{\lambda} := \lambda_{\min}(\mathcal{T}^*) := \min_{j \in [m]} \lambda_{r_j}(\mathcal{M}_j(\mathcal{T}^*))$. Here $\lambda_r(\cdot)$ denotes the r -th largest singular value of a matrix. Thus, $\underline{\lambda}$ represents the smallest non-zero singular value

among all the matricizations of \mathcal{T}^* . Similarly, denote $\bar{\lambda} := \lambda_{\max}(\mathcal{T}^*) := \max_{j \in [m]} \lambda_1(\mathcal{M}_j(\mathcal{T}^*))$ and define $\kappa_0 := \bar{\lambda} \underline{\lambda}^{-1}$ to be the condition number of \mathcal{T}^* .

Define

$$\text{Err}_{2\mathbf{r}} := \sup_{\mathcal{M} \in \mathbb{M}_{2\mathbf{r}}, \|\mathcal{M}\|_{\text{F}} \leq 1} \langle \nabla \mathcal{L}(\mathcal{T}^* + \mathcal{S}^*), \mathcal{M} \rangle \quad (4.5)$$

and $\text{Err}_{\infty} := \max \{ \|\nabla \mathcal{L}(\mathcal{T}^* + \mathcal{S}^*)\|_{\ell_{\infty}}, \min_{\|\mathcal{X}\|_{\ell_{\infty}} \leq k_{\text{pr}}} \|\nabla \mathcal{L}(\mathcal{X})\|_{\ell_{\infty}} \}$, where k_{pr} is the tuning parameter in gradient pruning Algorithm 1. The quantity $\text{Err}_{2\mathbf{r}}$ is typical in the aforementioned literature in exact low-rank matrix and tensor estimation. But the special quantity Err_{∞} appears in our paper for investigating the performance of gradient pruning algorithm. The first term in Err_{∞} comes from the gradient of loss function at the ground truth characterizing the stochastic error in many statistical models, while the second term is due to the setting of tuning parameter k_{pr} .

Theorem 4.1 displays the general performance bounds of Algorithm 2. For simplicity, we denote Ω^* the support of \mathcal{S}^* , $\bar{r} = \max_j r_j$, $\bar{d} = \max_j d_j$, $\underline{d} = \min_j d_j$, $r^* = r_1 \cdots r_m$ and $d^* := d_j d_j^- = d_1 \cdots d_m$. Let $\|\cdot\|_{\ell_{\infty}}$ denote the vectorized ℓ_{∞} -norm of tensors.

Theorem 4.1. *Let $\gamma > 1$, $k_{\text{pr}} > 0$ be the parameters used in Algorithm 2. Suppose that Assumptions 1, 2 and 3 hold with $\mathbb{B}_2^* = \{\mathcal{T} + \mathcal{S} : \|\mathcal{T} + \mathcal{S} - \mathcal{T}^* - \mathcal{S}^*\|_{\text{F}} \leq C_{0,m}\underline{\lambda}, \mathcal{T} \in \mathbb{M}_{\mathbf{r}}, \mathcal{S} \in \mathbb{S}_{\gamma\alpha}\}$, $\mathbb{B}_{\infty}^* = \{\mathcal{T} + \mathcal{S} : \|\mathcal{T} + \mathcal{S} - \mathcal{T}^* - \mathcal{S}^*\|_{\ell_{\infty}} \leq k_{\infty}, \mathcal{T} \in \mathbb{M}_{\mathbf{r}}, \mathcal{S} \in \mathbb{S}_{\gamma\alpha}\}$ where $k_{\infty} = C_{1,m}\mu_1^{2m}(\bar{r}^{m-1}/\underline{d}^{m-1})^{1/2}\underline{\lambda} + k_{\text{pr}} + \|\mathcal{S}^*\|_{\ell_{\infty}}$, $0.36b_l(b_u^2)^{-1} \leq 1$ and $b_u b_l^{-1} \leq 0.4(\sqrt{\delta})^{-1}$ for some $\delta \in (0, 1]$ and large absolute constants $C_{0,m}, C_{1,m} > 0$ depending only on m . Assume that*

- (a) *Initialization: $\|\hat{\mathcal{T}}_0 - \mathcal{T}^*\|_{\text{F}} \leq c_{1,m}\underline{\lambda} \cdot \min \{ \delta^2 \bar{r}^{-1/2}, (\kappa_0^{2m} \bar{r}^{1/2})^{-1} \}$, $\hat{\mathcal{T}}_0 \in \mathbb{B}_{\infty}^*$ and $\hat{\mathcal{T}}_0$ is $(2\mu_1\kappa_0)^2$ -incoherent*
- (b) *Signal-to-noise ratio: $\text{Err}_{2\mathbf{r}}/\underline{\lambda} + \text{Err}_{\infty}(b_u + 1)(|\Omega^*| + \gamma\alpha d^*)^{1/2}/(b_l \underline{\lambda}) \leq c_{2,m} \cdot \min \{ \delta^2 \bar{r}^{-1/2}, (\kappa_0^{2m} \bar{r}^{1/2})^{-1} \}$*
- (c) *Sparsity condition: $\alpha \leq c_{3,m}(\kappa_0^{4m} \mu_1^{4m} \bar{r}^m b_u^4 b_l^{-4})^{-1}$ and $\gamma \geq 1 + (4m)^{-1} b_u^4 b_l^{-4}$*

where $c_{1,m}, c_{2,m}, c_{3,m} > 0$ are small constants depending only on m . If the stepsize β is between $[0.005b_l/(b_u^2), 0.36b_l/(b_u^2)]$, we have

$$\begin{aligned} \|\hat{\mathcal{T}}_{l+1} - \mathcal{T}^*\|_{\text{F}}^2 &\leq (1 - \delta^2) \|\hat{\mathcal{T}}_l - \mathcal{T}^*\|_{\text{F}}^2 + C_{1,\delta} \text{Err}_{2\mathbf{r}}^2 + C_{1,b_u,b_l} (|\Omega^*| + \gamma\alpha d^*) \text{Err}_{\infty}^2 \\ \|\hat{\mathcal{S}}_{l+1} - \mathcal{S}^*\|_{\text{F}}^2 &\leq \frac{b_u^2}{b_l^2} \left(C_{2,m} \frac{1}{\gamma - 1} + C_{3,m} (\mu_1 \kappa_0)^{4m} \bar{r}^m \alpha \right) \|\hat{\mathcal{T}}_{l+1} - \mathcal{T}^*\|_{\text{F}}^2 + \frac{C_1}{b_l^2} (|\Omega^*| + \gamma\alpha d^*) \text{Err}_{\infty}^2 \end{aligned} \quad (4.6)$$

where $C_{1,\delta} = 6\delta^{-1}$ and $C_{1,b_u,b_l} = (C_2 + C_3 b_u + C_4 b_u^2) b_l^{-2}$ for absolute constants $C_1, \dots, C_4 > 0$ and $C_{2,m}, C_{3,m} > 0$ depending only on m . Therefore, for all $l \in [l_{\max}]$, we have

$$\|\hat{\mathcal{T}}_l - \mathcal{T}^*\|_{\text{F}}^2 \leq (1 - \delta^2)^l \|\hat{\mathcal{T}}_0 - \mathcal{T}^*\|_{\text{F}}^2 + \frac{C_{1,\delta} \text{Err}_{2\mathbf{r}}^2 + C_{1,b_u,b_l} (|\Omega^*| + \gamma\alpha d^*) \text{Err}_{\infty}^2}{\delta^2}. \quad (4.7)$$

By eq. (4.7), after suitably chosen l_{\max} iterations and treating b_l, b_u, δ as constants, we conclude with the following error bounds:

$$\|\widehat{\mathcal{T}}_{l_{\max}} - \mathcal{T}^*\|_{\text{F}}^2 \leq C_1 \text{Err}_{2\mathbf{r}}^2 + C_2(|\Omega^*| + \gamma \alpha d^*) \text{Err}_{\infty}^2 \quad (4.8)$$

and

$$\|\widehat{\mathcal{S}}_{l_{\max}} - \mathcal{S}^*\|_{\text{F}} \leq \frac{\alpha(\mu_1 \kappa_0)^{4m} \bar{r}^m (\gamma - 1) + 1}{\gamma - 1} \cdot (C_5 \text{Err}_{2\mathbf{r}}^2 + C_6(|\Omega^*| + \gamma \alpha d^*) \text{Err}_{\infty}^2) + C_7(|\Omega^*| + \gamma \alpha d^*) \text{Err}_{\infty}^2.$$

There exist two types of error as illustrated on the RHS of (4.8). The first term $\text{Err}_{2\mathbf{r}}^2$ comes from the model complexity of low-rank \mathcal{T}^* , and the term $|\Omega^*| \text{Err}_{\infty}^2$ is related to the model complexity of sparse \mathcal{S}^* . These two terms both reflect the intrinsic complexity of our model. On the other hand, the last term $\gamma \alpha d^* \text{Err}_{\infty}^2$ is a human-intervened complexity which originates from the tuning parameter γ in the algorithm design. If the cardinality of Ω^* happens to be of the same order as αd^* (it is the worse-case cardinality of Ω^* for $\mathcal{S}^* \in \mathbb{S}_{\alpha}$), the error bound is simplified into the following corollary. It is an immediate result from Theorem 4.1 and we hence omit the proof.

Corollary 4.2. *Suppose that the conditions of Theorem 4.1 hold and assume that $|\Omega^*| \asymp \alpha d^*$. Then for all $l = 1, \dots, l_{\max}$,*

$$\|\widehat{\mathcal{T}}_l - \mathcal{T}^*\|_{\text{F}}^2 \leq (1 - \delta^2)^l \|\widehat{\mathcal{T}}_0 - \mathcal{T}^*\|_{\text{F}}^2 + \frac{C_{1,\delta} \text{Err}_{2\mathbf{r}}^2 + C_{1,b_u,b_l} |\Omega^*| \text{Err}_{\infty}^2}{\delta^2}.$$

Remarks on the conditions of Theorem 4.1. The initialization is required to be as close to \mathcal{T}^* as $o(\lambda)$, if b_l, b_u, κ_0 and \bar{r} are all $O(1)$ constants. It is a common condition for non-convex methods for low-rank matrix and tensor related problems. Concerning the signal-to-noise ratio condition, Theorem 4.1 requires λ to dominate $\text{Err}_{2\mathbf{r}}$ and $(|\Omega^*| + \gamma \alpha d^*)^{1/2} \text{Err}_{\infty}$ if $b_l, b_u, \kappa_0, \bar{r} = O(1)$. This condition is mild and perhaps minimal. The sparsity requirement on \mathcal{S}^* is also mild. Assuming $b_l, b_u, \kappa_0, \bar{r}, \mu_1 = O(1)$, Theorem 4.1 merely requires $\alpha \leq c$ for a sufficiently small $c > 0$ which depends only on m , implying that Algorithm 2 allows a wide range of sparsity on \mathcal{S}^* . Similarly, Theorem 4.1 only requires $\gamma \geq C$ for a sufficiently large $C > 0$ which depends on m only.

We now investigate the recovery of the support of \mathcal{S}^* . Algorithm 2 usually over-estimates the size of the support of \mathcal{S}^* since the Level- $\gamma \alpha$ active indices are used for a γ strictly greater than 1.

Theorem 4.3. *Suppose conditions of Theorem 4.1 hold, $b_l, b_u = O(1)$, $|\Omega^*| \asymp \alpha d^*$ and l_{\max} is chosen such that (4.8) holds. Then,*

$$\|\widehat{\mathcal{S}}_{l_{\max}} - \mathcal{S}^*\|_{\ell_{\infty}} \leq C_{1,m} \kappa_0^{2m} \mu_1^{2m} \left(\frac{\bar{r}^m}{d^{m-1}} \right)^{1/2} \cdot (\text{Err}_{2\mathbf{r}} + (\gamma |\Omega^*|)^{1/2} \text{Err}_{\infty}) + C_{2,m} \text{Err}_{\infty}, \quad (4.9)$$

where $C_{1,m}, C_{2,m} > 0$ only depend on m .

If the non-zero entries of \mathcal{S}^* satisfy $|[\mathcal{S}^*]_\omega| > 2\delta^*$ for all $\omega \in \Omega^*$ where δ^* is the RHS of (4.9), we obtain $\widehat{\mathcal{S}}$ by a final-stage hard thresholding on $\widehat{\mathcal{S}}_{l_{\max}}$ so that $[\widehat{\mathcal{S}}]_\omega := [\widehat{\mathcal{S}}_{l_{\max}}]_\omega \cdot \mathbb{1}(|[\widehat{\mathcal{S}}_{l_{\max}}]_\omega| > \delta^*)$. By Theorem 4.3, we get $\text{supp}(\widehat{\mathcal{S}}) = \Omega^*$ and thus recovering the support of \mathcal{S}^* . The lower bound on the outliers is necessary for distinguishing the noise and outliers. If an entry in the outliers is of small magnitude, then it might be considered as noise. When the noise does not exist, we can set $k_{\text{pr}} = \infty$ implying $\delta^* = 0$.

5 Applications

We now apply the established results in Section 4 to more specific examples and elaborate the respective statistical performances. Our framework certainly covers many other interesting examples but we do not intend to exhaust them.

5.1 Sub-Gaussian Tensor Robust PCA with i.i.d. Noise

As introduced in Example 2.1, the goal of SG-RPCA is to extract low-rank *signal* from a noisy tensor observation $\mathcal{A} \in \mathbb{R}^{d_1 \times \dots \times d_m}$. Due to the linearity, we use the loss function $\mathcal{L}(\mathcal{T} + \mathcal{S}) := \frac{1}{2} \|\mathcal{T} + \mathcal{S} - \mathcal{A}\|_{\text{F}}^2$. Clearly, this loss is an entry-wise loss function, and satisfies the strongly-convex and smoothness conditions of Assumptions 2 and 3 with constants $b_l = b_u = 1$ within any subsets \mathbb{B}_2^* and \mathbb{B}_∞^* , or simply $\mathbb{B}_2^* = \mathbb{B}_\infty^* = \mathbb{R}^{d_1 \times \dots \times d_m}$. As a result, Theorem 4.1 and Theorem 4.3 are readily applicable by choosing $\delta = 0.15$, and setting the tuning parameter $k_{\text{pr}} = \infty$.

Theorem 5.1. *Suppose Assumption 1 holds and there exists $\sigma_z > 0$ such that $\mathbb{E} \exp\{t[\mathcal{Z}]_\omega\} \leq \exp\{t^2 \sigma_z^2 / 2\}$ for $\forall t \in \mathbb{R}$ and $\forall \omega \in [d_1] \times \dots \times [d_m]$. Let $r^* = r_1 \dots r_m$ and $\gamma > 1$ be the tuning parameter in Algorithm 2. Assume $|\Omega^*| \asymp \alpha d^*$ and*

- (a) *Initialization: $\|\widehat{\mathcal{T}}_0 - \mathcal{T}^*\|_{\text{F}} \leq c_{1,m} \underline{\lambda} \cdot (\kappa_0^{2m} \bar{r}^{1/2})^{-1}$ and $\widehat{\mathcal{T}}_0$ is $(2\mu_1 \kappa_0)^2$ -incoherent*
- (b) *Signal-to-noise ratio: $\underline{\lambda} / \sigma_z \geq C_{1,m} \kappa_0^{2m} \bar{r}^{1/2} \cdot (\bar{d} \bar{r} + r^* + \gamma |\Omega^*| \log \bar{d})^{1/2}$*
- (c) *Sparsity condition: $\alpha \leq c_{2,m} (\mu_1^{4m} \kappa_0^{4m} \bar{r}^m)^{-1}$ and $\gamma \geq 1 + 4m$*

where $c_{1,m}, c_{2,m}, C_{1,m} > 0$ are constants depending only on m . If the step size $\beta \in [0.005, 0.36]$, then after $l_{\max} > 1$ iterations, with probability at least $1 - \bar{d}^{-2}$, we have

$$\begin{aligned} \|\widehat{\mathcal{T}}_{l_{\max}} - \mathcal{T}^*\|_{\text{F}}^2 &\leq 0.98^{l_{\max}} \|\widehat{\mathcal{T}}_0 - \mathcal{T}^*\|_{\text{F}}^2 + C_{2,m} (\bar{d} \bar{r} + r^* + \gamma |\Omega^*| \log \bar{d}) \sigma_z^2 \\ \|\widehat{\mathcal{S}}_{l_{\max}} - \mathcal{S}^*\|_{\text{F}}^2 &\leq (C_{3,m} \alpha \bar{r}^m \mu_1^{4m} \kappa_0^{4m} + C_{4,m} (\gamma - 1)^{-1}) \cdot \|\widehat{\mathcal{T}}_{l_{\max}} - \mathcal{T}^*\|_{\text{F}}^2 + C_{5,m} \sigma_z^2 \cdot \gamma |\Omega^*| \log \bar{d} \end{aligned} \quad (5.1)$$

where $C_{2,m}, C_{3,m}, C_{4,m}, C_{5,m} > 0$ are constants depending only on m . Moreover, If l_{\max} is chosen large enough such that the second term on RHS of (5.1) dominates and assume $\mu_1^{4m} \kappa_0^{4m} \bar{r}^m (\bar{d} \bar{r} + r^*) \leq$

$C_{9,m}\underline{d}^{m-1}$, we get with probability at least $1 - \bar{d}^{-2}$ that

$$\|\widehat{\mathcal{S}}_{l_{\max}} - \mathcal{S}^*\|_{\ell_{\infty}} \leq \left(C_{6,m} \kappa_0^{2m} \mu_1^{2m} \bar{r}^{m/2} (\gamma |\Omega^*|)^{1/2} / \underline{d}^{(m-1)/2} + C_{7,m} \right) \cdot \sigma_z \log^{1/2} \bar{d}$$

where $C_{6,m}, C_{7,m} > 0$ are constants depending only on m .

Theorem 5.1 has several interesting implications. If the noise is absent meaning $\sigma_z = 0$, eq. (5.1) implies that, for an arbitrary $\varepsilon > 0$, after $l_{\max} \asymp \log(\varepsilon^{-1})$ iterations, Algorithm 2 outputs a $\widehat{\mathcal{T}}_{l_{\max}}$ satisfying $\|\widehat{\mathcal{T}}_{l_{\max}} - \mathcal{T}^*\|_{\text{F}} = O(\varepsilon)$. Therefore, Algorithm 2 can exactly recover the low-rank and sparse component, separately. On the other hand, if $\sigma_z > 0$ and $l_{\max} \asymp \log(\underline{\lambda} \sigma_z^{-1})$, eq. (5.1) implies that Algorithm 2 produces, with probability at least $1 - \bar{d}^{-2}$,

$$\|\widehat{\mathcal{T}}_{l_{\max}} - \mathcal{T}^*\|_{\text{F}}^2 \leq C_{2,m} \sigma_z^2 (\bar{d} \bar{r} + r^* + \gamma |\Omega^*| \log \bar{d}). \quad (5.2)$$

Since the intrinsic model complexity is of order $\bar{d} \bar{r} + r^* + |\Omega^*|$, the bound (5.2) is sharp up to logarithmic factors. Similar bounds also hold for $\|\widehat{\mathcal{S}}_{l_{\max}} - \mathcal{S}^*\|_{\text{F}}^2$. In addition, if $\mu_1^{4m} \kappa_0^{4m} \bar{r}^m (\bar{d} \bar{r} + r^* + \gamma |\Omega^*|) \leq C_{9,m} \underline{d}^{m-1}$, we get with probability at least $1 - \bar{d}^{-2}$,

$$\|\widehat{\mathcal{S}}_{l_{\max}} - \mathcal{S}^*\|_{\ell_{\infty}} \leq C_{7,m} \sigma_z \log^{1/2} \bar{d}. \quad (5.3)$$

Bound (5.3) is nearly optimal. To see it, consider the simpler model that $\mathcal{T}^* = \mathbf{0}$. Then, it is equivalent to estimate a sparse tensor from the data $\mathcal{S}^* + \mathcal{Z}$. Without further information, $O(\sigma_z \log^{1/2} \bar{d})$ is the best sup-norm performance one can expect in general.

Comparison with existing literature. In Lu et al. (2016); Zhou and Feng (2017), the authors studied noiseless RPCA assuming low tubal rank and proved that a convex program can exactly recover the underlying parameters. Their method works only for third order tensor and is not applicable to low Tucker-rank tensors, and there exists no statistical guarantee for the noisy setting. In Gu et al. (2014), the authors proposed the convex relaxation by unfolding a tensor into matrices. Their method is statistically sub-optimal and computationally more demanding. See Table 1 in Introduction. Interestingly, by setting $|\Omega^*| = 0$, our Theorem 5.1 degrades to well-established results for tensor PCA in the literature, e.g., higher order orthogonal iteration in Zhang and Xia (2018) and regularized jointly gradient descent in Han et al. (2020).

Initialization. We verify that the initialization conditions required by Theorem 5.1 can be satisfied under mild conditions. Recall that we denote the $\lfloor pd^* \rfloor$ -th largest entry of \mathcal{A} in absolute value by $|\mathcal{A}|^{(\lfloor pd^* \rfloor)}$. The idea of the initialization process is to first truncate the observed tensor \mathcal{A} defined by $[\text{Trunc}_{\tau}(\mathcal{A})]_{\omega} = \tau \cdot \text{Sign}([\mathcal{A}]_{\omega}) \cdot \mathbb{1}(|[\mathcal{A}]_{\omega}| > \tau) + [\mathcal{A}]_{\omega} \cdot \mathbb{1}(|[\mathcal{A}]_{\omega}| \leq \tau)$. We then apply the higher-order orthogonal iteration (HOOI) to $[\text{Trunc}_{\tau}(\mathcal{A})]_{\omega}$. The choice of τ is given in Algorithm 3. The details of HOOI can be found in the supplement. We remark that, in practice, the spikiness-related parameter μ_1 can be set to $2^m + \log \bar{d}$ and gradually double it if Algorithm 2 fails to converge. The theoretical guarantee is provided by the following lemma.

Lemma 5.2. Suppose Assumption 1 holds, the support of \mathcal{S}^* is Ω^* with cardinality $|\Omega^*|$, \mathcal{Z} has i.i.d entries with $\mathbb{E}[\mathcal{Z}]_\omega^2 = \sigma_z^2$ and $\mathbb{E} \exp\{t[\mathcal{Z}]_\omega\} \leq \exp\{c_1 t^2 \sigma_z^2\}$ for $\forall t \in \mathbb{R}$ and some absolute constant $c_1 > 0$. There exist absolute constants $C_{1,m}, C_{2,m}, C_{3,m}, c_{2,m} > 0$ such that if the maximum iteration of HOOI $t_{\max} \geq C_{1,m}(\log(\bar{d}\kappa_0) \vee 1)$ and

- (a) Sparsity condition: $|\Omega^*| \leq c_{2,m} \kappa_0^{-4m-2} \bar{r}^{-2} \mu_1^{-4} \log^{-2}(\bar{d}) \cdot \min\{(\underline{\lambda}/\sigma_z)^2, d^*\}$,
- (b) Signal-to-noise ratio: $\underline{\lambda}/\sigma_z \geq C_{2,m} \max\{\kappa_0^{2m} \bar{r}^{1/2} \mu_1[(r^*)^{1/2} + (\bar{d}\bar{r})^{1/2}] \log(\bar{d}), (d^*)^{1/4}\}$,

the output of Algorithm 3 satisfies the initialization condition in Theorem 5.1 with probability at least $1 - C_{3,m} \bar{d}^{-2}$.

Algorithm 3 Initialization for SG-RPCA

Take $p = \min\{(8\mu_1^2)^{-1}, (64m \log \bar{d})^{-1}\}$, and set $\tau_0 = |\mathcal{A}|^{(lp^{d^*})}$.

Define \mathcal{A}_0 by $[\mathcal{A}_0]_\omega = \begin{cases} [\mathcal{A}]_\omega, & \text{if } |[\mathcal{A}]_\omega| \leq \tau_0 \\ 0, & \text{otherwise.} \end{cases}$

Set $\tilde{\mathcal{A}} = \text{Trunc}_\tau(\mathcal{A})$ with $\tau = 10\sqrt{m \log(\bar{d})} \mu_1 \|\mathcal{A}_0\|_F / \sqrt{d^*}$.

$(\hat{\mathcal{T}}; \hat{\mathbf{U}}_1, \dots, \hat{\mathbf{U}}_m) = \text{HOOI}(\tilde{\mathcal{A}})$.

$\hat{\mathcal{T}}_0 = \text{Trim}_{\eta, \mathbf{r}}(\hat{\mathcal{T}})$ with $\eta = 16\mu_1 \|\hat{\mathcal{T}}\|_F / (7\sqrt{d^*})$.

5.2 Tensor PCA under Heavy-tailed Noise

Most aforementioned literature in Section 5.1 on tensor PCA focus on sub-Gaussian (Vershynin, 2011, 2018; Pan et al., 2018; Li et al., 2018). Nowadays, heavy-tailed noise routinely arise in diverse fields. However, the performances of most existing approaches for tensor PCA significantly deteriorate when noise have heavy tails. Interestingly, tensor PCA under heavy-tailed noise can be regarded as a special case of SG-RPCA. Suppose that the observed tensorial data \mathcal{A} satisfies $\mathcal{A} = \mathcal{T}^* + \mathcal{Z}$ with $\mathcal{T}^* \in \mathbb{U}_{\mathbf{r}, \mu_1}$. The noise tensor \mathcal{Z} satisfies the following tail assumption.

Assumption 4. (θ -tailed noise) The entries of \mathcal{Z} are i.i.d. with $\mathbb{E}[\mathcal{Z}]_\omega = 0$ and $\text{Var}([\mathcal{Z}]_\omega) \leq \sigma_z^2$. There exist $\theta > 2$ such that $\mathbb{P}(|[\mathcal{Z}]_\omega| \geq \sigma_z \cdot t) \leq t^{-\theta}$ for all $t > 1$.

If θ is only moderately large (e.g., $\theta = 3$), many entries of \mathcal{Z} can have large magnitudes such that the typical concentration properties of \mathcal{Z} (e.g., the bounds of $\text{Err}_{2\mathbf{r}}$ and Err_∞ in Section 5.1) disappear. Fix any $\alpha > 1$, we decompose $[\mathcal{Z}]_\omega = [\mathcal{S}_\alpha]_\omega + [\tilde{\mathcal{Z}}]_\omega$ such that

$$[\tilde{\mathcal{Z}}]_\omega = \mathbb{1}(|[\mathcal{Z}]_\omega| \geq \alpha\sigma_z) \cdot (\alpha\sigma_z) \text{sign}([\mathcal{Z}]_\omega) + \mathbb{1}(|[\mathcal{Z}]_\omega| < \alpha\sigma_z) \cdot [\mathcal{Z}]_\omega, \quad \forall \omega \in [d_1] \times \dots \times [d_m].$$

By definition, the entry $[\mathcal{S}_\alpha]_\omega \neq 0$ if and only if $|[\mathcal{Z}]_\omega| > \alpha\sigma_z$. Now, we write

$$\mathcal{A} = \mathcal{T}^* + \mathcal{S}_\alpha + \tilde{\mathcal{Z}} \tag{5.4}$$

Lemma 5.3. Suppose Assumption 4 holds and the distribution of $[\mathbf{Z}]_\omega$ is symmetric. For any $\alpha > 1$, we have $\mathbb{E}\tilde{\mathbf{Z}} = \mathbf{0}$. There exists an event \mathfrak{E}_1 with $\mathbb{P}(\mathfrak{E}_1) \geq 1 - \bar{d}^{-2}$ such that $\mathcal{S}_\alpha \in \mathbb{S}_{\alpha'}$ in the event \mathfrak{E}_1 where $\alpha' = \max\{2\alpha^{-\theta}, 10(\bar{d}/d^*)\log(m\bar{d}^3)\}$.

By Lemma 5.3, in the event \mathfrak{E}_1 , model (5.4) satisfies the SG-RPCA model such that $\mathcal{T}^* \in \mathbb{U}_{\mathbf{r}, \mu_1}$, $\mathcal{S}_\alpha \in \mathbb{S}_{\alpha'}$. Meanwhile, the entries of $\tilde{\mathbf{Z}}$ are sub-Gaussian for being uniformly bounded by $\alpha\sigma_z$. Therefore, conditioned on \mathfrak{E}_1 , Theorem 5.1 is readily applicable.

Theorem 5.4. Suppose Assumption 1 and the conditions of Lemma 5.3 hold. Choose $\alpha \asymp (d^*/\bar{d})^{1/\theta}$, $\gamma > 1$ as the tuning parameters in Algorithm 2. Assume $(\bar{d}/d^*)\log(m\bar{d}^3) \leq c_{2,m}(\mu_1^{4m}\kappa_0^{4m}\bar{r}^m)^{-1}$, $\gamma \geq 1 + 4m$ and

- (a) Initialization: $\|\hat{\mathcal{T}}_0 - \mathcal{T}^*\|_F \leq c_{1,m}\lambda \cdot (\kappa_0^{2m}\bar{r}^{1/2})^{-1}$ and $\hat{\mathcal{T}}_0$ is $(2\mu_1\kappa_0)^2$ -incoherent
- (b) Signal-to-noise ratio: $\lambda/(\alpha\sigma_z) \geq C_{1,m}\kappa_0^{2m}\bar{r}^{1/2} \cdot (\bar{d}\bar{r} + r^* + \gamma\bar{d}\log(m\bar{d}))^{1/2}$

where $c_{1,m}, c_{2,m}, C_{1,m} > 0$ are constants depending only on m . If the step size $\beta \in [0.005, 0.36]$, then after $l_{\max} > 1$ iterations, with probability at least $1 - 2\bar{d}^{-2}$, we have

$$\|\hat{\mathcal{T}}_{l_{\max}} - \mathcal{T}^*\|_F^2 \leq 0.98^{l_{\max}} \|\hat{\mathcal{T}}_0 - \mathcal{T}^*\|_F^2 + C_{2,m}\gamma(\bar{d}\bar{r} + r^* + \bar{d}\log(m\bar{d}))\alpha^2\sigma_z^2, \quad (5.5)$$

where $C_{2,m} > 0$ is a constant depending only on m .

By Theorem 5.4 and (5.5), if $\kappa_0, \gamma = O(1)$, $d_j \asymp d$ with $\alpha \asymp d^{(m-1)/\theta}$ and l_{\max} is properly chosen, we get with probability at least $1 - 2\bar{d}^{-2}$ that

$$\|\hat{\mathcal{T}}_{l_{\max}} - \mathcal{T}^*\|_F^2 \leq C_{2,m}(d\bar{r} + r^* + d\log(md))d^{2(m-1)/\theta} \cdot \sigma_z^2. \quad (5.6)$$

The bound (5.6) decreases as θ increases implying that the final estimate $\hat{\mathcal{T}}_{l_{\max}}$ becomes more accurate as the noise tail gets lighter. Moreover, if Assumption 4 holds with $\theta = 2(m-1)\log d$ so that $d^{2(m-1)/\theta} = O(1)$, bound (5.6) implies $\|\hat{\mathcal{T}}_{l_{\max}} - \mathcal{T}^*\|_F^2/\sigma_z^2 = O(d\bar{r} + r^* + d\log(md))$ which is sharp up to logarithmic factors. Similarly as Theorem 5.1, under Assumption 1, it is possible to derive an ℓ_∞ -norm bound for $\hat{\mathcal{T}}_{l_{\max}} - \mathcal{T}^*$.

Initialization. The initialization can be attained by Algorithm 3. Under bounded spikiness condition, we initially take $\mu_1 = 2^m + \log(\bar{d})$ and gradually double it if Algorithm 2 fails to converge. Similarly by Lemma 5.2, we have the following initialization guarantee for heavy-tailed tensor PCA.

Lemma 5.5. Under the setting of Theorem 5.4, there exist absolute constants $C_{1,m}, C_{2,m}, C_{3,m} > 0$ such that if the signal-noise-ratio

$$\lambda/(\alpha\sigma_z) \geq C_{1,m} \max \left\{ \kappa_0^{2m+1}\mu_1^2\bar{r}^{1/2}[(r^*)^{1/2} + (\bar{d}\bar{r})^{1/2}] \log^2(\bar{d}), (d^*)^{1/4} \right\},$$

after $t_{\max} \geq C_{2,m}(\log(\bar{d}\kappa_0) \vee 1)$ iterations, the output of Algorithm 3 satisfies the initialization condition in Theorem 5.4 with probability at least $1 - C_{3,m}\bar{d}^{-2}$.

5.3 Bernoulli Tensor Robust PCA

Following the Bernoulli tensor model in Example 2.2, based on a binary tensorial observation $\mathcal{A} \in \{0, 1\}^{d_1 \times \dots \times d_m}$, we choose the loss function to be the *negative* log-likelihood (without loss of generality, we set the scale parameter $\sigma = 1$ for ease of exposition)

$$\mathfrak{L}(\mathcal{T} + \mathcal{S}) = - \sum_{\omega} \left([\mathcal{A}]_{\omega} \log p([\mathcal{T} + \mathcal{S}]_{\omega}) + (1 - [\mathcal{A}]_{\omega}) \log (1 - p([\mathcal{T} + \mathcal{S}]_{\omega})) \right). \quad (5.7)$$

The RHS of (5.7) is an entry-wise loss, and Assumptions 2 and 3 are determined by the entry-wise second order derivatives. For $\forall \zeta > 0$, define

$$b_{u,\zeta} := \max \left\{ \sup_{|x| \leq \zeta} \frac{(p'(x))^2}{p^2(x)} - \frac{p''(x)}{p(x)}, \sup_{|x| \leq \zeta} \frac{(p'(x))^2}{(1-p(x))^2} + \frac{p''(x)}{1-p(x)} \right\}$$

$$b_{l,\zeta} := \min \left\{ \inf_{|x| \leq \zeta} \frac{(p'(x))^2}{p^2(x)} - \frac{p''(x)}{p(x)}, \inf_{|x| \leq \zeta} \frac{(p'(x))^2}{(1-p(x))^2} + \frac{p''(x)}{1-p(x)} \right\}$$

Assuming $b_{l,\zeta}, b_{u,\zeta} > 0$, then the loss function (5.7) satisfies Assumptions 2 and 3 with constants $b_{l,\zeta}$ and $b_{u,\zeta}$ for $\mathbb{B}_2^* = \mathbb{B}_{\infty}^* = \{\mathcal{T} + \mathcal{S} : \|\mathcal{T} + \mathcal{S}\|_{\ell_{\infty}} \leq \zeta, \mathcal{T} \in \mathbb{M}_r, \mathcal{S} \in \mathbb{S}_{\gamma\alpha}\}$ (more precisely, the low-rank and sparse conditions are unnecessary).

Notice that $b_{l,\zeta}$ and $b_{u,\zeta}$ can be extremely sensitive to large ζ . For instance (Wang and Li, 2020), we have

$$b_{l,\zeta} = \begin{cases} \frac{e^{\zeta}}{(1+e^{\zeta})^2}, & \text{if } p(x) = (1 + e^{-x})^{-1} \\ \gtrsim \frac{\zeta+1/6}{\sqrt{2\pi}} e^{-\zeta^2}, & \text{if } p(x) = \Phi(x) \end{cases} \quad \text{and} \quad b_{u,\zeta} = \begin{cases} \frac{1}{4}, & \text{if } p(x) = (1 + e^{-x})^{-1} \\ \geq 0.6, & \text{if } p(x) = \Phi(x) \end{cases}$$

implying that $b_{u,\zeta} b_{l,\zeta}^{-1}$ increases very fast as ζ becomes larger. Toward that end, we impose the following assumption which implies $\|\mathcal{T}^*\|_{\ell_{\infty}} \leq \zeta/2$ so that $\|\mathcal{S}^* + \mathcal{T}^*\|_{\ell_{\infty}} \leq \zeta$.

Assumption 5. *There exists a small $\zeta > 0$ such that $\|\mathcal{S}^*\|_{\ell_{\infty}} \leq \zeta/2$, \mathcal{T}^* satisfies Assumption 1 and its largest singular value $\bar{\lambda} \leq c_m(\mu_1 \kappa_0)^{-m}(\sqrt{d^*}/r^*) \cdot \zeta$ where $r^* = r_1 \cdots r_m$ and $d^* = d_1 \cdots d_m$.*

Meanwhile, we shall guarantee that the iterates $(\hat{\mathcal{T}}_l, \hat{\mathcal{S}}_l)$ produced by our algorithm satisfy $\|\hat{\mathcal{T}}_l\|_{\ell_{\infty}}, \|\hat{\mathcal{S}}_l\|_{\ell_{\infty}} = O(\zeta)$. The infinity norm bound for the sparse part is ensured by the choice of k_{pr} . And the low rank part is guaranteed by the following lemma.

Lemma 5.6. *Suppose that Assumptions 1 and 5 hold. Given any \mathcal{W} such that $\|\mathcal{W} - \mathcal{T}^*\|_{\text{F}} \leq \underline{\lambda}/8$, if we choose $\eta = 16\mu_1 \|\mathcal{W}\|_{\text{F}} / (7\sqrt{d^*})$, then $\|\text{Trim}_{\eta, \text{r}}(\mathcal{W})\|_{\ell_{\infty}} \leq (9\zeta/16) \cdot (\kappa_0 \mu_1)^m$.*

By Lemma 5.6, if $\kappa_0 \mu_1, m = O(1)$ and $\|\mathcal{W}_l - \mathcal{T}^*\|_{\text{F}} \leq \underline{\lambda}/8$, the trimming operator guarantees $\|\hat{\mathcal{T}}_{l+1}\|_{\ell_{\infty}} = O(\zeta)$. Equipped with (3.1) and by setting $k_{\text{pr}} = C_1 \zeta$ for some absolute $C_1 > 1$ depending only on $\kappa_0 \mu_1$ and m , we apply Algorithm 2 to minimize the RHS of (5.7).

Similarly, the error of final estimate relies on Err_{2r} and Err_∞ , both of which are related to the gradient of loss (5.7). Denote $L_\zeta := \sup_{|x| \leq \zeta} |p'(x)|/|p(x)(1-p(x))|$. Since $k_{\text{pr}} = C_1\zeta > \zeta$, by definition of Err_∞ , we have

$$\text{Err}_\infty \leq \max \left\{ L_\zeta, \min_{|x| \leq k_{\text{pr}}} \left| \frac{p'(x)}{p(x)(1-p(x))} \right| \right\} \leq L_\zeta. \quad (5.8)$$

In practice, due to sparsity, the value ζ is often small and it suffices to set $k_{\text{pr}} = 1$ in Algorithm 2 and for a cleaner bound of Theorem 5.7.

Theorem 5.7. *Let $\gamma > 1$, $k_{\text{pr}} := C_1\zeta$ be the parameters used in Algorithm 2 for a constant $C_1 > 1$ depending only on $\kappa_0\mu_1$ and m via Lemma 5.6. Suppose Assumptions 1 and 5 hold. Assume $|\Omega^*| \asymp \alpha d^*$, $0.36b_{l,\zeta'}b_{u,\zeta'}^{-2} \leq 1$, $b_{u,\zeta'}b_{l,\zeta'}^{-1} \leq 0.4(\sqrt{\delta})^{-1}$ for some $\delta \in (0, 1]$ and $\zeta' = (2C_1 + 1)\zeta$, and*

(a) *Initialization: $\|\hat{\mathcal{T}}_0 - \mathcal{T}^*\|_F \leq c_{1,m}\underline{\lambda} \cdot \min \{ \delta^2 \bar{r}^{-1/2}, (\kappa_0^{2m} \bar{r}^{1/2})^{-1} \}$, $\|\hat{\mathcal{T}}_0\|_{\ell_\infty} \leq c_{2,m}\zeta$ and $\hat{\mathcal{T}}_0$ is $(2\mu_1\kappa_0)^2$ -incoherent*

(b) *Signal-to-noise ratio:*

$$\underline{\lambda} \cdot \min \{ \delta^2 \bar{r}^{-1/2}, (\kappa_0^{2m} \bar{r}^{1/2})^{-1} \} \geq C_{2,m} \left(\sqrt{\bar{d}\bar{r}} + r^* + \gamma |\Omega^*| \frac{1 + b_{u,\zeta'}}{b_{l,\zeta'}} \right) \cdot L_\zeta$$

(c) *Sparsity condition: $\alpha \leq c_{3,m}b_{l,\zeta'}^4(b_{u,\zeta'}^4\kappa_0^{4m}\mu_1^{4m}\bar{r}^m)^{-1}$ and $\gamma \geq 1 + 4m \cdot b_{u,\zeta'}^4b_{l,\zeta'}^{-4}$*

where $c_{1,m}, c_{2,m}, c_{3,m}, C_{2,m} > 0$ are some constants depending on m only. If the stepsize $\beta \in [0.005b_{l,\zeta'}/(b_{u,\zeta'})^2, 0.36b_{l,\zeta'}/(b_{u,\zeta'})^2]$, after l_{\max} iterations, with probability at least $1 - \bar{d}^{-2}$,

$$\|\hat{\mathcal{T}}_{l_{\max}} - \mathcal{T}^*\|_F^2 \leq (1 - \delta^2)^{l_{\max}} \cdot \|\hat{\mathcal{T}}_0 - \mathcal{T}^*\|_F^2 + C_3 L_\zeta^2 \cdot (\bar{d}\bar{r} + r^* + \gamma |\Omega^*|) \quad (5.9)$$

$$\|\hat{\mathcal{S}}_{l_{\max}} - \mathcal{S}^*\|_F^2 \leq \frac{b_{u,\zeta'}^2}{b_{l,\zeta'}^2} (C_{4,m}\alpha \bar{r}^m (\mu_1\kappa_0)^{4m} + C_{5,m}(\gamma - 1)^{-1}) \|\hat{\mathcal{T}}_{l_{\max}} - \mathcal{T}^*\|_F^2 + \frac{C_{6,m}}{b_{l,\zeta'}^2} L_\zeta^2 \cdot \gamma |\Omega^*|$$

where $C_3 > 0$ depends only on $\delta, b_{l,\zeta'}, b_{u,\zeta'}, m$, and $C_{4,m}, C_{5,m}, C_{6,m} > 0$ are constants depending only on m . Moreover, if l_{\max} is chosen large enough such that the second term on RHS of (5.9) dominates and assume $\kappa_0^{4m}\mu_1^{4m}\bar{r}^m(\bar{d}\bar{r} + r^*) \lesssim_m O(\underline{d}^{m-1})$, we get with probability at least $1 - \bar{d}^{-2}$ that

$$\begin{aligned} \|\hat{\mathcal{T}}_{l_{\max}} - \mathcal{T}^*\|_{\ell_\infty} &\leq C_6 \kappa_0^{2m} \mu_1^{2m} (\bar{r}^m / \underline{d}^{m-1})^{1/2} (\bar{d}\bar{r} + r^* + \gamma |\Omega^*|)^{1/2} \cdot L_\zeta \\ \|\hat{\mathcal{S}}_{l_{\max}} - \mathcal{S}^*\|_{\ell_\infty} &\leq \left(C_7 \kappa_0^{2m} \mu_1^{2m} \bar{r}^{m/2} |\Omega^*|^{1/2} / \underline{d}^{(m-1)/2} + C_8 \right) \cdot L_\zeta \end{aligned}$$

where $C_6, C_7, C_8 > 0$ depend only on $\delta, b_{l,\zeta'}, b_{u,\zeta'}, m$.

By Theorem 5.7, after a properly chosen l_{\max} iterations and treating γ as a bounded constant, bound (5.9) implies $\|\hat{\mathcal{T}}_{l_{\max}} - \mathcal{T}^*\|_F^2 = O(L_\zeta^2 \cdot (\bar{d}\bar{r} + r^* + |\Omega^*|))$. Note that the term $\bar{d}\bar{r} + r^* + |\Omega^*|$ is the model complexity and thus this rate is sharp in general. If $\mathcal{S}^* = \mathbf{0}$ so that $|\Omega^*| = 0$, this rate is comparable to the existing ones in generalized low-rank tensor estimation (Wang and Li, 2020; Han

et al., 2020). Additionally, for the matrix case ($m = 2$), this rate matches the well-known results in (Davenport et al., 2014; Robin et al., 2020).

Initialization. The initialization for treating binary tensorial data can be obtained by unfolding \mathcal{A} into a $(d_1 \cdots d_{m_0}) \times (d_{m_0+1} \cdots d_m)$ matrix and applying 1 bit matrix estimation (Davenport et al., 2014). Here $m_0 = \lfloor m/2 \rfloor$. It is based on the solution to a convex program. See the supplement for more details. Its theoretical performance is guaranteed by Lemma 5.8. We write $d_1^* = d_1 \cdots d_{m_0}$, $d_2^* = d_{m_0+1} \cdots d_m$, and $\beta_\zeta = \sup_{|x| \leq \zeta} |p(x)(1 - p(x))|/(p'(x))^2$.

Lemma 5.8. *Suppose that Assumptions 1 and 5 hold and $\mathcal{S}^* \in \mathbb{S}_\alpha$. There exist absolute constants $C_{1,m}, C_{2,m}, C_{3,m} > 0$ such that if*

- (a) *Sparsity of \mathcal{S}^* :* $|\Omega^*| \leq \min \left\{ \frac{d^* r}{\min(d_1^*, d_2^*)}, C_{1,m} \zeta^{-2} \bar{\lambda}^2 \cdot \min \{ \delta^4 \bar{r}^{-1}, \kappa_0^{-4m} \bar{r}^{-1} \} \right\},$
- (b) *Signal-to-noise ratio:* $\underline{\lambda}^2 \cdot \min \{ \delta^4 \bar{r}^{-1}, \kappa_0^{-4m} \bar{r}^{-1} \} \geq C_{2,m} \zeta L_\zeta \beta_\zeta [r(d_1^* + d_2^*) d^*]^{1/2},$

the output of Algorithm 7 satisfies the initialization in Theorem 5.7 with probability at least $1 - C_{3,m}(d^)^{-1}$.*

Compared with Theorem 5.7, the required sparsity of \mathcal{S}^* and signal-to-noise ratio are more stringent to guarantee a warm initialization. It is typical that, oftentimes, the signal-to-noise ratio condition required by warm initialization is the primary bottleneck in tensor-related problems. See, for instance, Xia et al. (2021); Zhang and Xia (2018).

5.4 Poisson Tensor Robust PCA

In this section, we consider the Poisson tensor RPCA model. Suppose we observe $\mathcal{Y} \in \mathbb{N}^{d_1 \times \cdots \times d_m}$ that satisfies

$$\forall \omega \in [d_1] \times \cdots \times [d_m], [\mathcal{Y}]_\omega \sim \text{Poisson}(I \exp([\mathcal{T}^*]_\omega + [\mathcal{S}^*]_\omega)) \text{ independently,}$$

where $(\mathcal{T}^*, \mathcal{S}^*) \in (\mathbb{U}_{\mathbf{r}, \mu_1}, \mathbb{S}_\alpha)$ are the low rank part and sparse part respectively and $I > 0$ is the intensity parameter that is revealed as in Han et al. (2020). We choose the loss function to be the negative log-likelihood with scaling

$$\mathfrak{L}(\mathcal{T} + \mathcal{S}) = \frac{1}{I} \sum_{\omega} (-[\mathcal{Y}]_\omega [\mathcal{T} + \mathcal{S}]_\omega + I \exp([\mathcal{T} + \mathcal{S}]_\omega)).$$

This is an entry-wise loss, and simple calculation shows Assumptions 2 and 3 are satisfied with $\mathbb{B}_2^* = \mathbb{B}_\infty^* = \{\mathcal{T} + \mathcal{S} : \|\mathcal{T} + \mathcal{S}\|_{\ell_\infty} \leq \zeta, \mathcal{T} \in \mathbb{M}_{\mathbf{r}}, \mathcal{S} \in \mathbb{S}_{\gamma_\alpha}\}$ with $b_{l,\zeta} = e^{-\zeta}, b_{u,\zeta} = e^\zeta$. Since the parameter will become trivial in an unbounded set, we impose the following assumption which implies $\|\mathcal{T}^*\|_{\ell_\infty} \leq \frac{\zeta}{2}$ and thus $\|\mathcal{T}^* + \mathcal{S}^*\|_{\ell_\infty} \leq \zeta$.

Assumption 6. *There exists a small $\zeta > 0$ such that $\|\mathcal{S}^*\|_\infty \leq \frac{\zeta}{2}$, \mathcal{T}^* satisfies Assumption 1 with its largest singular value $\bar{\lambda} \leq c_m(\kappa_0\mu_1)^{-m}\sqrt{\frac{d^*}{r^*}}\zeta$ where $d^* = d_1 \cdots d_m$ and $r^* = r_1 \cdots r_m$.*

Similar with the binary case, we also need to show $\|\hat{\mathcal{T}}_l\|_{\ell_\infty}, \|\hat{\mathcal{S}}_l\|_{\ell_\infty} = O(\zeta)$. These are guaranteed by choosing $k_{pr} = C_1\zeta$ for some $C_1 > 1$ depending only on $\kappa_0\mu_1, m$ and from Lemma 5.6, when $\kappa_0\mu_1, m = O(1)$ and $\|\hat{\mathcal{T}}_l - \mathcal{T}^*\|_F \leq \underline{\lambda}/8$, we have $\|\hat{\mathcal{T}}_{l+1}\|_{\ell_\infty} = O(\zeta)$. We summarize the result in the following Theorem.

Theorem 5.9. *Let $\gamma > 1, k_{pr} := C_1\zeta$ be the parameters used in Algorithm 2 for a constant $C_1 > 1$ depending only on $\kappa_0\mu_1$ and m via Lemma 5.6. Suppose Assumptions 1 and 6 hold. Assume $|\Omega^*| \asymp \alpha d^*, e^{2\zeta'} \leq 0.4(\sqrt{\delta})^{-1}$ for some $\delta \in (0, 1]$ and $\zeta' = (2C_1 + 1)\zeta$, and*

(a) *Initialization: $\|\hat{\mathcal{T}}_0 - \mathcal{T}^*\|_F \leq c_{1,m}\underline{\lambda} \cdot \min\{\delta^2\bar{r}^{-1/2}, (\kappa_0^{2m}\bar{r}^{1/2})^{-1}\}$, $\|\hat{\mathcal{T}}_0\|_{\ell_\infty} \leq c_{2,m}\zeta$ and $\hat{\mathcal{T}}_0$ is $(2\mu_1\kappa_0)^2$ -incoherent*

(b) *Signal-to-noise ratio:*

$$\underline{\lambda} \cdot \min\{\delta^2\bar{r}^{-1/2}, (\kappa_0^{2m}\bar{r}^{1/2})^{-1}\} \geq C_{2,m}\left(\gamma|\Omega^*|\frac{1+e^{\zeta'}}{e^{-\zeta'}} \cdot e^\zeta + \sqrt{(r^* + \bar{d}\bar{r})e^\zeta/I}\right), \text{ and } I \geq Ce^\zeta \log(d^*)$$

(c) *Sparsity condition: $\alpha \leq c_{3,m}e^{-8\zeta'}(\kappa_0^{4m}\mu_1^{4m}\bar{r}^m)^{-1}$ and $\gamma \geq 1 + (4m)^{-1} \cdot e^{8\zeta'}$*

where $c_{1,m}, c_{2,m}, c_{3,m}, C_{2,m} > 0$ are some constants depending on m only. If the stepsize $\beta \in [0.005e^{-3\zeta'}, 0.36e^{-3\zeta'}]$, after l_{\max} iterations, with probability at least $1 - \frac{2}{d^*}$,

$$\|\hat{\mathcal{T}}_{l_{\max}} - \mathcal{T}^*\|_F^2 \leq (1 - \delta^2)^{l_{\max}} \cdot \|\hat{\mathcal{T}}_0 - \mathcal{T}^*\|_F^2 + C_{1,\delta} \frac{r^* + \bar{d}\bar{r}}{I/e^\zeta} + C_3 e^{2\zeta} \cdot \gamma|\Omega^*|$$

$$\|\hat{\mathcal{S}}_{l_{\max}} - \mathcal{S}^*\|_F^2 \leq e^{4\zeta'} (C_{4,m}\alpha\bar{r}^m(\mu_1\kappa_0)^{4m} + C_{5,m}(\gamma - 1)^{-1}) \|\hat{\mathcal{T}}_{l_{\max}} - \mathcal{T}^*\|_F^2 + C_{6,m}e^{2\zeta+2\zeta'} \cdot \gamma|\Omega^*|$$

where $C_3 > 0$ depends only on δ, ζ, m , and $C_{4,m}, C_{5,m}, C_{6,m} > 0$ are constants depending only on m . Moreover, if l_{\max} is chosen large enough such that the second term on RHS of (5.9) dominates and assume $\kappa_0^{4m}\mu_1^{4m}\bar{r}^m(\bar{r}\bar{d} + r^*) \lesssim_m O(\underline{d}^{m-1})$, we get with probability at least $1 - \frac{2}{d^*}$ that

$$\begin{aligned} \|\hat{\mathcal{T}}_{l_{\max}} - \mathcal{T}^*\|_{\ell_\infty} &\leq C_6\kappa_0^{2m}\mu_1^{2m}(\bar{r}^m/\underline{d}^{m-1})^{1/2} \left(\frac{r^* + \bar{d}\bar{r}}{I} + \gamma|\Omega^*|\right)^{1/2} \\ \|\hat{\mathcal{S}}_{l_{\max}} - \mathcal{S}^*\|_{\ell_\infty} &\leq C_7\kappa_0^{2m}\mu_1^{2m}\bar{r}^{m/2}/\underline{d}^{(m-1)/2} \cdot \left(\sqrt{(r^* + \bar{d}\bar{r})/I} + |\Omega^*|^{1/2}\right) + C_8 \end{aligned}$$

where $C_6, C_7, C_8 > 0$ depend only on γ, δ, ζ, m .

From Theorem 5.9, after a properly chosen l_{\max} iterations, we will obtain $\|\hat{\mathcal{T}}_{l_{\max}} - \mathcal{T}^*\|_F^2 = O(\frac{r^* + \bar{d}\bar{r}}{I/e^\zeta} + e^{2\zeta} \cdot \gamma|\Omega^*|)$. As a special case when $|\Omega^*| = 0$, our result matches the previous result in Poisson tensor PCA in Han et al. (2020) that is rate optimal under the same requirements on the intensity parameter I . When there are outliers, the error for the estimation of \mathcal{T}^* is further influenced by the outliers.

Initialization. We shall adopt the initialization proposed in Han et al. (2020) with slight modification. The theoretical guarantee is summarized in the following lemma.

Lemma 5.10. *Suppose that Assumptions 1 and 6 hold. There exist absolute constants $c, C > 0$ such that if $I \geq C \max\{\bar{d}, \underline{\lambda}^{-2} \sum_{i=1}^m (d_i r_i + d_i^- r_i) \bar{r}\}$, and the sparsity of \mathcal{S}^* satisfies $|\Omega^*| \leq c \zeta^{-2} \underline{\lambda}^2 \bar{r}^{-1}$, then the output of Algorithm 4 satisfies the initialization requirement in Theorem 5.9 with probability at least $1 - 1/d^*$.*

Algorithm 4 Initialization for Poisson RPCA

Set $\tilde{\mathcal{T}} = \log(\frac{\mathcal{Y}^{+1/2}}{I})$.
 Let $\tilde{\mathcal{T}}_0 = \mathcal{H}_{\mathbf{r}}^{\text{HO}}(\tilde{\mathcal{T}})$.
 Return $\hat{\mathcal{T}}_0 = \text{Trim}_{\eta, \mathbf{r}}(\tilde{\mathcal{T}}_0)$ with $\eta = 16\mu_1 \|\tilde{\mathcal{T}}_0\|_{\text{F}} / (7\sqrt{d^*})$.

6 When Sparse Component is Absent

In this section, we consider the special case when the sparse component is absent, i.e., $\mathcal{S}^* = \mathbf{0}$. For the exact low-rank tensor model, we observe that many conditions in Section 4 can be relaxed. A major difference is that the spikiness condition is generally not required for exact low-rank model. Consequently, the trimming step in Algorithm 2 is unnecessary. Therefore, it suffices to simply apply the Riemannian gradient descent algorithm to solve for the underlying low-rank tensor \mathcal{T}^* . For ease of exposition, the procedure is summarized in Algorithm 5 (largely the same as Algorithm 2).

Algorithm 5 Riemannian Gradient Descent for Exact Low-rank Estimate

Initialization: $\hat{\mathcal{T}}_0 \in \mathbb{M}_{\mathbf{r}}$ and stepsize $\beta > 0$
for $l = 0, 1, \dots, l_{\max}$ **do**
 $\mathcal{G}_l = \nabla \mathcal{L}(\hat{\mathcal{T}}_l)$
 $\mathcal{W}_l = \hat{\mathcal{T}}_l - \beta \mathcal{P}_{\mathbb{T}_l} \mathcal{G}_l$
 $\hat{\mathcal{T}}_{l+1} = \mathcal{H}_{\mathbf{r}}^{\text{HO}}(\mathcal{W}_l)$
end for
Output: $\hat{\mathcal{T}}_{l_{\max}}$

Algorithm 5 runs fast and guarantees favourable convergence performances under weaker conditions than Theorem 4.1. Indeed, since there is no sparse component, only Assumption 2 is required to guarantee the convergence of Algorithm 5. Similarly as Section 4, the error of final estimate produced by Algorithm 5 is characterized by the gradient at \mathcal{T}^* . With a slightly abuse of notation, denote $\text{Err}_{2\mathbf{r}} = \sup_{\mathcal{X} \in \mathbb{M}_{2\mathbf{r}}, \|\mathcal{X}\|_{\text{F}} \leq 1} \langle \nabla \mathcal{L}(\mathcal{T}^*), \mathcal{X} \rangle$.

Theorem 6.1. Suppose Assumption 2 holds with $\mathcal{S}^* = \mathbf{0}$ and $\mathbb{B}_2^* = \{\mathcal{T} : \|\mathcal{T} - \mathcal{T}^*\|_F \leq c_{0,m}\underline{\lambda}, \mathcal{T} \in \mathbb{M}_{\mathbf{r}}\}$ for a small constant $c_{0,m} > 0$ depending on m only, also suppose $1.5b_l b_u^{-2} \leq 1$ and $0.75b_l b_u^{-1} \geq \delta^{1/2}$ for some $\delta \in (0, 1]$ and the stepsize $\beta \in [0.4b_l b_u^{-2}, 1.5b_l b_u^{-2}]$ in Algorithm 5. Assume

- (a) Initialization: $\|\widehat{\mathcal{T}}_0 - \mathcal{T}^*\|_F \leq \underline{\lambda} \cdot c_{1,m} \delta \bar{r}^{-1/2}$
- (b) Signal-to-noise ratio: $\text{Err}_{2\mathbf{r}}/\underline{\lambda} \leq c_{2,m} \delta^2 \bar{r}^{-1/2}$

where $c_{1,m}, c_{2,m} > 0$ are small constants depending only on m . Then for all $l = 1, \dots, l_{\max}$,

$$\|\widehat{\mathcal{T}}_l - \mathcal{T}^*\|_F^2 \leq (1 - \delta^2)^l \|\widehat{\mathcal{T}}_0 - \mathcal{T}^*\|_F^2 + C_\delta \text{Err}_{2\mathbf{r}}^2$$

where $C_\delta > 0$ is a constant depending only on δ . Then after at most $l_{\max} \asymp \log(\underline{\lambda}/\text{Err}_{2\mathbf{r}})$ iterations (also depends on b_l, b_u, m, \bar{r} and β), we get

$$\|\widehat{\mathcal{T}}_{l_{\max}} - \mathcal{T}^*\|_F \leq C \cdot \text{Err}_{2\mathbf{r}},$$

where the constant $C > 0$ depends on only b_l, b_u, m, \bar{r} and β .

Note that Theorem 6.1 holds without spikiness condition in contrast with Theorem 4.1. It makes sense for the model has no missing values or sparse corruptions. The assumptions on loss function are also weaker (e.g., no need to be an entry-wise loss or entry-wisely smooth) than those in Theorem 4.1. As a result, Theorem 6.1 is also applicable to the low-rank tensor regression model among others. See (Han et al., 2020; Chen et al., 2019; Xia et al., 2020) and references therein. The initialization and signal-to-noise conditions are similar to those in Theorem 4.1, e.g., by setting $|\Omega^*| = \alpha = 0$ there. In addition, the error of final estimate depends only on $\text{Err}_{2\mathbf{r}}$. Interestingly, the contraction rate does not depend on the condition number κ_0 .

Comparison with existing literature In (Han et al., 2020), the authors proposed a general framework for exact low-rank tensor estimation based on regularized jointly gradient descent on the core tensor and associated low-rank factors. Their method is fast and achieves statistical optimality in various models. In contrast, our algorithm is based on Riemannian gradient descent, requires no regularization and also runs fast. An iterative tensor projection algorithm was studied in (Yu and Liu, 2016). But their method only applies to tensor regression. Other notable works focusing only on tensor regression include (Zhang et al., 2020a; Zhou et al., 2013; Hao et al., 2020; Sun et al., 2017; Li et al., 2018; Pan et al., 2018). A general projected gradient descent algorithm was proposed in (Chen et al., 2019) for generalized low-rank tensor estimation. For Tucker low-rank tensors, their algorithm is similar to our Algorithm 5 except that they use vanilla gradient \mathcal{G}_l while we use the Riemannian gradient $\mathcal{P}_{\mathbb{T}_l} \mathcal{G}_l$. As explained in Section 3, using the vanilla gradient can cause heavy computation burdens in the subsequent steps. Riemannian gradient descent algorithm for tensor completion was initially proposed by (Kressner et al., 2014). They focused only on tensor completion model and did not investigate its theoretical guarantees. Recently in (Cai et al.,

2020), the Riemannian gradient descent algorithm is applied for noiseless tensor regression and its convergence analysis is proved.

7 Numerical Comparisons with Existing Methods

We test the performances of our algorithms on synthetic datasets, specifically for the four applications studied in Section 5. Due to page limit, here we only present the comparative simulation results with competing methods on SG-RPCA and binary tensor learning. The comprehensive simulation results and the performance of proposed BIC-type criterion are collected in the supplementary file.

Choice of parameters. First of all, for the stepsize, we choose β that lies in the range we provide in the theories. For the spikiness parameter μ_1 , our theorem only requires it to be larger than the truth, we can initially set $\mu_1 = 2^m + \log(\bar{d})$ and gradually increase it by a factor of 2 if the algorithm fails to converge. For the rank \mathbf{r} and sparsity α , we treat them as given or select them by the BIC-type criterion (3.3). Note that γ *only* plays a role in the term $\gamma\alpha =: \alpha'$, i.e., the desired sparsity level. If the true α is unknown, then the BIC-type criterion actually searches for α' in which case γ is irrelevant and we simply set it to 1; if the true α is known, then we initially set $\gamma = 1.1$ or 2 and gradually increase it by a factor of 1.5 if the algorithm fails to converge. In the case of SG-RPCA and tensor PCA with heavy tailed noise, $k_{\text{pr}} = \infty$; and in the case of binary tensor, we follow the choice in Wang and Li (2020) and set $k_{\text{pr}} = 1$.

For the first experiment, we compare RGrad and PGD (Chen et al., 2019) on noisy tensor decomposition without outliers, i.e., no α or γ . The low-rank tensor $\mathcal{T}^* \in \mathbb{R}^{d \times d \times d}$ with $d = 300$ and Tucker rank $\mathbf{r} = (2, 2, 2)^\top$ is generated from the HOSVD of a trimmed standard normal tensor. The noise tensor \mathcal{Z} has i.i.d. entries sampled from $N(0, \sigma_z^2)$. Both algorithm terminate either when the relative error $\|\hat{\mathcal{T}}_l - \hat{\mathcal{T}}_{l-1}\|_F / \|\hat{\mathcal{T}}_l\|_F < 0.001$ or the maximum iteration (100) is reached. The noise level σ_z ranges from 0.01 to 0.05. For each fixed σ_z , 10 random instances for both algorithms are conducted. The result is displayed in the left plot of Figure 1a. We see that the statistical performance of RGrad and PGD, when there is no outliers, are similar. However, the right panel of Figure 1a shows that the per-step runtime using RGrad is only roughly 1/4 of the per-step runtime using PGD. This illustrates the computational efficiency of using RGrad over PGD.

For the second experiment, we set $d = 100$ and $\sigma_z = 0.01$. Given a sparsity level $\alpha \in (0, 1)$, the entries of sparse tensor \mathcal{S}^* are i.i.d. sampled from $\mathbf{S}_{\text{amp}} \times \text{Be}(\alpha) \times N(0, 1)$, which ensures $\mathcal{S}^* \in \mathbb{S}_{O(\alpha)}$ with high probability. Here the constant \mathbf{S}_{amp} is set as 0.1 or 1 modeling the two cases of small magnitude and large magnitude, respectively. The sparsity α is varied between 0.025 and 0.1, and $\gamma = 1.1$ for RGrad. We refer to Gu et al. (2014)’s method as convex relaxation and Lu et al.

(2016)’s method as tubal-tRPCA. The results are displayed in Figure 1b. Here RGrad (BIC) means that α is treated as unknown and selected by BIC-type criterion (3.3). It shows that the proposed BIC-type criterion works nicely in SG-RPCA. We can see the tubal-tRPCA performs poorly due to the ignorance of the low rank structure along the third direction. When the magnitude of the outliers is small, the performance of PGD and RGrad are similar. However, when the magnitude of the outliers is large, PGD performs poorly since it cannot deal with the outliers. The performance of convex relaxation is also worse than RGrad since it unfolds a tensor into an unbalanced matrix, and is statistically sub-optimal.

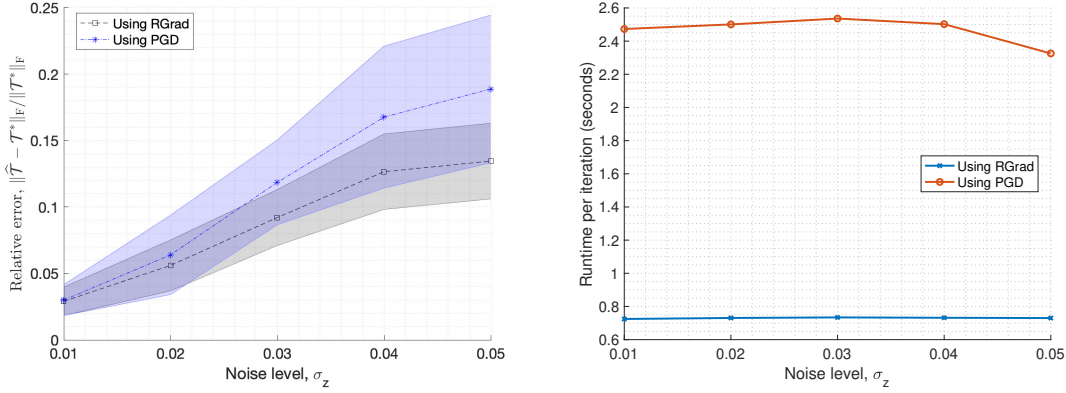
For the third experiment, we compare RGrad and PGD on binary tensor learning. Here $d = 100$ and $\mathbf{r} = (2, 2, 2)^\top$. The incoherent \mathcal{T}^* is generated such that $\|\mathcal{T}^*\|_{\ell_\infty} \approx 5$. The entries of \mathcal{S}^* are i.i.d. sampled from $\mathcal{S}_{\text{amp}} \times \text{Be}(\alpha)$. Here the constant \mathcal{S}_{amp} is set as 1 or 10 modeling the two cases of small magnitude and large magnitude, respectively. The sparsity α is varied between 0.005 and 0.02, and $\gamma = 1.1$ for RGrad. Initialization is obtained by the algorithm in the supplement. The link function is set to $p(x) = (1 + e^{-x/5})^{-1}$. Here RGrad (BIC) has a similar meaning as above. The results are displayed in Figure 1c. When the magnitude of outliers is small ($\mathcal{S}_{\text{amp}} = 1$), the performance of RGrad and PGD are comparable. However, when the magnitude of the outliers become large ($\mathcal{S}_{\text{amp}} = 10$), PGD cannot handle them well while our proposed algorithm has a much better performance.

8 Real Data: International Commodity Trade Flows

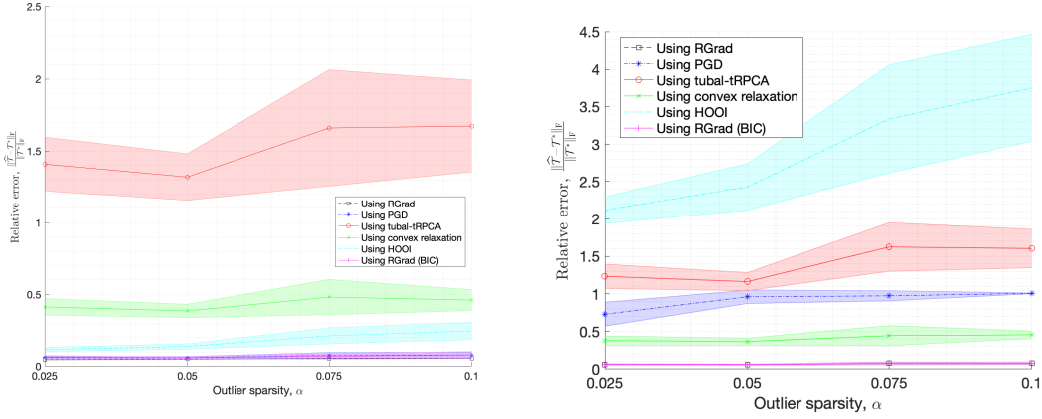
We collected the international commodity trade data from the API provided by UN website <https://comtrade.un.org>. The dataset contains the monthly information of imported commodities by countries from Jan. 2010 to Dec. 2016 (84 months in total). For simplicity, we focus on 50 countries among which 35 are from Europe, 9 from America, 5 from Asia² and 1 from Africa. All the commodities are classified into 100 categories based on the 2-digit HS code (<https://www.foreign-trade.com/reference/hscod.htm>). Thus, the raw data is a $50 \times 50 \times 100 \times 84$ tensor. At any month and for any category of commodity, there is a directed and weighted graph of size 50×50 depicting the trade flow between countries. The international trade has cyclic pattern annually. Since we are less interested in the time domain, we eliminate the fourth dimension by simply adding up the entries. Finally, we end up with a tensor \mathcal{A} of size $50 \times 50 \times 100$.

In Figure 2, circular plots are presented for illustrating the special trade patterns of some commodities. The countries are grouped and coloured by continent, i.e., Europe by red, Asia by

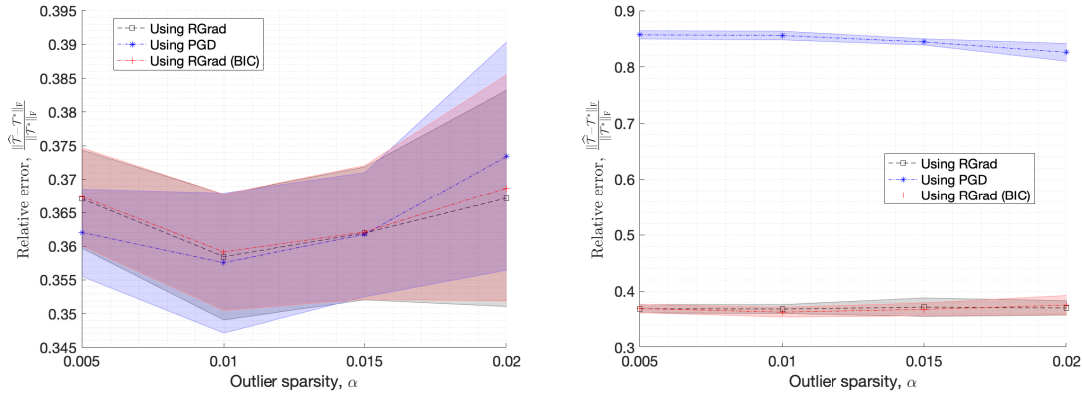
²Egypt is at the cross of Eastern Africa and Western Asia. For simplicity, we treat it as an Asian country. In addition, Turkey is treated as an Eastern European country rather than a Western Asian country.



(a) Tensor PCA without outliers. Left: Error bar of RGrad and PGD for 10 random instances. Right: Per-step runtime of RGrad and PGD.



(b) SG-RPCA. Left: Small amplitude of outlier with $S_{\text{amp}} = 0.1$; BIC suggested α : $\{0.025, 0.04, 0.065, 0.09\}$. Right: Large amplitude of outlier with $S_{\text{amp}} = 1$; BIC suggested α : $\{0.025, 0.05, 0.075, 0.1\}$.



(c) On binary tensor learning with outliers. Left: Small amplitude of outlier with $S_{\text{amp}} = 1$; BIC suggested α : $\{0.003, 0.008, 0.013, 0.015\}$. Right: Large amplitude of outlier with $S_{\text{amp}} = 10$; BIC suggested α : $\{0.003, 0.007, 0.012, 0.016\}$.

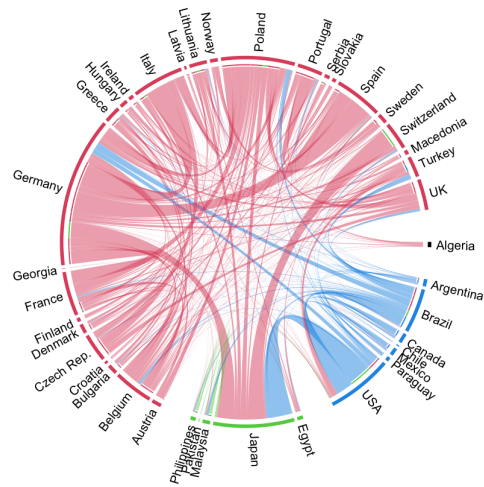
Figure 1: Comparison of RGrad, PGD (Chen et al., 2019), convex (Gu et al., 2014), tubal-tRPCA (Lu et al., 2016) and HOOI (Zhang and Xia, 2018).

green, America by blue and Africa by black. The links represent the directional trade flow between nations and are coloured based on the starting end of the link. The position of starting end of the link is shorter than the other end to give users the feeling that the link is moving out. The thickness of link indicates the volume of trade. From the top-left plot, we observe that Japan imports a large volume of tobacco related commodities; Germany is the largest exporter; Poland and Brazil are the second and third largest exporter; USA both import and export a large quantity of tobacco commodity. The top-right plot shows that USA and Canada import and export large volumes of mineral fuels; Malaysia exports lots of mineral fuels to Japan; Algeria exports a large quantity of miner fuels which plays the major role of international trade of this Africa country. The middle-left plot shows that Portugal is the largest exporter of Cork, and European countries are the major exporter and importer of this commodity. From the middle-right plot, we observe that Pakistan is the major exporter of Cotton in Asia; the European countries Turkey, Italy and Germany all export and import large volumes of cotton; USA exports a great deal of cotton to Mexico, Turkey and Philippines. The bottom-left plot shows that Malaysia and Belgium are the largest exporter of Tin and USA is the major importer. Finally, the bottom-right plot shows that Switzerland is the single largest exporter of clocks and watches; USA is the major importer; France and Germany both export and import large quantities of clocks and watches.

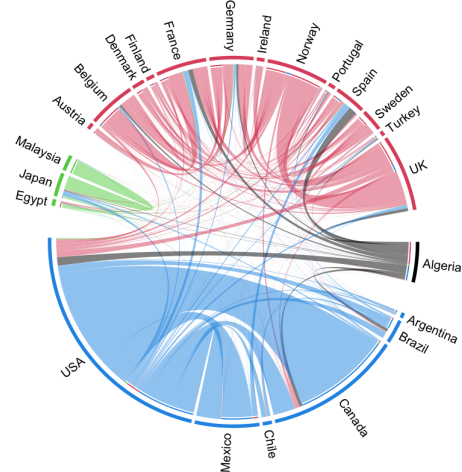
We implement the SG-RPCA framework as Section 5.1 to analyze the tensor $\log(1 + \mathcal{A})$, where a logarithmic transformation helps shrink the extremely large entries. The Tucker ranks are set as $(3, 3, 3)$, although most of the results seem insensitive to the ranks so long as they are bounded by 5 (BIC values within a 1% discrepancy). We apply the BIC-type criterion (3.3) and the detailed BIC result is postponed to the supplement. It suggests that any α between 0.002 and 0.03 yield similar (within 0.1% discrepancy) BIC values. See also top left and right panel in Figure 3. The algorithm is initialized by a HOSVD, which finally produces a low-rank $\hat{\mathcal{T}}$ and a sparse $\hat{\mathcal{S}}$. We shall use $\hat{\mathcal{T}}$ to uncover underlying relations among countries, and $\hat{\mathcal{S}}$ to examine distinctive trading patterns of certain commodities.

In particular, the singular vectors of $\hat{\mathcal{T}}$ are utilized to illustrate the community structure of nations. Note that the 1st-dim and 2nd-dim singular vectors of $\hat{\mathcal{T}}$ are distinct because the trading flows are directed. We observe that the 2nd-dim singular vectors often render better results. Then, a procedure of multi-dimensional scaling is adopted to visualize the rows of these singular vectors. We note that, though the BIC-type criterion suggests an $\alpha \in [0.002, 0.03]$, intriguing phenomenons are observed for larger values of α . The results are presented in Figure 3 for four choices of $\alpha \in \{0.003, 0.03, 0.1, 0.3\}$. All the plots in Figure 3 reveal certain degrees of the geographical relations among countries. It is reasonable since regional trade partnerships generally dominate the inter-continental trade relations. The European countries (coloured in blue) are mostly separated

HS Code 24: TOBACCO AND MANUFACTURED TOBACCO SUBSTITUTES



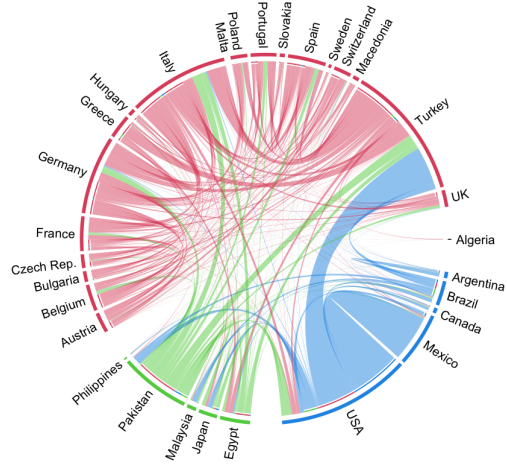
HS Code 27: MINERAL FUELS



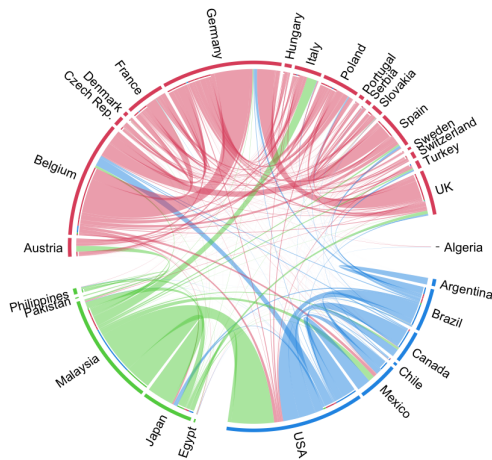
HS Code 45: CORK AND ARTICLES OF CORK



HS Code 52: COTTON



HS Code 80: TIN; ARTICLES THEREOF



HS Code 91: CLOCKS AND WATCHES AND PARTS THEREOF

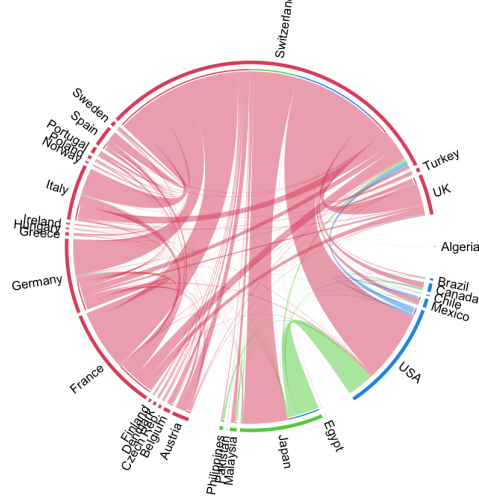
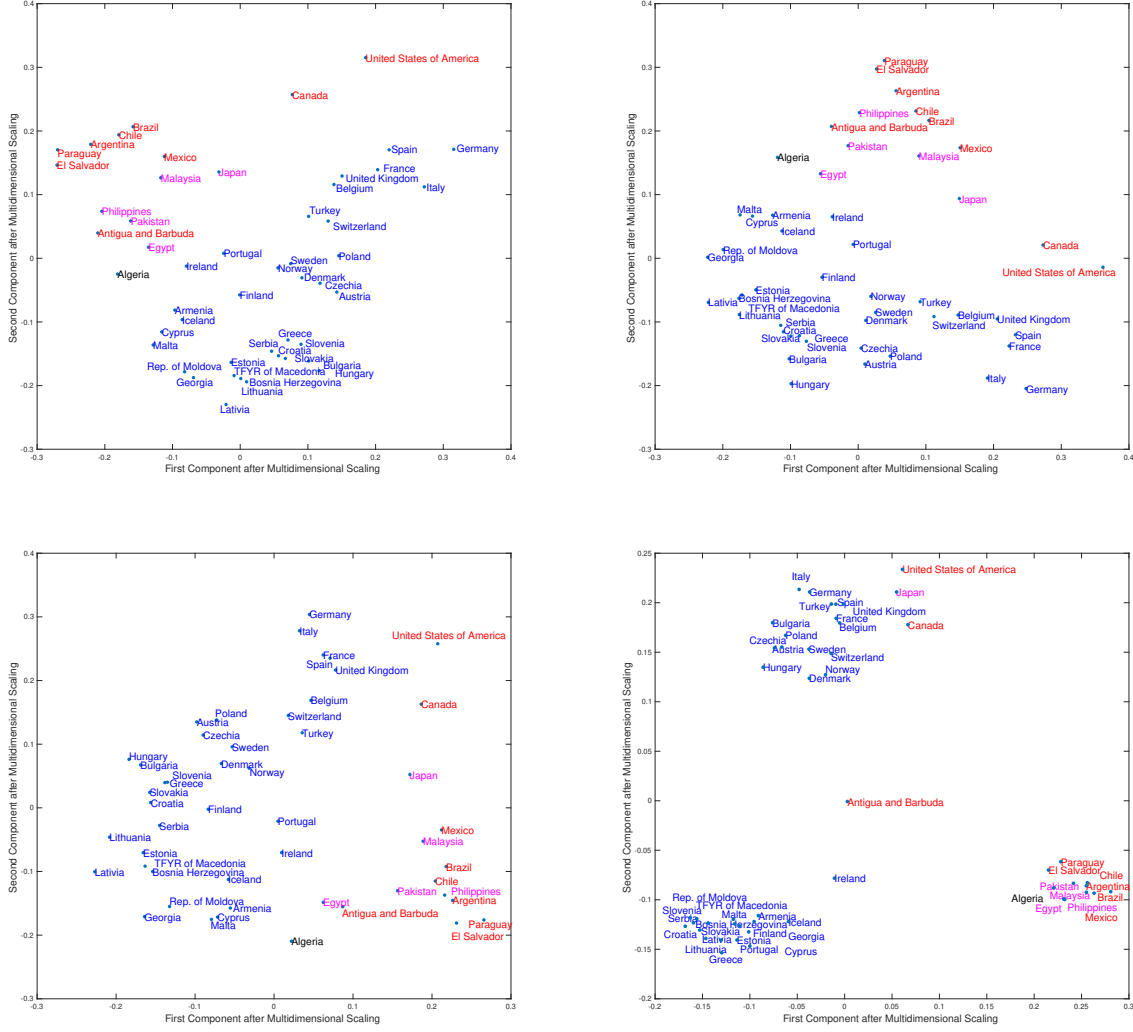


Figure 2: International Commodity Trade Flow₂₉ Import and export flow of some commodities.

from the others. Overall, countries from America (coloured in red) and Asia (coloured in magenta) are less separable especially when α is large. For small α like 0.003 or 0.03, the 5 Asian countries are clustered together and the major 8 American nations lie on the top-right corner of the plot. The two geographically close African countries Algeria and Egypt are also placed together in the top-left plot of Figure 3, as is the case with the Western European nations such as United Kingdom, Spain, France, Germany and Italy.

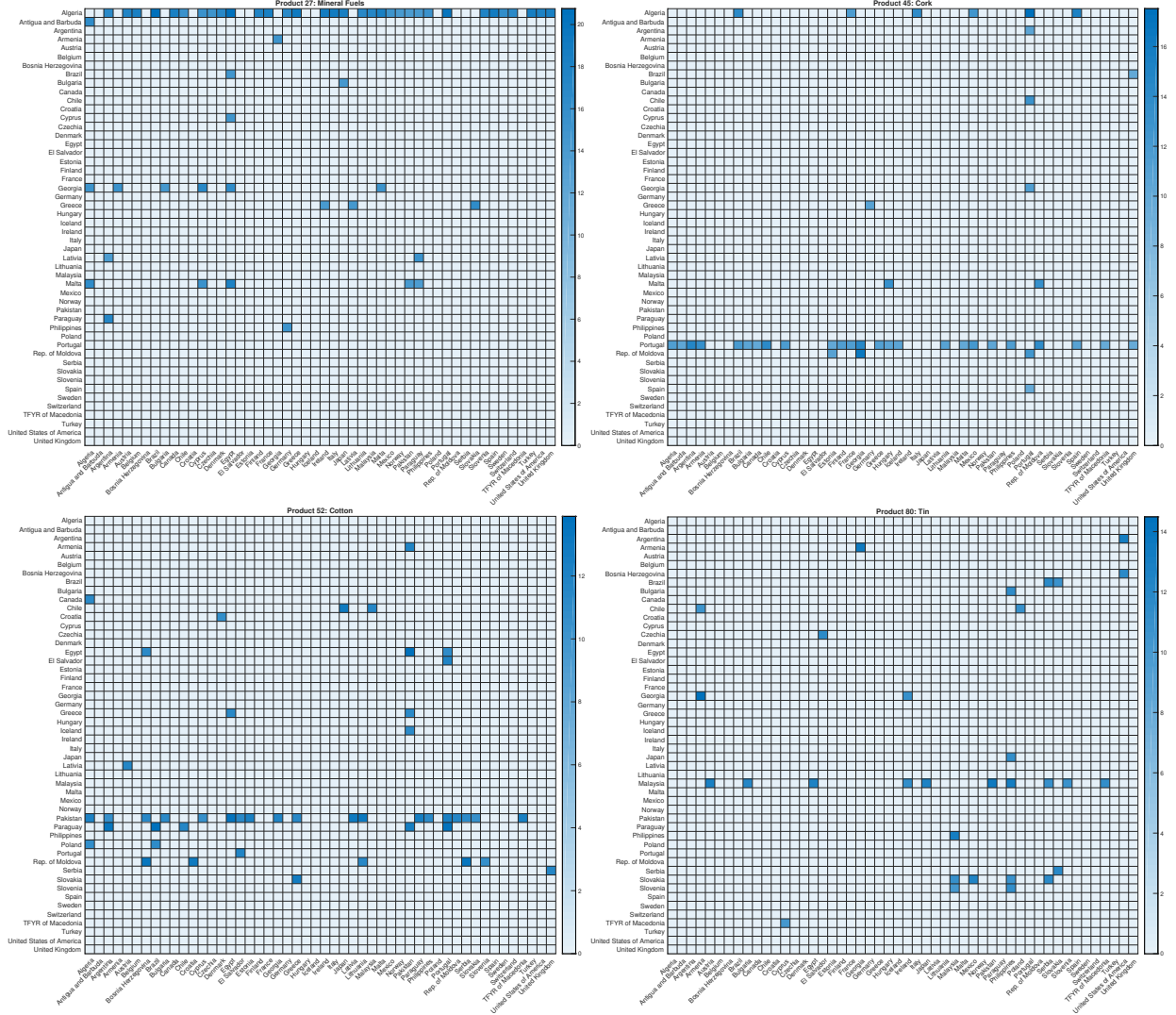
Figure 3 show that the low-rank estimate is sensitive to the larger sparsity ratio. Interesting shifts appear as α increases. Indeed, the geographical relations become a less important factor but the economic similarity plays the dominating role. For instance, some Asian and American nations split and merge into two clusters. The three large economies US, Canada and Japan are merged into one cluster, while the other small and less-developed Asian and American countries are merged into another cluster. It may be caused by that these three large economies are better at advanced technology and share similar structures in exporting high end commodities. Moreover, as α increases, the African country Algeria moves closer to the less-developed American and Asian nations. All these nations including Algeria rely heavily on exporting natural resources even if Algeria is geographically far from the others. Another significant shift is that the European countries split into two clusters as α increases. Moreover, one cluster comprising those wealthy and advanced Western European countries move closer to the group of US, Japan and Canada. These countries have close ties in trading high end products and components, although they belong to distinct continents. The other cluster includes mostly the Central and Eastern European countries, among which regional trade flows are particularly intense. Interestingly, there are two outlier countries Ireland (north-western Europe) and Antigua and Barbuda (a small island country in middle America). They do not merge into any clusters. The magnitudes of coordinates of these two points suggest that their international trade is not active.

We now look into the slices of the sparse estimate $\hat{\mathcal{S}}$ and investigate the distinctive trading patterns of certain commodities. As the sparsity ratio α grows, the slices of $\hat{\mathcal{S}}$ become denser whose patterns are more difficult to examine. For better exposition, we mainly focus on small values of α like 0.03. The results are presented in Figure 4. The top-left plot shows that Algeria exports exceptionally large volumes of mineral fuels that can not be explained by the low-rank tensor estimate. Similarly, based on the top-right plot, we observe that the exact low-rank tensor PCA fails to explain the trading export of cork by Portugal. Fortunately, these interesting and significant trading patterns can be easily captured by the additional sparse tensor estimate. The bottom-left and bottom-right plots of Figure 4 showcase the unusual exports of cotton by Pakistan and exports of Tin by Malaysia, respectively. These findings echo some trading patterns displayed in Figure 2.



(a) Sparsity level: top-left, $\alpha = 0.003$; top-right, $\alpha = 0.03$; bottom-left, $\alpha = 0.1$; bottom-right, $\alpha = 0.3$.

Figure 3: Visualize the relations between countries by spectral estimates. Tucker ranks are set as $(3, 3, 3)$ and the low-rank tensor is estimated by SG-RPCA as in Section 5.1 with HOSVD initialization. Blue coloured countries are from Europe, red from America, magenta from Asia and black from Africa. When α is small, clusters have strong implications on the geographical closeness between nations; As α becomes large, economic structures become the major factor in that large and advanced economies tend to merge, and so do low end economies and natural resource reliant economies. But our BIC-type criterion suggests to choose $\alpha \in [0.002, 0.03]$.



(a) Commodity: top-left, Mineral Fuels; top-right, Cork; bottom-left, Cotton; bottom-right, Tin.

Figure 4: Heatmaps of the slices of $\hat{\mathcal{S}}$. They reveal distinctive trading patterns of certain commodities. The sparsity ratio is set at $\alpha = 0.03$.

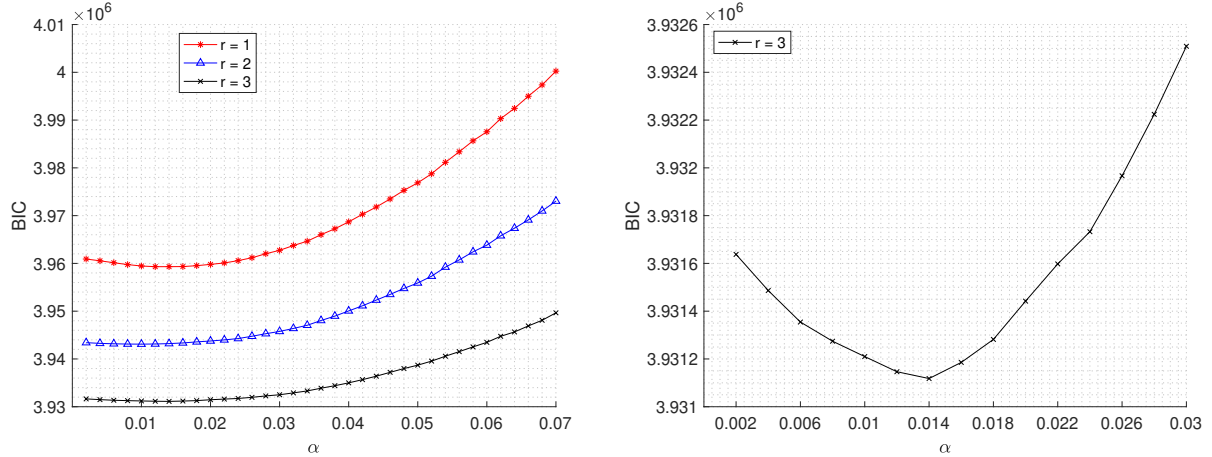


Figure 5: BIC values on the International Trade Flow Data. Left: BIC values for different rank and sparsity; Right: Zoom in on the case $r = 3$.

We now compare Gu et al. (2014)’s method (convex relaxation) and Lu et al. (2016)’s method (tubal-tRPCA) with our method in terms of prediction error on the international trade flow dataset. As in Section 8, we analyze the tensor $\log(1 + \mathcal{A})$. We split $\log(1 + \mathcal{A})$ into two parts, namely $\log(1 + \mathcal{A}) =: \mathcal{A}_{\text{train}} + \mathcal{A}_{\text{test}}$, where $\mathcal{A}_{\text{test}}$ is generated by randomly taking 10% of the non-zero entries of $\log(1 + \mathcal{A})$. We then apply tubal-tRPCA with the default parameter the authors provide³ and convex relaxation with carefully tuned parameters⁴. We use the proposed BIC-type criterion to select the rank and sparsity. As the left panel of Figure 5 suggests, we choose $\mathbf{r} = (3, 3, 3)^\top$, and the right panel of Figure 5 shows the BIC is less sensitive to α for a small range. Therefore we set the rank as $\mathbf{r} = (3, 3, 3)^\top$ and try $\alpha = 0.01, 0.02, 0.03$. The error is measured in terms of the test error $\|[\hat{\mathcal{T}} + \hat{\mathcal{S}}]_{\Omega_{\text{test}}} - \mathcal{A}_{\text{test}}\|_F$ and the results are presented in Table 2.

When $\alpha = 0$, all methods perform poorly because the existence of outliers distort the low-rank estimate making it ineffective in prediction. Meanwhile, if α is too large, say 0.1, the sparse component might incorrectly absorb useful information from the low-rank component which, as a result, sabotages its prediction accuracy. Fortunately, our method with the BIC suggested α indeed significantly outperforms other methods.

References

Animashree Anandkumar, Rong Ge, Daniel Hsu, Sham M Kakade, and Matus Telgarsky. Tensor decompositions for learning latent variable models. *Journal of Machine Learning Research*, 15:

³Their codes are available at <https://github.com/canyilu/tensor-completion-under-linear-transform>.

⁴The codes in Gu et al. (2014) is not publicly released so we have to tune the parameters by ourselves.

Method	Convex Gu et al. (2014)	tubal-tRPCA Lu et al. (2016)	Our method ($\alpha = 0$)	Our method ($\alpha = 0.01$)	Our method ($\alpha = 0.02$)	Our method ($\alpha = 0.03$)
Pred. Error	1892.3	1894.2	1891.2	693.5	800.5	980.1

Table 2: Comparison of our method with convex relaxation Gu et al. (2014) and tubal-tRPCA Lu et al. (2016) in terms of prediction error on the international trade flow data. Our BIC criterion suggests any α between 0.002 and 0.03. We note that our method with $\alpha = 0.003$ yields a prediction error 566.0.

2773–2832, 2014.

Xuan Bi, Annie Qu, and Xiaotong Shen. Multilayer tensor factorization with applications to recommender systems. *Annals of Statistics*, 46(6B):3308–3333, 2018.

Xuan Bi, Xiwei Tang, Yubai Yuan, Yanqing Zhang, and Annie Qu. Tensors in statistics. *Annual Review of Statistics and Its Application*, 8, 2020.

Changxiao Cai, Gen Li, H Vincent Poor, and Yuxin Chen. Nonconvex low-rank tensor completion from noisy data. In *Advances in Neural Information Processing Systems*, pages 1863–1874, 2019.

Jian-Feng Cai, Lizhang Miao, Yang Wang, and Yin Xian. Provable near-optimal low-multilinear-rank tensor recovery. *arXiv preprint arXiv:2007.08904*, 2020.

Emmanuel J Candès, Xiaodong Li, Yi Ma, and John Wright. Robust principal component analysis? *Journal of the ACM (JACM)*, 58(3):1–37, 2011.

Raymond B Cattell. The scree test for the number of factors. *Multivariate behavioral research*, 1(2):245–276, 1966.

Han Chen, Garvesh Raskutti, and Ming Yuan. Non-convex projected gradient descent for generalized low-rank tensor regression. *The Journal of Machine Learning Research*, 20(1):172–208, 2019.

Yuxin Chen, Jianqing Fan, Cong Ma, and Yuling Yan. Bridging convex and nonconvex optimization in robust pca: Noise, outliers, and missing data. *arXiv preprint arXiv:2001.05484*, 2020.

Mark A Davenport, Yaniv Plan, Ewout Van Den Berg, and Mary Wootters. 1-bit matrix completion. *Information and Inference: A Journal of the IMA*, 3(3):189–223, 2014.

- Alan Edelman, Tomás A Arias, and Steven T Smith. The geometry of algorithms with orthogonality constraints. *SIAM journal on Matrix Analysis and Applications*, 20(2):303–353, 1998.
- Xing Fan, Marianna Pensky, Feng Yu, and Teng Zhang. Alma: Alternating minimization algorithm for clustering mixture multilayer network. *arXiv preprint arXiv:2102.10226*, 2021.
- Quanquan Gu, Huan Gui, and Jiawei Han. Robust tensor decomposition with gross corruption. *Advances in Neural Information Processing Systems*, 27:1422–1430, 2014.
- Rungang Han, Rebecca Willett, and Anru Zhang. An optimal statistical and computational framework for generalized tensor estimation. *arXiv preprint arXiv:2002.11255*, 2020.
- Botao Hao, Anru Zhang, and Guang Cheng. Sparse and low-rank tensor estimation via cubic sketchings. *IEEE Transactions on Information Theory*, 2020.
- Pengsheng Ji and Jiashun Jin. Coauthorship and citation networks for statisticians. *The Annals of Applied Statistics*, 10(4):1779–1812, 2016.
- Jiashun Jin. Fast community detection by score. *Annals of Statistics*, 43(1):57–89, 2015.
- Bing-Yi Jing, Ting Li, Zhongyuan Lyu, and Dong Xia. Community detection on mixture multi-layer networks via regularized tensor decomposition. *arXiv preprint arXiv:2002.04457*, 2020.
- Zheng Tracy Ke, Feng Shi, and Dong Xia. Community detection for hypergraph networks via regularized tensor power iteration. *arXiv preprint arXiv:1909.06503*, 2019.
- Tamara G Kolda and Brett W Bader. Tensor decompositions and applications. *SIAM review*, 51(3):455–500, 2009.
- Daniel Kressner, Michael Steinlechner, and Bart Vandereycken. Low-rank tensor completion by riemannian optimization. *BIT Numerical Mathematics*, 54(2):447–468, 2014.
- Xiaoshan Li, Da Xu, Hua Zhou, and Lexin Li. Tucker tensor regression and neuroimaging analysis. *Statistics in Biosciences*, 10(3):520–545, 2018.
- Tianqi Liu, Ming Yuan, and Hongyu Zhao. Characterizing spatiotemporal transcriptome of human brain via low rank tensor decomposition. *arXiv preprint arXiv:1702.07449*, 2017.
- Canyi Lu, Jiashi Feng, Yudong Chen, Wei Liu, Zhouchen Lin, and Shuicheng Yan. Tensor robust principal component analysis: Exact recovery of corrupted low-rank tensors via convex optimization. In *Proceedings of the IEEE conference on computer vision and pattern recognition*, pages 5249–5257, 2016.

- Yuetian Luo and Anru R Zhang. Tensor clustering with planted structures: Statistical optimality and computational limits. *arXiv preprint arXiv:2005.10743*, 2020.
- Yuqing Pan, Qing Mai, and Xin Zhang. Covariate-adjusted tensor classification in high dimensions. *Journal of the American Statistical Association*, 2018.
- Subhadeep Paul and Yuguo Chen. Spectral and matrix factorization methods for consistent community detection in multi-layer networks. *The Annals of Statistics*, 48(1):230–250, 2020.
- Marianna Pensky and Teng Zhang. Spectral clustering in the dynamic stochastic block model. *Electronic Journal of Statistics*, 13(1):678–709, 2019.
- Garvesh Raskutti, Ming Yuan, and Han Chen. Convex regularization for high-dimensional multiresponse tensor regression. *The Annals of Statistics*, 47(3):1554–1584, 2019.
- Emile Richard and Andrea Montanari. A statistical model for tensor pca. *Advances in Neural Information Processing Systems*, 27:2897–2905, 2014.
- Geneviève Robin, Olga Klopp, Julie Josse, Éric Moulines, and Robert Tibshirani. Main effects and interactions in mixed and incomplete data frames. *Journal of the American Statistical Association*, 115(531):1292–1303, 2020.
- Will Wei Sun and Lexin Li. Dynamic tensor clustering. *Journal of the American Statistical Association*, 114(528):1894–1907, 2019.
- Will Wei Sun, Junwei Lu, Han Liu, and Guang Cheng. Provable sparse tensor decomposition. *Journal of the Royal Statistical Society: Series B (Statistical Methodology)*, 79(3):899–916, 2017.
- Roman Vershynin. Spectral norm of products of random and deterministic matrices. *Probability theory and related fields*, 150(3):471–509, 2011.
- Roman Vershynin. *High-dimensional probability: An introduction with applications in data science*, volume 47. Cambridge university press, 2018.
- Lu Wang, Zhengwu Zhang, and David Dunson. Common and individual structure of brain networks. *Ann. Appl. Stat.*, 13(1):85–112, 03 2019. doi: 10.1214/18-AOAS1193. URL <https://doi.org/10.1214/18-AOAS1193>.
- Miaoyan Wang and Lexin Li. Learning from binary multiway data: Probabilistic tensor decomposition and its statistical optimality. *Journal of Machine Learning Research*, 21(154):1–38, 2020.

- Miaoyan Wang and Yuchen Zeng. Multiway clustering via tensor block models. *arXiv preprint arXiv:1906.03807*, 2019.
- Dong Xia. Normal approximation and confidence region of singular subspaces, 2019.
- Dong Xia and Ming Yuan. On polynomial time methods for exact low-rank tensor completion. *Foundations of Computational Mathematics*, 19(6):1265–1313, 2019.
- Dong Xia and Fan Zhou. The sup-norm perturbation of hosvd and low rank tensor denoising. *J. Mach. Learn. Res.*, 20:61–1, 2019.
- Dong Xia, Anru R Zhang, and Yuchen Zhou. Inference for low-rank tensors—no need to debias. *arXiv preprint arXiv:2012.14844*, 2020.
- Dong Xia, Ming Yuan, and Cun-Hui Zhang. Statistically optimal and computationally efficient low rank tensor completion from noisy entries. *Annals of Statistics*, 49(1):76–99, 2021.
- Rose Yu and Yan Liu. Learning from multiway data: Simple and efficient tensor regression. In *International Conference on Machine Learning*, pages 373–381, 2016.
- Ming Yuan and Cun-Hui Zhang. Incoherent tensor norms and their applications in higher order tensor completion. *IEEE Transactions on Information Theory*, 63(10):6753–6766, 2017.
- Anru Zhang and Dong Xia. Tensor svd: Statistical and computational limits. *IEEE Transactions on Information Theory*, 64(11):7311–7338, 2018.
- Anru R Zhang, Yuetian Luo, Garvesh Raskutti, and Ming Yuan. Islet: Fast and optimal low-rank tensor regression via importance sketching. *SIAM Journal on Mathematics of Data Science*, 2(2):444–479, 2020a.
- Chenyu Zhang, Rungang Han, Anru R Zhang, and Paul M Voyles. Denoising atomic resolution 4d scanning transmission electron microscopy data with tensor singular value decomposition. *Ultramicroscopy*, 219:113123, 2020b.
- Xiao Zhang, Lingxiao Wang, and Quanquan Gu. A unified framework for nonconvex low-rank plus sparse matrix recovery. In *International Conference on Artificial Intelligence and Statistics*, pages 1097–1107. PMLR, 2018.
- Hua Zhou, Lexin Li, and Hongtu Zhu. Tensor regression with applications in neuroimaging data analysis. *Journal of the American Statistical Association*, 108(502):540–552, 2013.
- Pan Zhou and Jiashi Feng. Outlier-robust tensor pca. In *Proceedings of the IEEE Conference on Computer Vision and Pattern Recognition*, pages 2263–2271, 2017.

SUPPLEMENTARY MATERIAL for “Generalized Low-rank plus Sparse
Tensor Estimation by Fast Riemannian Optimization”

9 Higher Order Orthogonal Iteration Algorithm

The HOOI algorithm is summarized as follows which is applied for the initialization in Section 5.1 and 5.2.

Algorithm 6 HOOI

Input: $\mathcal{Y} \in \mathbb{R}^{d_1 \times \dots \times d_m}$, $\mathbf{r} = (r_1, \dots, r_m)$, maximum number of iteration: t_{\max} .

Let $t = 0$, initiate $\hat{\mathbf{U}}_i^0 = \text{SVD}_{r_i}(\mathcal{M}_i(\mathcal{Y}))$, $i \in [m]$.

for $t = 1, \dots, t_{\max}$ **do**

for $i = 1, \dots, m$ **do**

$$\hat{\mathbf{U}}_i^t = \text{SVD}_{r_i}(\mathcal{M}_i(\mathcal{Y})(\hat{\mathbf{U}}_m^{t-1} \otimes \dots \otimes \hat{\mathbf{U}}_{i+1}^{t-1} \otimes \hat{\mathbf{U}}_{i-1}^t \otimes \dots \otimes \hat{\mathbf{U}}_1^{t-1}))$$

end for

end for

Output: $\hat{\mathbf{U}}_i = \hat{\mathbf{U}}_i^{t_{\max}}$, $\hat{\mathcal{T}} = \mathcal{Y} \times_{i=1}^m \hat{\mathbf{U}}_i \hat{\mathbf{U}}_i^T$.

10 More Numerical Simulations

In Section 10.1, we apply the proposed BIC-type criterion for SG-RPCA and binary tensor learning and demonstrate its effectiveness on synthetic data. Through Section 10.2-10.5, we treat \mathbf{r} and α as given and test the performance of our estimator with respect to different choices of γ . Other algorithmic parameters like μ_1 and k_{pr} are decided as explained in Section 7.

10.1 Performance of BIC-type Criterion

We test the performance of BIC-type criterion (3.3) for SG-RPCA and binary tensor learning. As explained in Section 7, γ is set to 1 and $\mu_1 = 2^m + \log(\bar{d})$. More exactly, the BIC-type criterion for SG-RPCA (assuming Gaussian noise with equal but unknown variances) is

$$\text{BIC}(\mathbf{r}, \alpha) := (\|\hat{\mathcal{S}}_{\mathbf{r}, \alpha}\|_{\ell_0} + \sum_{i=1}^m r_i d_i) \cdot \log(d^*) + d^* \log(\|\mathcal{A} - \hat{\mathcal{T}}_{\mathbf{r}, \alpha} - \hat{\mathcal{S}}_{\mathbf{r}, \alpha}\|_{\text{F}}^2).$$

The true tensor $\mathcal{T}^* \in \mathbb{R}^{d \times d \times d}$ with $d = 100$ and $\mathbf{r} = (3, 3, 3)^\top$. We test two true sparsity levels $\alpha \in \{0.05, 0.1\}$. The true tensor \mathcal{T}^* satisfies $\|\mathcal{T}^*\|_{\ell_\infty} = 0.1$, and \mathcal{S}^* is generated as above satisfying $\|\mathcal{S}^*\|_{\ell_\infty} = 4$, and all entries of \mathcal{Z}^* satisfy i.i.d. $N(0, \sigma_z^2)$ with $\sigma_z = 0.01$. For each $\alpha \in \{0.05, 0.1\}$, we test, in our algorithm, $\mathbf{r} \in \{(1, 1, 1), (2, 2, 2), (3, 3, 3), (4, 4, 4), (5, 5, 5)\}$ and $\alpha \in (0.02, 0.2)$. The

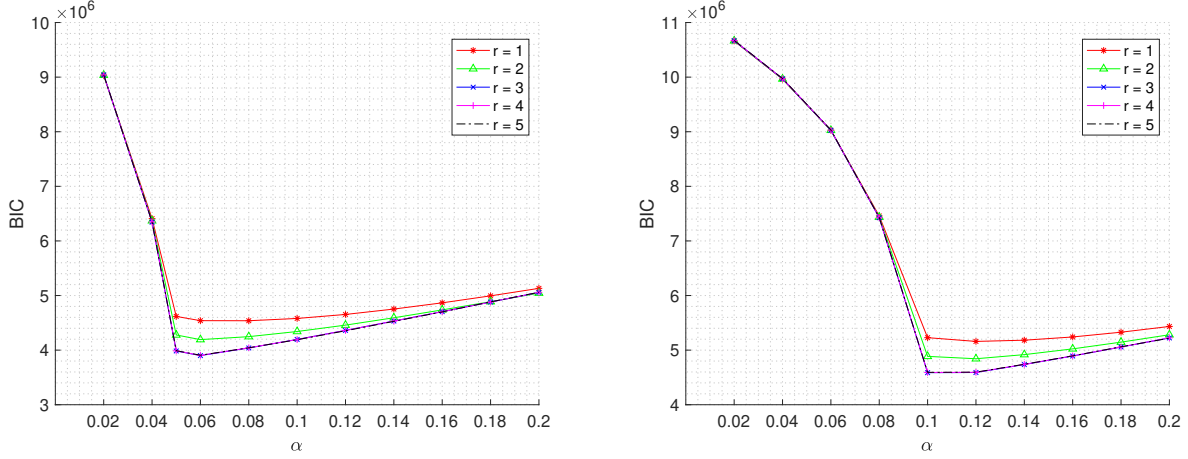


Figure 6: BIC values for SG-RPCA; the true rank $\mathbf{r} = (3, 3, 3)^\top$. Left: true $\alpha = 0.05$; Right: true $\alpha = 0.1$.

results are displayed in Figure 6. The BIC-values are sensitive to both \mathbf{r} and α . We note that the BIC-values for $\mathbf{r} > 3$ are strictly larger than that of $\mathbf{r} = (3, 3, 3)$, but the difference is too small to be spotted in the figures.

For robust binary tensor learning, we also set $\mathbf{r} = (3, 3, 3)^\top$ and $\mathcal{T}^* \in \mathbb{R}^{d \times d \times d}$ with $d = 100$, and \mathcal{S}^* is generated as above. The true $\alpha \in \{0.005, 0.01\}$. We fix $p(x) = (1 + e^{-10x})^{-1}$. The BIC criterion for the binary case is:

$$\text{BIC}(\mathbf{r}, \alpha) := (\|\hat{\mathcal{S}}\|_{\ell_0} + \sum_{i=1}^m r_i d_i) \cdot \log(d^*) - 2 \sum_{\omega} ([\mathcal{A}]_{\omega} \log p([\hat{\mathcal{T}} + \hat{\mathcal{S}}]_{\omega}) + (1 - [\mathcal{A}]_{\omega}) \log(1 - p([\hat{\mathcal{T}} + \hat{\mathcal{S}}]_{\omega}))).$$

For each true $\alpha \in \{0.005, 0.01\}$, we test BIC for $\mathbf{r} \in \{(1, 1, 1), (2, 2, 2), (3, 3, 3), (4, 4, 4), (5, 5, 5)\}$ and α varying from 0.001 to 0.015. The results are displayed in Figure 7 showing that BIC is more sensitive to \mathbf{r} and less sensitive to α for a small range. After the true \mathbf{r} is identified, the BIC criterion works reasonably well for selecting α .

10.2 Tensor Sub-Gaussian Robust PCA

The low-rank tensor $\mathcal{T}^* \in \mathbb{R}^{d \times d \times d}$ with $d = 100$ and Tucker ranks $\mathbf{r} = (2, 2, 2)^\top$ is generated from the HOSVD of a trimmed standard normal tensor. It satisfies the spikiness condition, with high probability, and has singular values $\bar{\lambda} \approx 3$ and $\underline{\lambda} \approx 1$. Given a sparsity level $\alpha \in (0, 1)$, the entries of sparse tensor \mathcal{S}^* are i.i.d. sampled from $\text{Be}(\alpha) \times \mathcal{N}(0, 1)$, which ensures $\mathcal{S}^* \in \mathbb{S}_{O(\alpha)}$ with high probability. This ensures that the non-zero entries of \mathcal{S}^* have typically much larger magnitudes than the entries of \mathcal{T}^* . The noise tensor \mathcal{Z} has i.i.d. entries sampled from $\mathcal{N}(0, \sigma_z^2)$. The default choice of γ is 2, $k_{\text{pr}} = \infty$ and μ_1 is set as previously. The convergence performances of

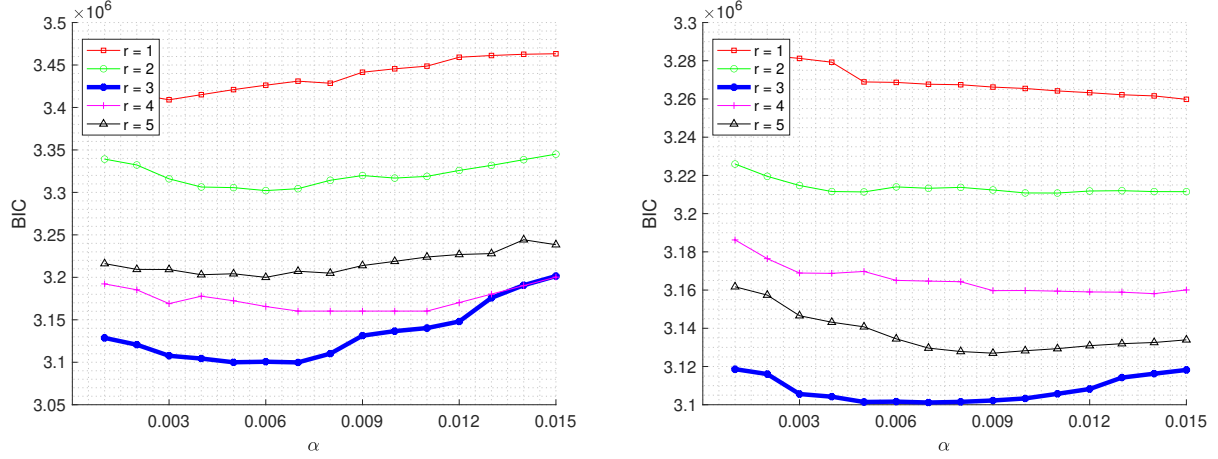


Figure 7: BIC values for binary tensor learning; the true rank $\mathbf{r} = (3, 3, 3)^\top$. Left: true $\alpha = 0.005$; Right: true $\alpha = 0.01$. The BIC curve for $\mathbf{r} = (3, 3, 3)^\top$ is highlighted.

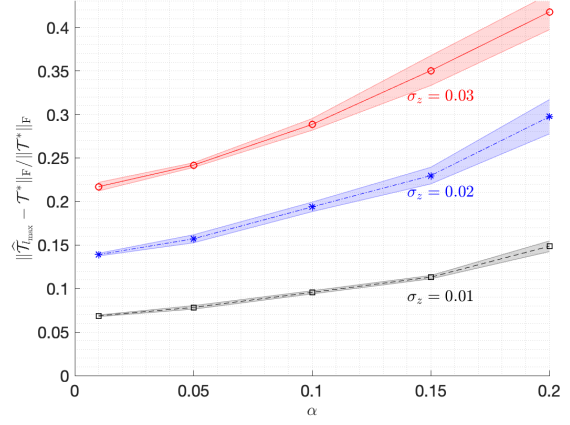
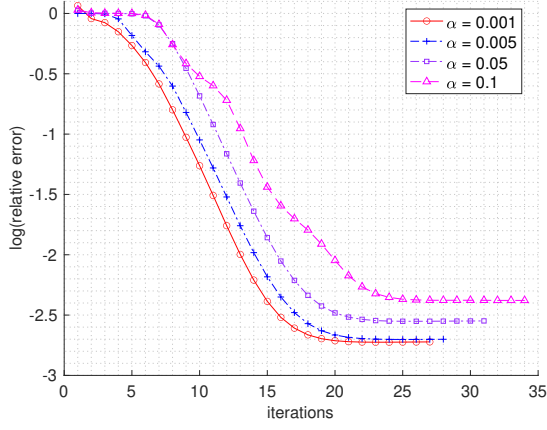
$\log(\|\hat{\mathcal{T}}_l - \mathcal{T}^*\|_F / \|\mathcal{T}^*\|_F)$ by Algorithm 2 are examined and presented in the left panels of Figure 8.

The top-left plot in Figure 8 displays the effects of α on the convergence of Algorithm 2. It shows that the convergence speed of Algorithm 2 is insensitive to α , while the error of final estimates $\hat{\mathcal{T}}_{l_{\max}}$ is related to α . This is consistent with the claims of Theorem 5.1. In the middle-left plot of Figure 8, we observe that, for a fixed sparsity level α , the error of final estimates grows as the tuning parameter γ becomes larger. The bottom-left plot of Figure 8 shows the convergence of Algorithm 2 for different noise levels. All these plots confirm the fast convergence of our Riemannian gradient descent algorithm. In particular, there are stages during which the log relative error decreases linearly w.r.t. the number of iterations, as proved in Theorem 4.1.

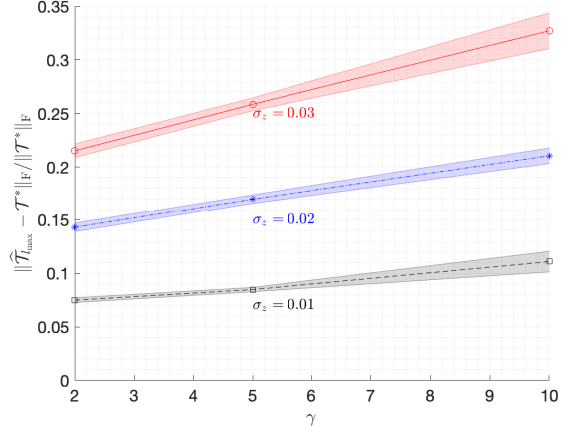
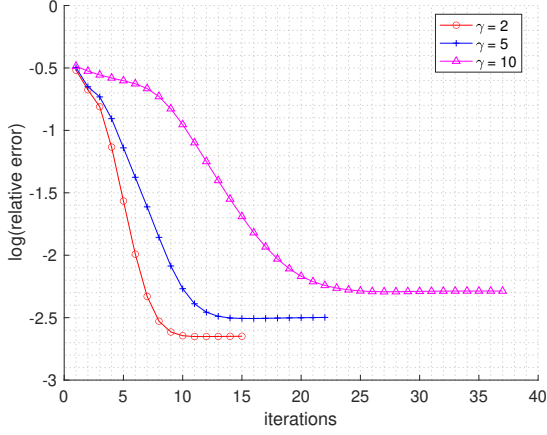
The statistical stability of the final estimates by Algorithm 2 is demonstrated in the right panels of Figure 8. Each curve represents the average relative error of $\hat{\mathcal{T}}_{l_{\max}}$ based on 10 simulations, and the error bar shows the confidence region by one empirical standard deviation. Based on these plots, we observe that the standard deviations of $\|\hat{\mathcal{T}}_{l_{\max}} - \mathcal{T}^*\|_F$ grow as the noise level σ_z , the sparsity level α or the tuning parameter γ increases.

10.3 Tensor PCA with Heavy-tailed Noise

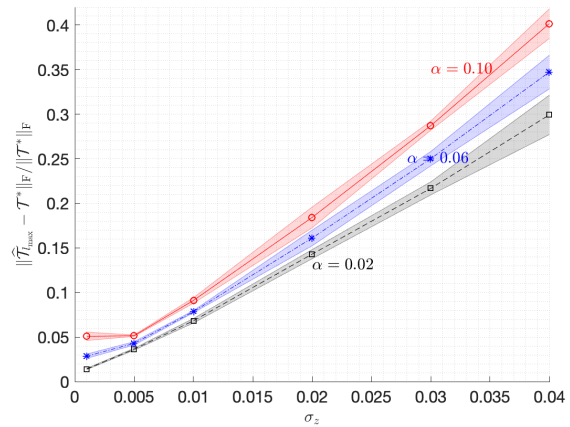
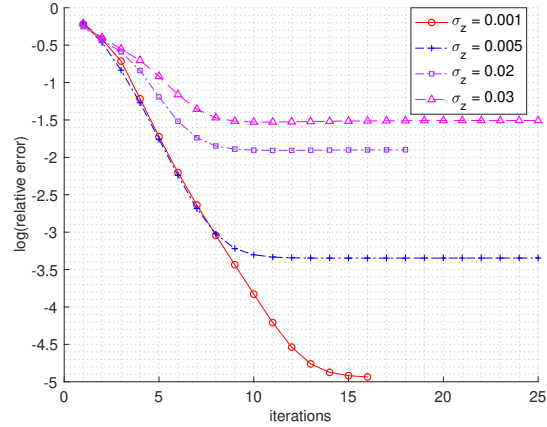
The low-rank tensor $\mathcal{T}^* \in \mathbb{R}^{d \times d \times d}$ with $d = 100$ and Tucker ranks $\mathbf{r} = (2, 2, 2)^\top$ is generated from the HOSVD of a trimmed standard normal tensor, as in Section 10.2. Given a parameter θ , we generate the noisy tensor whose entries are i.i.d. and satisfy the Student-t distribution with degree of freedom θ . But notice here we also apply a global scaling to better control the noise standard deviation. We denote the noisy tensor after scaling by \mathcal{Z} . This generated tensor \mathcal{Z} satisfies



(a) Change of sparsity α . Left: $\sigma_z = 0.01, \gamma = 2$; Right: $\gamma = 2$



(b) Change of γ . Left: $\alpha = 0.02, \sigma_z = 0.01$; Right: $\alpha = 0.02$



(c) Change of noise size σ_z . Left: $\alpha = 0.02, \gamma = 2$; Right: $\gamma = 2$

Figure 8: Performances of Algorithm 2 for SG-RPCA. The low-rank \mathcal{T}^* has size $d \times d \times d$ with $d = 100$ and has Tucker ranks $\mathbf{r} = (2, 2, 2)^\top$. The relative error on left panels is defined by $\|\hat{\mathcal{T}}_l - \mathcal{T}^*\|_F / \|\mathcal{T}^*\|_F$. The error bars on the right panels are based on 1 standard deviation from 10 replications. Here the default γ is 2.

Assumption 4 with the same parameter θ . Once the parameter θ and global scaling are given, we are able to calculate the variance σ_z^2 . The convergence performances of $\log(\|\hat{\mathcal{T}}_l - \mathcal{T}^*\|_F / \|\mathcal{T}^*\|_F)$ by Algorithm 2 are examined and presented in the upper panels of Figure 9.

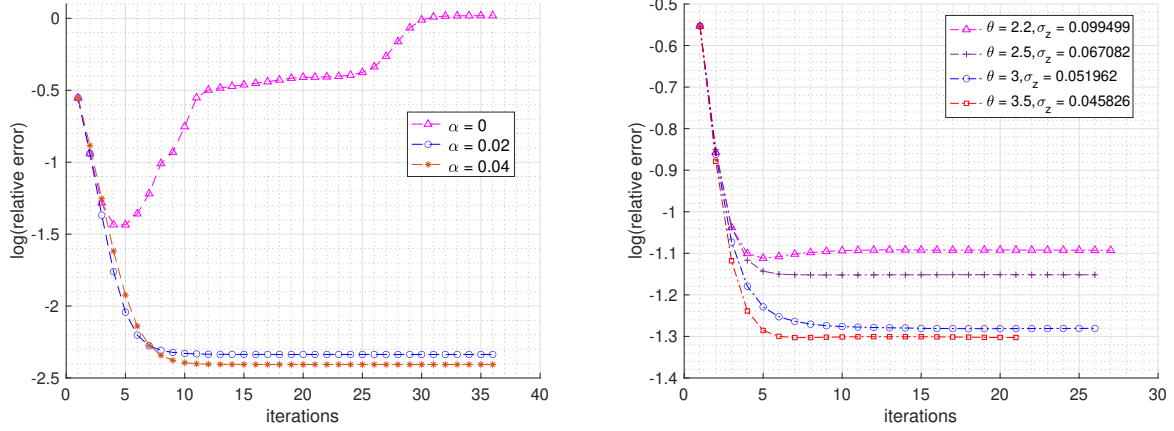
In this experiment, we set $\gamma = 2$, $k_{pr} = \infty$ and μ_1 as previously. The top-left plot in Figure 9 displays the effects of α on the convergence of Algorithm 2. The case $\alpha = 0$ reduces to the normal Riemannian gradient descent, which cannot output a satisfiable result due to the heavy-tailed noise, even if a warm initialization is provided. This shows the importance of gradient pruning in Algorithm 2. When $\alpha > 0$, the convergence speed of the algorithm is insensitive to α , but the final estimates $\hat{\mathcal{T}}_{l_{\max}}$ is related to α . In the top-right plot of Figure 9, we observe the error becomes larger as θ decreases (or equivalently, as σ_z^2 increases). All these results match the claim of Theorem 5.4 and confirm the fast convergence of Riemannian gradient descent. And there are indeed stages where the log relative error decreases linearly w.r.t. the number of iterations.

The statistical stability of the final estimates by Algorithm 2 applied to tensor PCA with heavy-tailed noise is demonstrated in the bottom panel of Figure 9. Each curve represents the average relative error of $\hat{\mathcal{T}}_{l_{\max}}$ based on 5 simulations, and the error bar shows the confidence region by one empirical standard deviation. Based on these plots, we observe that for each fixed θ (or σ_z^2 , equivalently), we need to choose α carefully to achieve the best performance. This is reasonable since in the heavy-tail noise setting, we do not know the sparsity of outliers. Also, the figure shows that Algorithm 2 is stable for different α and θ .

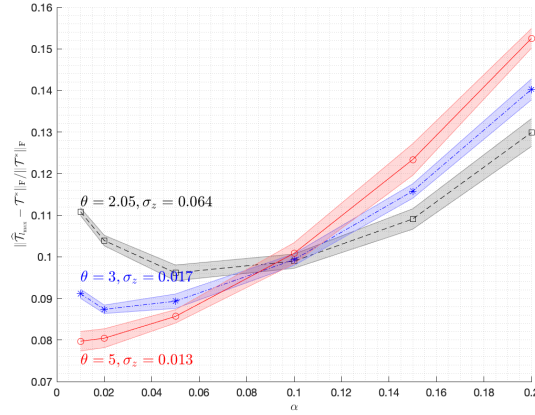
10.4 Binary Tensor Learning

In the binary tensor setting, we generate the low-rank tensor $\mathcal{T}^* \in \mathbb{R}^{d \times d \times d}$ with $d = 100$ and Tucker ranks $\mathbf{r} = (2, 2, 2)^\top$ from the HOSVD of a trimmed standard normal tensor. But here we did a scaling to \mathcal{T}^* so that the singular value $\bar{\lambda} \approx 300$ and $\underline{\lambda} \approx 100$. Given a sparsity level $\alpha \in (0, 1)$, the entries of sparse tensor \mathcal{S}^* are i.i.d. sampled from $\text{Be}(\alpha) \times \text{N}(0, 1)$, which ensures $\mathcal{S}^* \in \mathbb{S}_{O(\alpha)}$ with high probability. We generate the tensor \mathcal{T}^* and \mathcal{S}^* in this way in order to meet the requirements of Assumption 5. In the following experiments, we are considering the logistic link function with the scaling parameter σ , i.e., $p(x) = (1 + e^{-x/\sigma})^{-1}$. The default choice of γ is 1.1, $k_{pr} = 1$ and μ_1 is set as previously. The convergence performances of $\log(\|\hat{\mathcal{T}}_l - \mathcal{T}^*\|_F / \|\mathcal{T}^*\|_F)$ by Algorithm 2 are examined and presented in the top two panels of Figure 10.

The top-left plot in Figure 10 shows the effect of α on the convergence of Algorithm 2. From the figure, it is clear that the error of final estimates $\hat{\mathcal{T}}_{l_{\max}}$ is related to α . This again verifies the results in Theorem 5.7. In the top-right plot in Figure 10, we can see the error of the final estimates increases as the parameter γ becomes larger. All these experiments show that Riemannian gradient descent converges fast and there are stages when the log relative error decreases linearly w.r.t. the



(a) Left: Change of α , $\theta = 2.2(\sigma_z = 0.332)$; Right: Change of θ , $\alpha = 0.01$



(b) Change of θ

Figure 9: Performances of Algorithm 2 for tensor PCA with heavy-tailed noise. The low-rank \mathcal{T}^* has size $d \times d \times d$ with $d = 100$ and has Tucker ranks $\mathbf{r} = (2, 2, 2)^\top$. The relative error on upper panels is defined by $\|\hat{\mathcal{T}}_l - \mathcal{T}^*\|_F / \|\mathcal{T}^*\|_F$. The error bars on the lower panels are based on 1 standard deviation from 5 replications. Here the default choice of γ is 2.

number of iterations.

The statistical stability of the final estimates by Algorithm 2 is demonstrated in the bottom panel of Figure 10. Each curve represents the average relative error of $\hat{\mathcal{T}}_{l_{\max}}$ based on 5 simulations, and the error bar shows the confidence region by one empirical standard deviation. From these plots, we observe that the standard deviations of $\|\hat{\mathcal{T}}_{l_{\max}} - \mathcal{T}^*\|_F$ grow as the noise level, the sparsity level α or the tuning parameter γ increases.

10.5 Tensor Poisson Robust PCA

In the Poisson tensor RPCA case, we generate $\mathcal{T}^* \in \mathbb{R}^{d \times d \times d}$ with $d = 100$ and Tucker rank $\mathbf{r} = (2, 2, 2)^\top$ such that $\|\mathcal{T}^*\|_{\ell_\infty} = 0.5$. Meanwhile, the sparse outliers \mathcal{S}^* is generated such that all its entries are i.i.d. sampled from $\text{Be}(\alpha) \times \text{N}(0, 1)$ and scaled such that $\|\mathcal{S}^*\|_{\ell_\infty} = 0.5$. Throughout the experiments, both ζ and k_{pr} is set to 0.5, and the default choice of γ is 1.1.

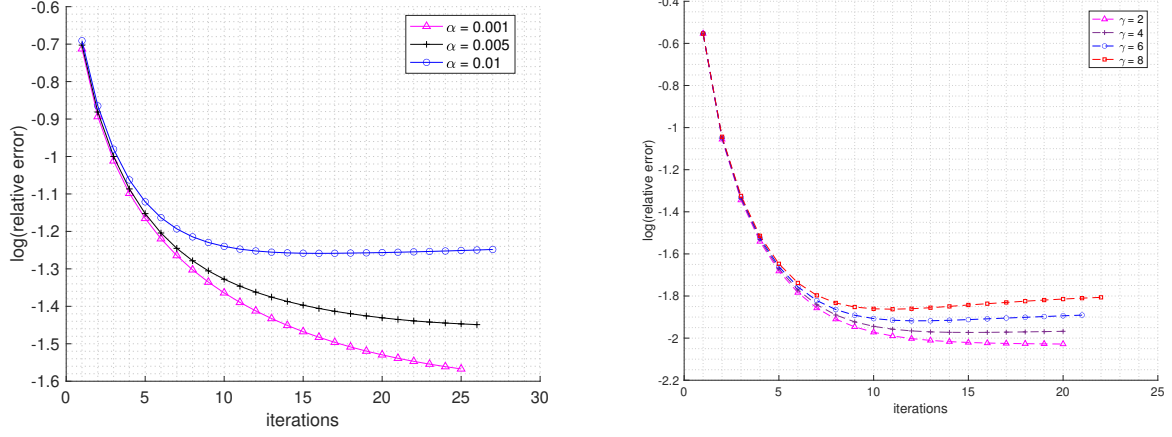
In the first experiment, we fix the intensity $I = 10$ and change the sparsity level. The convergence performances of $\log(\|\hat{\mathcal{T}}_l - \mathcal{T}^*\|_F / \|\mathcal{T}^*\|_F)$ by Algorithm 2 is displayed in the left panel of Figure 11. In the second experiment, for different values of α and I , we conduct 5 i.i.d. instances and plot the error bar. The results are displayed in the right panel of Figure 11.

11 Real Data: Statisticians Hypergraph Co-authorship Network

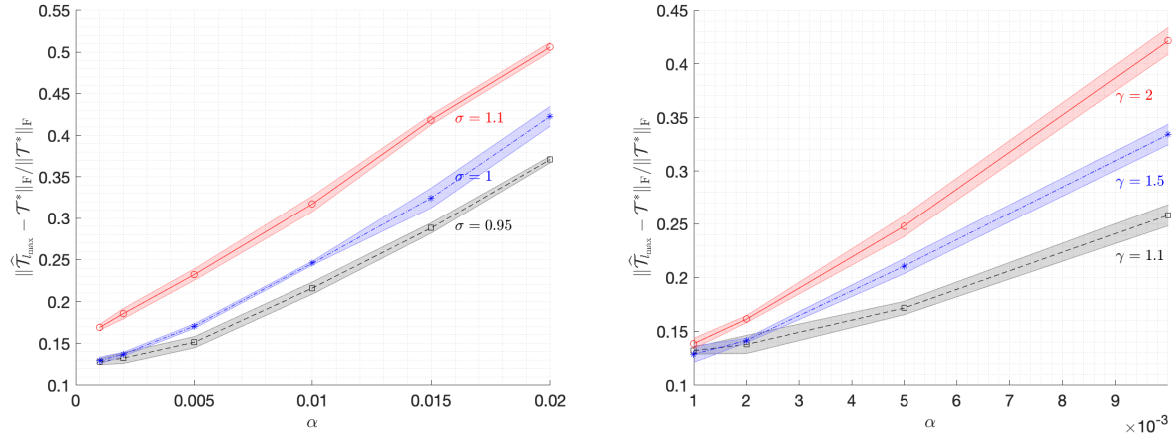
This dataset (Ji and Jin, 2016) contains the co-authorship relations of 3607 statisticians based on 3248 papers published in four prestigious statistics journals during 2003-2012. The co-authorship network thus has 3607 nodes and two nodes are connected by an edge if they collaborated on at least one paper. A giant connected component of this network consisting of 236 nodes is seen to be the ‘‘High-Dimensional Data Analysis’’ community. They also carried out community detection analysis to discover substructures in this giant component. See more details in (Ji and Jin, 2016).

We analyze the substructures of the giant component by treating it as a hypergraph co-authorship network. These 236 statisticians co-authored 542 papers⁵, among which 356 papers have two co-authors, 162 papers have three co-authors and 24 papers have four co-authors. A 3-uniform hypergraph co-authorship network is constructed by, for $i \neq j \neq k$, adding the hyperedge (i, j, k) if the authors i, j, k co-authored at least one paper, and adding the hyperedges (i, i, j) and (i, j, j) if the authors i, j co-authored at least one paper. The hyperedges are *undirected* resulting into a symmetric adjacency tensor \mathcal{A} . We adopt the framework from Section 5.1 to learn the latent low-rank tensor $\hat{\mathcal{T}}$ in \mathcal{A} , which is used to detect communities in the giant component. We

⁵There are 328 single-authored papers. They provide no information to co-authorship relations, and are left out in our analysis.



(a) Left: Change of sparsity α , $\sigma = 1, \gamma = 1.1$; Right: Change of γ , $\alpha = 0.001, \sigma = 1$



(b) Left: Change of σ , $\gamma = 1.1$; Right: Change of γ , $\alpha = 0.001$

Figure 10: Performances of Algorithm 2 for binary tensor learning. The low-rank \mathcal{T}^* has size $d \times d \times d$ with $d = 100$ and has Tucker ranks $\mathbf{r} = (2, 2, 2)^\top$. The relative error on left panels is defined by $\|\hat{\mathcal{T}}_l - \mathcal{T}^*\|_F / \|\mathcal{T}^*\|_F$. The error bars on the bottom panels are based on 1 standard deviation from 5 replications. The default choice of γ is 1.1.

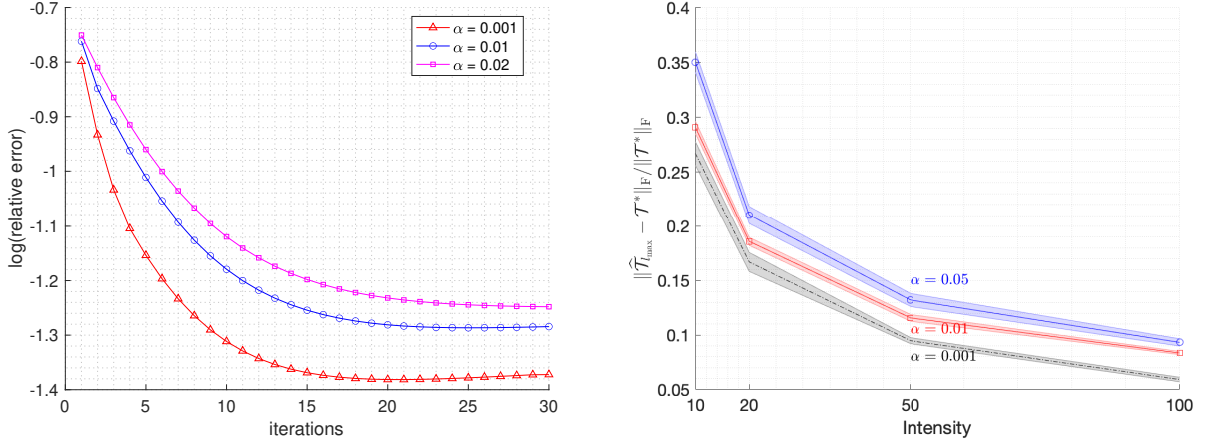
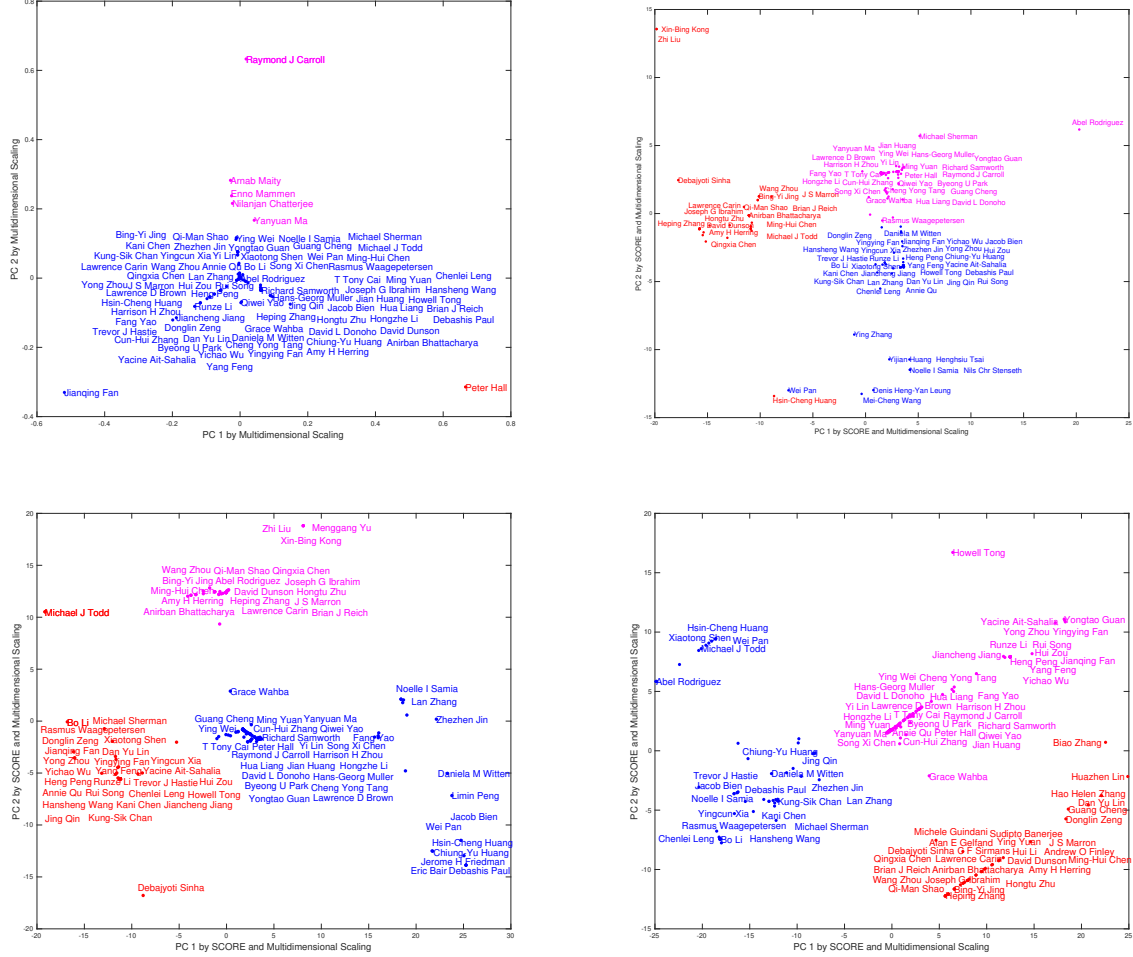


Figure 11: Performance of Algorithm 2 for tensor Poisson RPCA. The Tucker rank of \mathcal{T}^* is $\mathbf{r} = (2, 2, 2)^\top$. Left: Convergence behaviors with different α and I is fixed with $I = 10$; Right: Error bar with each setting repeated 5 i.i.d. times. Here $\gamma = 1.1$ and $k_{\text{pr}} = 0.5$.

emphasize that our primary goal is to present the new findings by taking into consideration of higher-order interactions among co-authors and applying novel robust tensor methods. It is not our intention to label an author with a certain community.

The Tucker ranks are set as $(4, 4, 4)$ and sparsity ratio α is varied at $\{0, 10^{-4}, 5 \times 10^{-4}\}$. The number of communities is set at $K = 3$ and the algorithm is initialized by the HOSVD of \mathcal{A} . To uncover community structures, we apply spectral clustering to the singular vectors of $\hat{\mathcal{T}}$. The node degrees are severely heterogeneous with Peter Hall, Jianqing Fan and Raymond Carroll being the top-3 statisticians in terms of $\#$ of co-authors. The naive spectral clustering often performs poorly in the existence of heterogeneity, skewing to the high-degree nodes. Indeed, the top-left plot in Figure 12 shows that the naive spectral clustering identifies these three statisticians as the corners in a triangle, and puts Peter Hall in a single community. To mitigate the influence of node heterogeneity, we apply SCORE (Jin, 2015) for community detection, which uses the leading singular vector of $\hat{\mathcal{T}}$ as normalization.

The community structures found by SCORE are displayed in Figure 12. The top-right plot shows the three clusters identified by SCORE when the sparsity ratio is zero. The three communities are: 1). “North Carolina” group including researchers from Duke University, University of North Carolina and North Carolina State University, together with their close collaborators such as Debajyoti Sinha, Qi-Man Shao, Bing-Yi Jing, Michael J Todd and etc.; 2). “Carroll-Hall” group including researchers in non-parametric and semi-parametric statistics, functional estimation and



(a) Top-left: $\alpha = 10^{-4}$ and naive spectral clustering; top-right: $\alpha = 0$ and SCORE; bottom-left: $\alpha = 10^{-4}$ and SCORE; bottom-right: $\alpha = 5 \times 10^{-4}$ and SCORE.

Figure 12: Sub-structures detected in the “High-Dimensional Data Analysis” community based on the hypergraph co-authorship network. The Tucker ranks are set as $(4, 4, 4)$ with varied sparsity ratio at $\{0, 10^{-4}, 5 \times 10^{-4}\}$ and the algorithm is initialized by the HOSVD of adjacency tensor \mathcal{A} .

high-dimensional statistics, together with collaborators; 3). “Fan and Others” group⁶ including *primarily* the researchers collaborating closely with Jianqing Fan or his co-authors, and other researchers who do not *obviously* belong to the first two groups. We note that the fields of researchers in “Fan and Others” group are quite diverse, some of which overlap with those in “Carroll-Hall” group and “North Carolina” group. However, unlike the results in (Ji and Jin, 2016), the top-right plot in Figure 12 does not cluster the “Fan and Others” group into either the “North Carolina” group or “Carroll-Hall” group.

We then set the sparsity ratio of $\hat{\mathcal{S}}$ by $\alpha = 10^{-4}$. The communities identified by SCORE based on the singular vectors of $\hat{\mathcal{T}}$ are illustrated in the bottom-left plot of Figure 12. Compared with the top-right plot ($\alpha = 0$), the three communities displayed in the bottom-left plot largely remain the same. But the group memberships of some authors do change. Notably, Debajyoti Sinha and Michael J Todd move from the “North Carolina” group to “Fan and Others” group; Abel Rodriguez moves from the “Carroll-Hall” group to “North-Carolina” group; several authors (e.g. Daniela M Witten, Jacob Bien, Pan Wei, Chiung-Yu Huang, Debashis Paul, Zhezhen Jin, Lan Zhang and etc.) move from the “Fan and Others” group to “Carroll-Hall” group; Hsin-Cheng Huang moves from the “North Carolina” group to “Carroll-Hall” group; Rasmus Waggepetersen moves from the “Carroll-Hall” group to “Fan and Others” group. These changes of memberships suggest that these authors may not have strong ties to the “North Carolina”, “Carroll-Hall” group or be the co-authors of Jianqing Fan. It may be more reasonable that these authors constitute a separate group.

This indeed happens when the sparsity ratio α increases to a certain level. The bottom-right plot of Figure 12 shows the clustering result of SCORE when $\alpha = 5 \times 10^{-4}$. Compared with the top-right ($\alpha = 0$) and bottom-left ($\alpha = 10^{-4}$) plots, the community structure has a significant change. Indeed, the “Fan and Others” group now splits into a “Fan” group including Jianqing Fan and his co-authors, and an “Others” group including the researchers who do not have obvious ties with “Fan” group. Moreover, the “Fan” group merges into the “Carroll-Hall” group, which coincides with the clustering result of SCORE when applied onto the graph co-authorship network (Fig. 6 in (Ji and Jin, 2016)). Consequently, we name the three communities in the top-right plot by the “North Carolina”, “Carroll-Fan-Hall” and “Others” group. Interestingly, many of the authors in the “Others” group are those whose memberships change when the sparsity ratio α increases from 0 to 10^{-4} . See the top-right and bottom-left plots of Figure 12. In addition, we observe that, as α increases from 10^{-4} to 5×10^{-4} , Donglin Zeng and Dan Yu Lin in the “Fan and Others” group moves to “North Carolina” group. This might be more reasonable since they both work at the

⁶We name it the “Fan and Others” group simply because many researchers in this group are the co-authors of Jianqing Fan. It is not our intention to rank/label the authors.

12 Proofs of theorems

12.1 Proof of Theorem 4.1

We prove the theorem by induction on $\|\widehat{\mathcal{T}}_l - \mathcal{T}^*\|_F$ and $\|\widehat{\mathcal{S}}_l - \mathcal{S}^*\|_F$ alternatively. From the initialization condition we have $\|\widehat{\mathcal{T}}_0 - \mathcal{T}^*\|_F \leq c_{1,m} \min\{\frac{\delta^2}{\sqrt{\bar{r}}}, (\kappa_0^{2m} \sqrt{\bar{r}})^{-1}\} \cdot \underline{\lambda}$ and $\widehat{\mathcal{T}}_0 \in \mathbb{B}_\infty^*$ is $(2\mu_1 \kappa_0)^2$ -incoherent.

Step 1: Bounding $\|\widehat{\mathcal{S}}_l - \mathcal{S}^*\|_F$ for all $l \geq 0$. Suppose we have $\widehat{\mathcal{T}}_l \in \mathbb{B}_\infty^*$ is $(2\mu_1 \kappa_0)^2$ -incoherent and $\|\widehat{\mathcal{T}}_l - \mathcal{T}^*\|_F \leq c_{1,m} \min\{\frac{\delta^2}{\sqrt{\bar{r}}}, (\kappa_0^{2m} \sqrt{\bar{r}})^{-1}\} \cdot \underline{\lambda}$.

Now we estimate $\|\widehat{\mathcal{S}}_l - \mathcal{S}^*\|_F$. Denote $\Omega_l = \text{supp}(\widehat{\mathcal{S}}_l)$ and $\Omega^* = \text{supp}(\mathcal{S}^*)$. For $\forall \omega \in \Omega_l$, from the construction of $\widehat{\mathcal{S}}_l$ in Algorithm 1, we have by the definition of Err_∞ ,

$$|[\nabla \mathcal{L}(\widehat{\mathcal{T}}_l + \widehat{\mathcal{S}}_l)]_\omega| \leq \min_{\|\mathcal{X}\|_{\ell_\infty} \leq k_{\text{pr}}} \|\nabla \mathcal{L}(\mathcal{X})\|_{\ell_\infty} \leq \text{Err}_\infty \quad (12.1)$$

From Assumption 3, we get

$$|[\nabla \mathcal{L}(\widehat{\mathcal{T}}_l + \widehat{\mathcal{S}}_l)]_\omega - [\nabla \mathcal{L}(\widehat{\mathcal{T}}_l + \mathcal{S}^*)]_\omega| \geq b_l |[\widehat{\mathcal{S}}_l - \mathcal{S}^*]_\omega|. \quad (12.2)$$

Note that to use (12.2), we shall verify the neighborhood condition. From the upper bound of $\|\widehat{\mathcal{T}}_l - \mathcal{T}^*\|_F$ we have $\|\widehat{\mathcal{T}}_l - \mathcal{T}^*\|_F \leq \underline{\lambda}/8$, and $\widehat{\mathcal{T}}_l$ is $(2\mu_1 \kappa_0)^2$ -incoherent. Therefore, from Lemma 13.7, we have:

$$|[\widehat{\mathcal{T}}_l - \mathcal{T}^*]_\omega|^2 \leq C_{1,m} \bar{r}^m \underline{d}^{-(m-1)} (\mu_1 \kappa_0)^{4m} \|\widehat{\mathcal{T}}_l - \mathcal{T}^*\|_F^2.$$

So we have

$$|[\widehat{\mathcal{T}}_l - \mathcal{T}^*]_\omega| \leq C_{1,m} \sqrt{\frac{\bar{r}^m}{\underline{d}^{m-1}}} (\mu_1 \kappa_0)^{2m} \|\widehat{\mathcal{T}}_l - \mathcal{T}^*\|_F \leq C_{1,m} \mu_1^{2m} \sqrt{\frac{\bar{r}^{m-1}}{\underline{d}^{m-1}}} \underline{\lambda},$$

where the last inequality is from the upper bound of $\|\widehat{\mathcal{T}}_l - \mathcal{T}^*\|_F$. As a result, we have

$$|[\widehat{\mathcal{T}}_l + \widehat{\mathcal{S}}_l - \mathcal{T}^* - \mathcal{S}^*]_\omega| \leq |[\widehat{\mathcal{T}}_l - \mathcal{T}^*]_\omega| + |[\widehat{\mathcal{S}}_l]_\omega| + |[\mathcal{S}^*]_\omega| \leq C_{1,m} \mu_1^{2m} \sqrt{\frac{\bar{r}^{m-1}}{\underline{d}^{m-1}}} \underline{\lambda} + k_{\text{pr}} + \|\mathcal{S}^*\|_{\ell_\infty}.$$

Thus, both $\widehat{\mathcal{T}}_l + \widehat{\mathcal{S}}_l$ and $\widehat{\mathcal{T}}_l + \mathcal{S}^*$ belong to the ball \mathbb{B}_∞^* and thus (12.2) holds.

As a result of (12.1) and (12.2), we get for any $\omega \in \Omega_l$

$$b_l |[\widehat{\mathcal{S}}_l - \mathcal{S}^*]_\omega| \leq |[\nabla \mathcal{L}(\widehat{\mathcal{T}}_l + \mathcal{S}^*)]_\omega| + \text{Err}_\infty.$$

Therefore,

$$\begin{aligned}
\|\mathcal{P}_{\Omega_l}(\widehat{\mathcal{S}}_l - \mathcal{S}^*)\|_{\mathbb{F}}^2 &\leq \frac{2}{b_l^2} \|\mathcal{P}_{\Omega_l}(\nabla \mathcal{L}(\widehat{\mathcal{T}}_l + \mathcal{S}^*))\|_{\mathbb{F}}^2 + \frac{2|\Omega_l|}{b_l^2} \text{Err}_{\infty}^2 \\
&= \frac{2}{b_l^2} \|\mathcal{P}_{\Omega_l}(\nabla \mathcal{L}(\widehat{\mathcal{T}}_l + \mathcal{S}^*)) - \mathcal{P}_{\Omega_l}(\nabla \mathcal{L}(\mathcal{T}^* + \mathcal{S}^*)) + \mathcal{P}_{\Omega_l}(\nabla \mathcal{L}(\mathcal{T}^* + \mathcal{S}^*))\|_{\mathbb{F}}^2 + \frac{2|\Omega_l|}{b_l^2} \text{Err}_{\infty}^2 \\
&\leq \frac{4}{b_l^2} \|\mathcal{P}_{\Omega_l}(\nabla \mathcal{L}(\widehat{\mathcal{T}}_l + \mathcal{S}^*)) - \mathcal{P}_{\Omega_l}(\nabla \mathcal{L}(\mathcal{T}^* + \mathcal{S}^*))\|_{\mathbb{F}}^2 + \frac{4}{b_l^2} \|\mathcal{P}_{\Omega_l}(\nabla \mathcal{L}(\mathcal{T}^* + \mathcal{S}^*))\|_{\mathbb{F}}^2 + \frac{2|\Omega_l|}{b_l^2} \text{Err}_{\infty}^2 \\
&\leq \frac{4b_u^2}{b_l^2} \|\mathcal{P}_{\Omega_l}(\widehat{\mathcal{T}}_l - \mathcal{T}^*)\|_{\mathbb{F}}^2 + \frac{6|\Omega_l|}{b_l^2} \text{Err}_{\infty}^2,
\end{aligned} \tag{12.3}$$

where the last inequality is due to $\|\mathcal{P}_{\Omega_l}(\nabla \mathcal{L}(\mathcal{T}^* + \mathcal{S}^*))\|_{\mathbb{F}}^2 \leq |\Omega_l| \text{Err}_{\infty}^2$ and Assumption 3 since $\widehat{\mathcal{T}}_l + \mathcal{S}^* \in \mathbb{B}_{\infty}^*$.

From (12.3), Lemma 13.8, we have

$$\|\mathcal{P}_{\Omega_l}(\widehat{\mathcal{S}}_l - \mathcal{S}^*)\|_{\mathbb{F}}^2 \leq \frac{C_{2,m} b_u^2}{b_l^2} (\mu_1 \kappa_0)^{4m} \bar{r}^m \alpha \|\widehat{\mathcal{T}}_l - \mathcal{T}^*\|_{\mathbb{F}}^2 + \frac{6|\Omega_l|}{b_l^2} \text{Err}_{\infty}^2 \tag{12.4}$$

here $C_{2,m} > 0$ is an absolute constant depending only on m .

For $\forall \omega = (\omega_1, \dots, \omega_m) \in \Omega^* \setminus \Omega_l$, we have $|\widehat{\mathcal{S}}_l - \mathcal{S}^*|_{\omega} = |\mathcal{S}^*|_{\omega}$. Since the loss function is entry-wise by Assumption 3, we have $[\nabla \mathcal{L}(\widehat{\mathcal{T}}_l)]_{\omega} = [\nabla \mathcal{L}(\widehat{\mathcal{T}}_l + \widehat{\mathcal{S}}_l)]_{\omega}$. Clearly, $\widehat{\mathcal{T}}_l$ and $\widehat{\mathcal{T}}_l + \mathcal{S}^*$ both belong to \mathbb{B}_{∞}^* , by Assumption 3 we get

$$|[\nabla \mathcal{L}(\widehat{\mathcal{T}}_l)]_{\omega} - [\nabla \mathcal{L}(\widehat{\mathcal{T}}_l + \mathcal{S}^*)]_{\omega}| \geq b_l |\mathcal{S}^*|_{\omega}.$$

Now we bound $|\widehat{\mathcal{S}}_l - \mathcal{S}^*|_{\omega}$ as follows. For any $\omega \in \Omega^* \setminus \Omega_l$,

$$\begin{aligned}
|\widehat{\mathcal{S}}_l - \mathcal{S}^*|_{\omega} &= |\mathcal{S}^*|_{\omega} \leq \frac{1}{b_l} |[\nabla \mathcal{L}(\widehat{\mathcal{T}}_l)]_{\omega} - [\nabla \mathcal{L}(\widehat{\mathcal{T}}_l + \mathcal{S}^*)]_{\omega}| \\
&\leq \frac{1}{b_l} \left(|[\nabla \mathcal{L}(\widehat{\mathcal{T}}_l)]_{\omega}| + |[\nabla \mathcal{L}(\widehat{\mathcal{T}}_l + \mathcal{S}^*)]_{\omega}| \right) \\
&\leq \frac{1}{b_l} \left(|[\nabla \mathcal{L}(\widehat{\mathcal{T}}_l)]_{\omega}| + |[\nabla \mathcal{L}(\widehat{\mathcal{T}}_l + \mathcal{S}^*) - \nabla \mathcal{L}(\mathcal{T}^* + \mathcal{S}^*)]_{\omega}| + |[\nabla \mathcal{L}(\mathcal{T}^* + \mathcal{S}^*)]_{\omega}| \right) \\
&\leq \frac{1}{b_l} |[\nabla \mathcal{L}(\widehat{\mathcal{T}}_l)]_{\omega}| + \frac{b_u}{b_l} |\widehat{\mathcal{T}}_l - \mathcal{T}^*|_{\omega} + \frac{1}{b_l} \text{Err}_{\infty},
\end{aligned}$$

where the last inequality is again due to Assumption 3 since $\widehat{\mathcal{T}}_l + \mathcal{S}^* \in \mathbb{B}_{\infty}^*$. Therefore we have

$$\|\mathcal{P}_{\Omega^* \setminus \Omega_l}(\widehat{\mathcal{S}}_l - \mathcal{S}^*)\|_{\mathbb{F}}^2 \leq \frac{2}{b_l^2} \|\mathcal{P}_{\Omega^* \setminus \Omega_l}(\nabla \mathcal{L}(\widehat{\mathcal{T}}_l))\|_{\mathbb{F}}^2 + \frac{4b_u^2}{b_l^2} \|\mathcal{P}_{\Omega^* \setminus \Omega_l}(\widehat{\mathcal{T}}_l - \mathcal{T}^*)\|_{\mathbb{F}}^2 + \frac{4}{b_l^2} |\Omega^* \setminus \Omega_l| \text{Err}_{\infty}^2 \tag{12.5}$$

Since $\omega \in \Omega^* \setminus \Omega_l$, we have

$$|[\nabla \mathcal{L}(\widehat{\mathcal{T}}_l)]_{\omega}| \leq \max_{i=1}^m |\mathbf{e}_{\omega_i}^{\top} \mathcal{M}_i(\nabla \mathcal{L}(\widehat{\mathcal{T}}_l))|^{(\gamma \alpha d_i^-)} \tag{12.6}$$

Now since we have $\mathcal{S}^* \in \mathbb{S}_\alpha$, we have

$$\begin{aligned} |[\nabla \mathcal{L}(\widehat{\mathcal{T}}_l)]_\omega| &\leq \max_{i=1}^m |\mathbf{e}_{\omega_i}^T \mathcal{M}_i(\nabla \mathcal{L}(\widehat{\mathcal{T}}_l + \mathcal{S}^*))|^{((\gamma-1)\alpha d_i^-)} \\ &\leq \max_{i=1}^m \left| \mathbf{e}_{\omega_i}^\top \left(\mathcal{M}_i(\nabla \mathcal{L}(\widehat{\mathcal{T}}_l + \mathcal{S}^*)) - \mathcal{M}_i(\nabla \mathcal{L}(\mathcal{T}^* + \mathcal{S}^*)) \right) \right|^{((\gamma-1)\alpha d_i^-)} + \text{Err}_\infty \end{aligned} \quad (12.7)$$

Using AM-GM inequality, we have:

$$\begin{aligned} |[\nabla \mathcal{L}(\widehat{\mathcal{T}}_l)]_\omega|^2 &\leq 2 \max_{i=1}^m \frac{\left\| \mathbf{e}_{\omega_i}^\top \left(\mathcal{M}_i(\nabla \mathcal{L}(\widehat{\mathcal{T}}_l + \mathcal{S}^*)) - \mathcal{M}_i(\nabla \mathcal{L}(\mathcal{T}^* + \mathcal{S}^*)) \right) \right\|_F^2}{(\gamma-1)\alpha d_i^-} + 2\text{Err}_\infty^2 \\ &\leq 2 \sum_{i=1}^m \frac{\left\| \mathbf{e}_{\omega_i}^\top \left(\mathcal{M}_i(\nabla \mathcal{L}(\widehat{\mathcal{T}}_l + \mathcal{S}^*)) - \mathcal{M}_i(\nabla \mathcal{L}(\mathcal{T}^* + \mathcal{S}^*)) \right) \right\|_F^2}{(\gamma-1)\alpha d_i^-} + 2\text{Err}_\infty^2 \end{aligned} \quad (12.8)$$

Now for all fixed $i \in [m]$, for all $\omega_i \in [d_i]$, ω_i appears at most αd_i^- times since $\Omega^* \setminus \Omega_l$ is an α -fraction set. This observation together with (12.8) lead to the following:

$$\begin{aligned} \|\mathcal{P}_{\Omega^* \setminus \Omega_l}(\nabla \mathcal{L}(\widehat{\mathcal{T}}_l))\|_F^2 &\leq 2 \sum_{i=1}^m \frac{\|\nabla \mathcal{L}(\widehat{\mathcal{T}}_l + \mathcal{S}^*) - \nabla \mathcal{L}(\mathcal{T}^* + \mathcal{S}^*)\|_F^2}{\gamma-1} + 2|\Omega^* \setminus \Omega_l| \text{Err}_\infty^2 \\ &\leq \frac{2mb_u^2}{\gamma-1} \|\widehat{\mathcal{T}}_l - \mathcal{T}^*\|_F^2 + 2|\Omega^* \setminus \Omega_l| \text{Err}_\infty^2. \end{aligned} \quad (12.9)$$

Therefore together with (12.5) and (12.9) and Lemma 13.8, we have

$$\|\mathcal{P}_{\Omega^* \setminus \Omega_l}(\widehat{\mathcal{S}}_l - \mathcal{S}^*)\|_F^2 \leq \left(\frac{4mb_u^2}{b_l^2} \frac{1}{\gamma-1} + C_{4,m} \frac{b_u^2}{b_l^2} (\mu_1 \kappa_0)^{4m} \bar{r}^m \alpha \right) \|\widehat{\mathcal{T}}_l - \mathcal{T}^*\|_F^2 + \frac{16}{b_l^2} |\Omega^* \setminus \Omega_l| \text{Err}_\infty^2 \quad (12.10)$$

where $C_{4,m} > 0$ are constants depending only on m . Now we combine (12.4) and (12.10) and we get

$$\|\widehat{\mathcal{S}}_l - \mathcal{S}^*\|_F^2 \leq \left(\frac{4mb_u^2}{b_l^2} \frac{1}{\gamma-1} + C_{5,m} (\mu_1 \kappa_0)^{4m} \bar{r}^m \frac{b_u^2}{b_l^2} \alpha \right) \|\widehat{\mathcal{T}}_l - \mathcal{T}^*\|_F^2 + \frac{C_1}{b_l^2} |\Omega^* \cup \Omega_l| \text{Err}_\infty^2 \quad (12.11)$$

where $C_{5,m} > 0$ depending only on m and $C_1 > 0$ an absolute constant.

Now if we choose $\alpha \leq (C_{5,m} \kappa_0^{4m} \mu_0^{4m} \bar{r}^m \frac{b_u^4}{b_l^4})^{-1}$ and $\gamma-1 \geq 4m \frac{b_u^4}{b_l^4}$ for some sufficient large constants $C_{5,m} > 0$ depending only on m , then we have

$$\|\widehat{\mathcal{S}}_l - \mathcal{S}^*\|_F^2 \leq \frac{b_l^2}{b_u^2} \|\widehat{\mathcal{T}}_l - \mathcal{T}^*\|_F^2 + \frac{C_1}{b_l^2} |\Omega^* \cup \Omega_l| \text{Err}_\infty^2 \quad (12.12)$$

and

$$\|\widehat{\mathcal{S}}_l - \mathcal{S}^*\|_F \leq \frac{b_l}{b_u} \|\widehat{\mathcal{T}}_l - \mathcal{T}^*\|_F + \frac{C_1}{b_l} \sqrt{|\Omega^* \cup \Omega_l|} \text{Err}_\infty \quad (12.13)$$

In addition, from the upper bound of $\|\mathcal{T}_l - \mathcal{T}^*\|_F$, (12.13) implies that $\|\widehat{\mathcal{S}}_l - \mathcal{S}^*\|_F \leq c_0 \lambda$ for a small $c_0 > 0$. This fact is helpful later since it implies that $\widehat{\mathcal{T}}_l + \widehat{\mathcal{S}}_l$ belongs to the ball \mathbb{B}_2^* and thus activates the conditions in Assumption 2.

Step 2: bounding $\|\widehat{\mathcal{T}}_l - \mathcal{T}^*\|_{\mathbb{F}}^2$ for all $l \geq 1$. From previous step, we have verified

$$\|\widehat{\mathcal{S}}_{l-1} - \mathcal{S}^*\|_{\mathbb{F}} \leq \frac{b_l}{b_u} \|\widehat{\mathcal{T}}_l - \mathcal{T}^*\|_{\mathbb{F}} + \frac{C_1}{b_l} \sqrt{|\Omega^* \cup \Omega_l|} \text{Err}_{\infty} \leq c_0 \underline{\lambda}. \quad (12.14)$$

And from the Algorithm 2, $\widehat{\mathcal{T}}_l = \text{Trim}_{\zeta_l, \mathbf{r}}(\mathcal{W}_{l-1})$. Now from Lemma 13.6, we get,

$$\begin{aligned} \|\widehat{\mathcal{T}}_l - \mathcal{T}^*\|_{\mathbb{F}}^2 &= \|\text{Trim}_{\zeta_l, \mathbf{r}}(\mathcal{W}_{l-1}) - \mathcal{T}^*\|_{\mathbb{F}}^2 \\ &\leq \|\mathcal{W}_{l-1} - \mathcal{T}^*\|_{\mathbb{F}}^2 + C_m \frac{\sqrt{\bar{r}}}{\underline{\lambda}} \|\mathcal{W}_{l-1} - \mathcal{T}^*\|_{\mathbb{F}}^3 \\ &\leq (1 + \frac{\delta}{4}) \|\mathcal{W}_{l-1} - \mathcal{T}^*\|_{\mathbb{F}}^2 \\ &\leq (1 - \delta^2) \|\widehat{\mathcal{T}}_{l-1} - \mathcal{T}^*\|_{\mathbb{F}}^2 + 6\delta^{-1} \text{Err}_{2\mathbf{r}} + C_1 (1 + b_u + b_u^2) b_l^{-2} (|\Omega^*| + \gamma \alpha d^*) \text{Err}_{\infty}^2 \end{aligned} \quad (12.15)$$

Notice to use Lemma 13.6, we need to verify $\|\mathcal{W}_{l-1} - \mathcal{T}^*\|_{\mathbb{F}} \leq \underline{\lambda}/8$, which we will check momentarily. Also, from (12.15) and the signal-to-noise ration condition, we get

$$\|\widehat{\mathcal{T}}_l - \mathcal{T}^*\|_{\mathbb{F}} \leq c_1 \min\{\delta^2 \bar{r}^{-1/2}, \kappa_0^{-2m} \bar{r}^{-1/2}\} \cdot \underline{\lambda}.$$

On the other hand, from lemma 13.6, we have $\widehat{\mathcal{T}}_l$ is $(2\mu_1 \kappa_0)^2$ -incoherent. Further, from Lemma 13.7 and the definition of \mathbf{k}_{∞} we have $\widehat{\mathcal{T}}_l \in \mathbb{B}_{\infty}^*$. This finishes the induction for the error $\|\widehat{\mathcal{T}}_l - \mathcal{T}^*\|_{\mathbb{F}}$. Now the only thing we need to check is the upper bound for $\|\mathcal{W}_{l-1} - \mathcal{T}^*\|_{\mathbb{F}}$.

Step 2.1: bounding $\|\mathcal{W}_{l-1} - \mathcal{T}^*\|_{\mathbb{F}}$. From the Algorithm 2, we have for arbitrary $1 \geq \delta > 0$,

$$\begin{aligned} \|\mathcal{W}_{l-1} - \mathcal{T}^*\|_{\mathbb{F}}^2 &= \|\widehat{\mathcal{T}}_{l-1} - \mathcal{T}^* - \beta \mathcal{P}_{\mathbb{T}_{l-1}}(\mathcal{G}_{l-1} - \mathcal{G}^*) - \beta \mathcal{P}_{\mathbb{T}_{l-1}} \mathcal{G}^*\|_{\mathbb{F}}^2 \\ &\leq (1 + \frac{\delta}{2}) \|\widehat{\mathcal{T}}_{l-1} - \mathcal{T}^* - \beta \mathcal{P}_{\mathbb{T}_{l-1}}(\mathcal{G}_{l-1} - \mathcal{G}^*)\|_{\mathbb{F}}^2 + (1 + \frac{2}{\delta}) \beta^2 \|\mathcal{P}_{\mathbb{T}_{l-1}}(\mathcal{G}^*)\|_{\mathbb{F}}^2 \end{aligned} \quad (12.16)$$

Now we consider the bound for $\|\widehat{\mathcal{T}}_{l-1} - \mathcal{T}^* - \beta \mathcal{P}_{\mathbb{T}_{l-1}}(\mathcal{G}_{l-1} - \mathcal{G}^*)\|_{\mathbb{F}}^2$,

$$\begin{aligned} \|\widehat{\mathcal{T}}_{l-1} - \mathcal{T}^* - \beta \mathcal{P}_{\mathbb{T}_{l-1}}(\mathcal{G}_{l-1} - \mathcal{G}^*)\|_{\mathbb{F}}^2 &= \|\widehat{\mathcal{T}}_{l-1} - \mathcal{T}^*\|_{\mathbb{F}}^2 - 2\beta \langle \widehat{\mathcal{T}}_{l-1} - \mathcal{T}^*, \mathcal{P}_{\mathbb{T}_{l-1}}(\mathcal{G}_{l-1} - \mathcal{G}^*) \rangle \\ &\quad + \beta^2 \|\mathcal{P}_{\mathbb{T}_{l-1}}(\mathcal{G}_{l-1} - \mathcal{G}^*)\|_{\mathbb{F}}^2 \end{aligned} \quad (12.17)$$

The upper bound of $\|\widehat{\mathcal{S}}_{l-1} - \mathcal{S}^*\|_{\mathbb{F}}$ ensures that $\widehat{\mathcal{T}}_{l-1} + \widehat{\mathcal{S}}_{l-1} \in \mathbb{B}_2^*$. Using the smoothness condition in Assumption 2, we get

$$\beta^2 \|\mathcal{P}_{\mathbb{T}_{l-1}}(\mathcal{G}_{l-1} - \mathcal{G}^*)\|_{\mathbb{F}}^2 \leq \beta^2 b_u^2 \|\widehat{\mathcal{T}}_{l-1} + \widehat{\mathcal{S}}_{l-1} - \mathcal{T}^* - \mathcal{S}^*\|_{\mathbb{F}}^2 \quad (12.18)$$

Now we consider the bound for $|\langle \widehat{\mathcal{T}}_{l-1} - \mathcal{T}^*, \mathcal{P}_{\mathbb{T}_{l-1}}(\mathcal{G}_{l-1} - \mathcal{G}^*) \rangle|$. First we have:

$$\langle \widehat{\mathcal{T}}_{l-1} - \mathcal{T}^*, \mathcal{P}_{\mathbb{T}_{l-1}}(\mathcal{G}_{l-1} - \mathcal{G}^*) \rangle = \langle \widehat{\mathcal{T}}_{l-1} - \mathcal{T}^*, \mathcal{G}_{l-1} - \mathcal{G}^* \rangle - \langle \widehat{\mathcal{T}}_{l-1} - \mathcal{T}^*, \mathcal{P}_{\mathbb{T}_{l-1}}^{\perp}(\mathcal{G}_{l-1} - \mathcal{G}^*) \rangle.$$

The estimation of $\langle \widehat{\mathcal{T}}_{l-1} - \mathcal{T}^*, \mathcal{G}_{l-1} - \mathcal{G}^* \rangle$ is as follows:

$$\begin{aligned} \langle \widehat{\mathcal{T}}_{l-1} - \mathcal{T}^*, \mathcal{G}_{l-1} - \mathcal{G}^* \rangle &= \langle \widehat{\mathcal{T}}_{l-1} - \mathcal{T}^* + \widehat{\mathcal{S}}_{l-1} - \mathcal{S}^*, \mathcal{G}_{l-1} - \mathcal{G}^* \rangle - \langle \widehat{\mathcal{S}}_{l-1} - \mathcal{S}^*, \mathcal{G}_{l-1} - \mathcal{G}^* \rangle \\ &\geq b_l \|\widehat{\mathcal{T}}_{l-1} - \mathcal{T}^* + \widehat{\mathcal{S}}_{l-1} - \mathcal{S}^*\|_{\text{F}}^2 - \langle \widehat{\mathcal{S}}_{l-1} - \mathcal{S}^*, \mathcal{G}_{l-1} - \mathcal{G}^* \rangle, \end{aligned} \quad (12.19)$$

where the last inequality follows from Assumption 2. And the estimation of $\langle \widehat{\mathcal{T}}_{l-1} - \mathcal{T}^*, \mathcal{P}_{\mathbb{T}_{l-1}}^\perp(\mathcal{G}_{l-1} - \mathcal{G}^*) \rangle$ is as follows:

$$\begin{aligned} |\langle \widehat{\mathcal{T}}_{l-1} - \mathcal{T}^*, \mathcal{P}_{\mathbb{T}_{l-1}}^\perp(\mathcal{G}_{l-1} - \mathcal{G}^*) \rangle| &\leq \|\mathcal{P}_{\mathbb{T}_{l-1}}^\perp(\widehat{\mathcal{T}}_{l-1} - \mathcal{T}^*)\|_{\text{F}} \|\mathcal{G}_{l-1} - \mathcal{G}^*\|_{\text{F}} \\ &\leq \frac{C_{1,m}b_u}{\lambda} \|\widehat{\mathcal{T}}_{l-1} - \mathcal{T}^*\|_{\text{F}}^2 \|\widehat{\mathcal{T}}_{l-1} - \mathcal{T}^* + \widehat{\mathcal{S}}_{l-1} - \mathcal{S}^*\|_{\text{F}} \end{aligned} \quad (12.20)$$

where the last inequality follows from Lemma 13.1. Together with (12.19) and (12.20), we get,

$$\begin{aligned} \langle \widehat{\mathcal{T}}_{l-1} - \mathcal{T}^*, \mathcal{P}_{\mathbb{T}_{l-1}}(\mathcal{G}_{l-1} - \mathcal{G}^*) \rangle &\geq b_l \|\widehat{\mathcal{T}}_{l-1} - \mathcal{T}^* + \widehat{\mathcal{S}}_{l-1} - \mathcal{S}^*\|_{\text{F}}^2 - \langle \widehat{\mathcal{S}}_{l-1} - \mathcal{S}^*, \mathcal{G}_{l-1} - \mathcal{G}^* \rangle \\ &\quad - \frac{C_{1,m}b_u}{\lambda} \|\widehat{\mathcal{T}}_{l-1} - \mathcal{T}^*\|_{\text{F}}^2 \|\widehat{\mathcal{T}}_{l-1} - \mathcal{T}^* + \widehat{\mathcal{S}}_{l-1} - \mathcal{S}^*\|_{\text{F}} \end{aligned} \quad (12.21)$$

Together with (12.18) and (12.21), we get

$$\begin{aligned} \|\widehat{\mathcal{T}}_{l-1} - \mathcal{T}^* - \beta \mathcal{P}_{\mathbb{T}_{l-1}}(\mathcal{G}_{l-1} - \mathcal{G}^*)\|_{\text{F}}^2 &\leq \left(1 + 2\beta b_u \frac{C_{1,m}}{\lambda} \|\widehat{\mathcal{T}}_{l-1} - \mathcal{T}^* + \widehat{\mathcal{S}}_{l-1} - \mathcal{S}^*\|_{\text{F}}\right) \|\widehat{\mathcal{T}}_{l-1} - \mathcal{T}^*\|_{\text{F}}^2 \\ &\quad + (\beta^2 b_u^2 - 2\beta b_l) \|\widehat{\mathcal{T}}_{l-1} - \mathcal{T}^* + \widehat{\mathcal{S}}_{l-1} - \mathcal{S}^*\|_{\text{F}}^2 \\ &\quad + 2\beta |\langle \widehat{\mathcal{S}}_{l-1} - \mathcal{S}^*, \mathcal{G}_{l-1} - \mathcal{G}^* \rangle| \end{aligned} \quad (12.22)$$

In order to bound (12.22), we derive separately the bound for each terms.

Bounding $\|\widehat{\mathcal{T}}_{l-1} - \mathcal{T}^* + \widehat{\mathcal{S}}_{l-1} - \mathcal{S}^*\|_{\text{F}}^2$. From the bound for $\|\widehat{\mathcal{S}}_{l-1} - \mathcal{S}^*\|_{\text{F}}$ in (12.14), we get,

$$\begin{aligned} \|\widehat{\mathcal{T}}_{l-1} - \mathcal{T}^* + \widehat{\mathcal{S}}_{l-1} - \mathcal{S}^*\|_{\text{F}}^2 &\leq 2\|\widehat{\mathcal{T}}_{l-1} - \mathcal{T}^*\|_{\text{F}}^2 + 2\|\widehat{\mathcal{S}}_{l-1} - \mathcal{S}^*\|_{\text{F}}^2 \\ &\leq 4\|\widehat{\mathcal{T}}_{l-1} - \mathcal{T}^*\|_{\text{F}}^2 + \frac{C_1}{b_l^2} |\Omega^* \cup \Omega_{l-1}| \text{Err}_\infty^2 \end{aligned} \quad (12.23)$$

Thus,

$$\|\widehat{\mathcal{T}}_{l-1} - \mathcal{T}^* + \widehat{\mathcal{S}}_{l-1} - \mathcal{S}^*\|_{\text{F}} \leq 2\|\widehat{\mathcal{T}}_{l-1} - \mathcal{T}^*\|_{\text{F}} + \frac{C_1}{b_l} \sqrt{|\Omega^* \cup \Omega_{l-1}|} \text{Err}_\infty \quad (12.24)$$

Bounding $|\langle \mathcal{G}_{l-1} - \mathcal{G}^*, \widehat{\mathcal{S}}_{l-1} - \mathcal{S}^* \rangle|$. We first bound $\|\mathcal{G}_{l-1} - \mathcal{G}^*\|_{\text{F}}$ by (12.24):

$$\begin{aligned} \|\mathcal{G}_{l-1} - \mathcal{G}^*\|_{\text{F}} &\leq b_u \|\widehat{\mathcal{T}}_{l-1} - \mathcal{T}^* + \widehat{\mathcal{S}}_{l-1} - \mathcal{S}^*\|_{\text{F}} \\ &\leq 2b_u \|\widehat{\mathcal{T}}_{l-1} - \mathcal{T}^*\|_{\text{F}} + \frac{C_1 b_u}{b_l} \sqrt{|\Omega^* \cup \Omega_{l-1}|} \text{Err}_\infty \end{aligned} \quad (12.25)$$

Now we estimate $|\langle \mathcal{G}_{l-1} - \mathcal{G}^*, \widehat{\mathcal{S}}_{l-1} - \mathcal{S}^* \rangle|$ from (12.14) and (12.25) as follows,

$$\begin{aligned} |\langle \mathcal{G}_{l-1} - \mathcal{G}^*, \widehat{\mathcal{S}}_{l-1} - \mathcal{S}^* \rangle| &\leq \|\mathcal{G}_{l-1} - \mathcal{G}^*\|_F \|\widehat{\mathcal{S}}_{l-1} - \mathcal{S}^*\|_F \\ &\leq (0.02b_l + 0.01\beta b_u^2) \|\widehat{\mathcal{T}}_{l-1} - \mathcal{T}^*\|_F^2 + \frac{1}{\beta} \frac{C_1}{b_l^2} |\Omega^* \cup \Omega_{l-1}| \text{Err}_\infty^2 + \frac{C_1 b_u}{b_l^2} |\Omega^* \cup \Omega_{l-1}| \text{Err}_\infty^2 \end{aligned} \quad (12.26)$$

Bounding $|\langle \widehat{\mathcal{T}}_{l-1} - \mathcal{T}^*, \widehat{\mathcal{S}}_{l-1} - \mathcal{S}^* \rangle|$. From (12.14), we have

$$\begin{aligned} |\langle \widehat{\mathcal{T}}_{l-1} - \mathcal{T}^*, \widehat{\mathcal{S}}_{l-1} - \mathcal{S}^* \rangle| &\leq \|\widehat{\mathcal{T}}_{l-1} - \mathcal{T}^*\|_F \|\widehat{\mathcal{S}}_{l-1} - \mathcal{S}^*\|_F \\ &\leq (0.01 \frac{b_l}{b_u} \|\widehat{\mathcal{T}}_{l-1} - \mathcal{T}^*\|_F + \frac{C_1}{b_l} \sqrt{|\Omega^* \cup \Omega_{l-1}|} \text{Err}_\infty) \|\widehat{\mathcal{T}}_{l-1} - \mathcal{T}^*\|_F \\ &\leq 0.02 \|\widehat{\mathcal{T}}_{l-1} - \mathcal{T}^*\|_F^2 + \frac{C_1}{b_l^2} |\Omega^* \cup \Omega_{l-1}| \text{Err}_\infty^2 \end{aligned} \quad (12.27)$$

Now we go back to (12.22) and from (12.23) - (12.27), we get:

$$\begin{aligned} &\|\widehat{\mathcal{T}}_{l-1} - \mathcal{T}^* - \beta \mathcal{P}_{\mathbb{T}_{l-1}}(\mathcal{G}_{l-1} - \mathcal{G}^*)\|_F^2 \\ &\leq (1 - 1.84\beta b_l + 5\beta^2 b_u^2) \|\widehat{\mathcal{T}}_{l-1} - \mathcal{T}^*\|_F^2 + C_1(1 + b_u + b_u^2) b_l^{-2} |\Omega^* \cup \Omega_{l-1}| \text{Err}_\infty^2 \end{aligned} \quad (12.28)$$

where the condition $\underline{\lambda} \geq C_{1,m} \frac{b_u}{b_l} \|\widehat{\mathcal{T}}_{l-1} - \mathcal{T}^*\|_F$ is used in the last step.

By combining (12.17) and (12.28), we get

$$\begin{aligned} \|\mathcal{W}_{l-1} - \mathcal{T}^*\|_F^2 &= \|\widehat{\mathcal{T}}_{l-1} - \mathcal{T}^* - \beta \mathcal{P}_{\mathbb{T}_{l-1}} \mathcal{G}_{l-1}\|_F^2 \\ &\leq (1 + \frac{\delta}{2}) \|\widehat{\mathcal{T}}_{l-1} - \mathcal{T}^* - \beta \mathcal{P}_{\mathbb{T}_{l-1}}(\mathcal{G}_{l-1} - \mathcal{G}^*)\|_F^2 + (1 + \frac{2}{\delta}) \beta^2 \|\mathcal{P}_{\mathbb{T}_{l-1}}(\mathcal{G}^*)\|_F^2 \\ &\leq (1 + \frac{\delta}{2}) (1 - 1.84\beta b_l + 5\beta^2 b_u^2) \|\widehat{\mathcal{T}}_{l-1} - \mathcal{T}^*\|_F^2 + (1 + \frac{2}{\delta}) \beta^2 \text{Err}_{2r}^2 \\ &\quad + C_1 (1 + \beta b_u + \beta^2 b_u^2) b_u^{-2} |\Omega^* \cup \Omega_{l-1}| \text{Err}_\infty^2 \\ &\leq (1 + \frac{\delta}{2}) (1 - 1.84\beta b_l + 5\beta^2 b_u^2) \|\widehat{\mathcal{T}}_{l-1} - \mathcal{T}^*\|_F^2 + (1 + \frac{2}{\delta}) \beta^2 \text{Err}_{2r}^2 \\ &\quad + C_1 (1 + \beta b_u + \beta^2 b_u^2) \frac{1}{b_u^2} (|\Omega^*| + \gamma \alpha d^*) \text{Err}_\infty^2 \end{aligned} \quad (12.29)$$

where in the second inequality we used

$$\|\mathcal{P}_{\mathbb{T}_{l-1}}(\mathcal{G}^*)\|_F = \sup_{\|\mathcal{Y}\|_F=1} \langle \mathcal{P}_{\mathbb{T}_{l-1}}(\mathcal{G}^*), \mathcal{Y} \rangle = \sup_{\|\mathcal{Y}\|_F=1} \langle \mathcal{G}^*, \mathcal{P}_{\mathbb{T}_{l-1}}(\mathcal{Y}) \rangle \leq \text{Err}_{2r} \quad (12.30)$$

since $\mathcal{P}_{\mathbb{T}_{l-1}}(\mathcal{Y}) \in \mathbb{M}_{2r}$ and in the last inequality we use $|\Omega^* \cup \Omega_{l-1}| \leq |\Omega^*| + |\Omega_{l-1}| \leq |\Omega^*| + \gamma \alpha d^*$.

Now we choose proper $\beta \in [0.005b_l/(b_u^2), 0.36b_l/(b_u^2)]$ so $1 - 1.84\beta b_l + 5\beta^2 b_u^2 \leq 1 - \delta$, and we get

$$\|\mathcal{W}_{l-1} - \mathcal{T}^*\|_F \leq (1 - \delta)(1 + \delta/2) \|\widehat{\mathcal{T}}_{l-1} - \mathcal{T}^*\|_F + 3\delta^{-1} \text{Err}_{2r} + C_1(b_u + 1) b_l^{-1} \sqrt{|\Omega^*| + \alpha \gamma d^*} \text{Err}_\infty \quad (12.31)$$

where we use the fact that $\beta \leq 1$. From the signal-to-noise ratio condition, we have $3\delta^{-1} \text{Err}_{2r} + C_1(b_u + 1) b_l^{-1} \sqrt{|\Omega^*| + \alpha \gamma d^*} \text{Err}_\infty \leq \frac{\delta}{4} \frac{\underline{\lambda}}{C_m \sqrt{r}}$. This implies that $\|\mathcal{W}_{l-1} - \mathcal{T}^*\|_F \leq \underline{\lambda}/8$ holds.

12.2 Proof of Theorem 4.3

Let $\widehat{\Omega}$ and Ω^* denote the support of $\widehat{\mathcal{S}}_{l_{\max}}$ and \mathcal{S}^* , respectively. By the proof of Theorem 4.1, we have

$$|[\widehat{\mathcal{S}}_{l_{\max}} - \mathcal{S}^*]_{\omega}| \leq \begin{cases} \frac{b_u}{b_l} |[\widehat{\mathcal{T}}_{l_{\max}} - \mathcal{T}^*]_{\omega}| + \frac{2\text{Err}_{\infty}}{b_l} & , \text{ if } \omega \in \widehat{\Omega} \\ \frac{2b_u}{b_l} \|\widehat{\mathcal{T}}_{l_{\max}} - \mathcal{T}^*\|_{\ell_{\infty}} + \frac{2\text{Err}_{\infty}}{b_l} & , \text{ if } \omega \in \Omega^* \setminus \widehat{\Omega} \end{cases}$$

Therefore, we conclude that

$$\|\widehat{\mathcal{S}}_{l_{\max}} - \mathcal{S}^*\|_{\ell_{\infty}} \leq \frac{2b_u}{b_l} \|\widehat{\mathcal{T}}_{l_{\max}} - \mathcal{T}^*\|_{\ell_{\infty}} + \frac{2\text{Err}_{\infty}}{b_l}. \quad (12.32)$$

Now, we can apply Lemma 13.7 and we obtain

$$\|\widehat{\mathcal{T}}_{l_{\max}} - \mathcal{T}^*\|_{\ell_{\infty}} \leq C_{1,m} \bar{r}^{m/2} \underline{d}^{-(m-1)/2} \mu_1^{2m} \kappa_0^{2m} \|\widehat{\mathcal{T}}_{l_{\max}} - \mathcal{T}^*\|_{\text{F}} \quad (12.33)$$

Now, by putting together (12.32), (12.33) and (4.8), we get

$$\|\widehat{\mathcal{S}}_{l_{\max}} - \mathcal{S}^*\|_{\ell_{\infty}} \leq C_{2,m} \kappa_0^{2m} \mu_1^{2m} \left(\frac{\bar{r}^m}{\underline{d}^{m-1}} \right)^{1/2} \cdot (\text{Err}_{2\mathbf{r}} + (|\Omega^*| + \gamma \alpha d^*)^{1/2} \text{Err}_{\infty}) + \frac{2\text{Err}_{\infty}}{b_l},$$

where $C_{1,m}$ and $C_{2,m}$ are constants depending only on m . Now since we assume $b_l, b_u = O(1)$, we finish the proof of Theorem 4.3.

12.3 Proof of Theorem 5.1

We first estimate the probability of the following two events.

$$\text{Err}_{2\mathbf{r}} \leq C_{0,m} \sigma_z \cdot (\bar{d}\bar{r} + r^*)^{1/2} \quad (12.34)$$

$$\text{Err}_{\infty} \leq C'_{0,m} \sigma_z \log^{1/2} \bar{d} \quad (12.35)$$

for some constants $C_{0,m}, C'_{0,m} > 0$ depending only on m . Notice here the first event (12.34) holds with probability at least $1 - \exp(-c_m \bar{r} \bar{d})$ by Lemma 13.3. And for the second event (12.35), we have from the definition,

$$\text{Err}_{\infty} = \max \left\{ \|\nabla \mathcal{L}(\mathcal{T}^* + \mathcal{S}^*)\|_{\ell_{\infty}}, \min_{\|\mathcal{X}\|_{\ell_{\infty}} \leq \infty} \|\nabla \mathcal{L}(\mathcal{X})\|_{\ell_{\infty}} \right\} = \|\mathcal{Z}\|_{\ell_{\infty}} \quad (12.36)$$

So we have (12.35) holds with probability at least $1 - 0.5\bar{d}^{-2}$ from Lemma 13.4. Taking union bounds and we get both (12.35) and (12.34) hold with probability at least $1 - \bar{d}^{-2}$. And finally applying Theorem 4.1 and Theorem 4.3 gives the desired result.

12.4 Proof of Lemma 5.2

Denote the event $\mathcal{E}_1 = \{\|\mathbf{Z}\|_{\ell_\infty} \leq 2\sqrt{m}\sigma_z\sqrt{\log(\bar{d})}\}$, then from Lemma 13.4, we have \mathcal{E}_1 holds with probability at least $1 - 2(d^*)^{-1}$. Now we set $\tau_l = 2\sqrt{m}\sigma_z\sqrt{\log(\bar{d})} + (d^*)^{-1/2}\mu_1\|\mathbf{T}^*\|_F$, then under \mathcal{E}_1 , we have $\|\mathbf{T}^* + \mathbf{Z}\|_{\ell_\infty} \leq \tau_l$. From the definition of τ_0 , we have $|\tau_0| \leq |\mathbf{T}^* + \mathbf{Z}|^{(\lfloor pd^* - |\Omega^*| \rfloor)} \leq \tau_l$. Denote $\Omega_1 = \{\omega : |\mathcal{A}_\omega| \leq \tau_0\}$. From the definition of \mathcal{A}_0 , we have

$$\begin{aligned}
\|\mathcal{A}_0\|_F^2 &= \sum_{\omega \in \Omega_1} [\mathbf{T}^* + \mathbf{S}^* + \mathbf{Z}]_\omega^2 \\
&\geq \sum_{\omega \in \Omega_1} [\mathbf{T}^* + \mathbf{Z}]_\omega^2 + 2 \sum_{\omega \in \Omega_1 \cap \Omega^*} [\mathbf{S}^*]_\omega [\mathbf{T}^* + \mathbf{Z}]_\omega \\
&\geq \sum_{\omega \in \Omega_1} [\mathbf{T}^* + \mathbf{Z}]_\omega^2 - 4|\Omega^*|\tau_l^2 \\
&= \|\mathbf{T}^* + \mathbf{Z}\|_F^2 - \sum_{\omega \in \Omega_1^c} [\mathbf{T}^* + \mathbf{Z}]_\omega^2 - 4|\Omega^*|\tau_l^2 \\
&\geq \|\mathbf{T}^* + \mathbf{Z}\|_F^2 - (pd^* + 4|\Omega^*|)\tau_l^2,
\end{aligned} \tag{12.37}$$

where the penultimate inequality holds since for all ω , $|\mathbf{T}^* + \mathbf{Z}]_\omega| \leq \tau_l$ and for all $\omega \in \Omega_1$, we have $|\mathbf{S}^*]_\omega| \leq |\mathbf{T}^* + \mathbf{Z}]_\omega| + \tau_0 \leq 2\tau_l$. Now we estimate the lower bound for $\|\mathbf{T}^* + \mathbf{Z}\|_F^2$. Since \mathbf{Z} has i.i.d. subgaussian entries, we have $\|\mathbf{Z}\|_F^2 \geq \frac{1}{2}d^*\sigma_z^2$ with probability at least $1 - 2\exp(-cd^*)$ for some absolute constant $c > 0$, and $2\langle \mathbf{T}^*, \mathbf{Z} \rangle \leq \frac{1}{2}\|\mathbf{T}^*\|_F^2 + 2\sigma_z^2 \log(\bar{d})$ with probability at least $1 - 2(d^*)^{-1}$. Put these altogether, we see

$$\|\mathbf{T}^* + \mathbf{Z}\|_F^2 = \|\mathbf{T}^*\|_F^2 + \|\mathbf{Z}\|_F^2 + 2\langle \mathbf{T}^*, \mathbf{Z} \rangle \geq \frac{1}{2}\|\mathbf{T}^*\|_F^2 + \frac{1}{4}\sigma_z^2 d^*. \tag{12.38}$$

Combine (12.37) and (12.38), we have

$$\|\mathcal{A}_0\|_F^2 \geq \frac{1}{2}\|\mathbf{T}^*\|_F^2 + \frac{1}{4}\sigma_z^2 d^* - (pd^* + 4|\Omega^*|)\tau_l^2. \tag{12.39}$$

Therefore with the choice $\tau = 10\sqrt{m}\sqrt{\log(\bar{d})}\mu_1 \frac{\|\mathcal{A}_0\|_F}{\sqrt{d^*}}$, we see that $\tau \geq \tau_l$ and $\tau_u := 10\sqrt{m}\sqrt{\log(\bar{d})}\mu_1\tau_l \geq \tau$. With such a choice of τ , since for $\omega \in (\Omega^*)^c$, we have $|\mathbf{T}^*]_\omega| + |\mathbf{Z}]_\omega| \leq \tau_l \leq \tau$, so we obtain

$$\begin{aligned}
\tilde{\mathcal{A}} &= \mathcal{P}_{(\Omega^*)^c}(\mathcal{A}) + \mathcal{P}_{\Omega^*}(\tilde{\mathcal{A}}) = \mathcal{P}_{(\Omega^*)^c}(\mathbf{T}^* + \mathbf{Z}) + \mathcal{P}_{\Omega^*}(\text{Trunc}_\tau(\mathcal{A})) \\
&= \mathbf{T}^* + \mathbf{Z} + \mathcal{P}_{\Omega^*}(\text{Trunc}_\tau(\mathcal{A}) - \mathbf{T}^* - \mathbf{Z}) \\
&=: \mathbf{T}^* + \mathbf{Z} + \mathcal{E},
\end{aligned}$$

where $\mathcal{E} = \mathcal{P}_{\Omega^*}(\text{Trunc}_\tau(\mathcal{A}) - \mathbf{T}^* - \mathbf{Z})$ and the first equality holds since for $\omega \in (\Omega^*)^c$, $|\mathcal{A}_\omega| \leq |\mathbf{T}^*]_\omega| + |\mathbf{Z}]_\omega| \leq \tau_u$. Under event \mathcal{E}_1 , we have $\|\mathcal{E}\|_F \leq 2|\Omega^*|^{1/2}\tau_u$.

Now we use bold-face capital letters as shorthand notation for the unfolding of corresponding calligraphic-font bold-face letters, for example, $\mathbf{T}_i^* = \mathcal{M}_i(\mathbf{T}^*)$, $i \in [m]$. We denote $\mathcal{X} = \mathbf{T}^* + \mathcal{E}$.

We also denote \mathbf{U}_i^* be the top r_i left singular vectors of \mathbf{T}_i^* , \mathbf{V}_i be the top r_i left singular vectors of \mathbf{X}_i and $\widehat{\mathbf{U}}_i^0$ be the top r_i left singular vectors of $\widehat{\mathbf{A}}_i$.

From Wedin's $\sin\Theta$ theorem, we have from condition (a),

$$d_c(\mathbf{U}_i^*, \mathbf{V}_i) \leq \frac{C|\Omega^*|^{1/2}\tau_u}{\underline{\lambda}}, \quad (12.40)$$

where $d_c(\mathbf{U}, \mathbf{V}) = \min_{\mathbf{R} \in \mathbb{O}_r} \|\mathbf{UR} - \mathbf{V}\|$. Meanwhile, from $\|\mathbf{X}_i - \mathbf{T}_i^*\|_F = \|\boldsymbol{\mathcal{E}}\|_F \leq |\Omega^*|^{1/2}\tau_u$, we also have $\sigma_{r_i}(\mathbf{X}_i) \geq \frac{3\underline{\lambda}}{4}$, $\sigma_{r_i+1}(\mathbf{X}_i) \leq \frac{\underline{\lambda}}{4}$ and $\|\mathbf{X}_i\| \leq \frac{5\underline{\lambda}}{4}$.

Since subtracting a multiple of identity matrix does not change the top eigenvectors, in order to bound the distance $d_c(\mathbf{V}_i, \widehat{\mathbf{U}}_i^0)$, we consider $\|\widetilde{\mathbf{A}}_i \widetilde{\mathbf{A}}_i^T - \mathbf{X}_i \mathbf{X}_i^T - \sigma_v^2 d_i^- \mathbf{I}_{d_i}\|$, where σ_v^2 is the variance of the entry of \mathbf{Z} and $d_i^- = d^*/d_i$. In fact, we have

$$\widetilde{\mathbf{A}}_i \widetilde{\mathbf{A}}_i^T - \mathbf{X}_i \mathbf{X}_i^T - \sigma_v^2 d_i^- \mathbf{I}_{d_i} = \mathbf{X}_i \mathbf{Z}_i^T + \mathbf{Z}_i \mathbf{X}_i^T + \mathbf{Z}_i \mathbf{Z}_i^T - \sigma_v^2 d_i^- \mathbf{I}_{d_i}.$$

Now we first consider the operator norm of $\mathbf{X}_i \mathbf{Z}_i^T$ under the event \mathcal{E}_1 . From Talagrand's concentration inequality, we have

$$\mathbb{P}\left(\left|\|\mathbf{X}_i \mathbf{Z}_i^T\| - \mathbb{E}\|\mathbf{X}_i \mathbf{Z}_i^T\|\right| \leq C_m \sqrt{\log(\bar{d})} \sigma_z \|\mathbf{X}_i\| \cdot t \middle| \mathcal{E}_1\right) \geq 1 - 2\exp(-ct^2).$$

Since $\mathbb{P}(\mathcal{E}_1) \geq 1/2$ and from (Vershynin, 2011, Theorem 1.1), we have $\mathbb{E}[\|\mathbf{X}_i \mathbf{Z}_i^T\| | \mathcal{E}_1] \leq 2\mathbb{E}\|\mathbf{X}_i \mathbf{Z}_i^T\| \leq C\sqrt{\bar{d}_i} \sigma_z \|\mathbf{X}_i\|$. Therefore setting $t = \sqrt{\log(\bar{d})}$ and the event

$$\mathcal{E}_2^i = \{\|\mathbf{X}_i \mathbf{Z}_i^T\| \leq C_m \sqrt{\bar{d}_i} \|\mathbf{X}_i\| \sigma_z\}, \quad \mathcal{E}_2 = \cap_{i=1}^m \mathcal{E}_2^i,$$

we know that $\mathbb{P}(\mathcal{E}_2 | \mathcal{E}_1) \geq 1 - 2m\bar{d}^{-1}$ and thus $\mathbb{P}(\mathcal{E}_2) \geq (1 - 2m\bar{d}^{-1})(1 - 2(d^*)^{-1})$.

Now we turn to bounding $\|\mathbf{Z}_i \mathbf{Z}_i^T - d_i^- \sigma_z^2 \mathbf{I}_{d_i}\|$. From (Vershynin, 2018, Theorem 4.6.1), we have with probability exceeding $1 - 2\exp(-d_i)$,

$$\|\mathbf{Z}_i \mathbf{Z}_i^T - d_i^- \sigma_z^2 \mathbf{I}_{d_i}\| \leq C(d^*)^{1/2} \sigma_z^2.$$

Denote the event $\mathcal{E}_3^i = \{\|\mathbf{Z}_i \mathbf{Z}_i^T - d_i^- \sigma_z^2 \mathbf{I}_{d_i}\| \leq C(d^*)^{1/2} \sigma_z^2\}$ and $\mathcal{E}_3 = \cap_{i=1}^m \mathcal{E}_3^i$ and we have $\mathbb{P}(\mathcal{E}_3) \geq 1 - 2\sum_{i=1}^m \exp(-d_i)$. Therefore under the event $\mathcal{E}_2, \mathcal{E}_3$, and from condition (b), we have

$$d_c(\mathbf{V}_i, \widehat{\mathbf{U}}_i^0) \leq \frac{C_m \sqrt{\bar{d}} \sigma_z \bar{\lambda} + C(d^*)^{1/2} \sigma_z^2}{\underline{\lambda}^2}.$$

Together with (12.40), we have

$$d_c(\mathbf{U}_i^*, \widehat{\mathbf{U}}_i^0) \leq \frac{C_m \sqrt{\bar{d}} \sigma_z \bar{\lambda} + C(d^*)^{1/2} \sigma_z^2}{\underline{\lambda}^2} + \frac{C|\Omega^*|^{1/2} \tau_u}{\underline{\lambda}}. \quad (12.41)$$

Denote the event

$$\mathcal{E}_4 = \left\{ \max_{i=1}^m \max_{\|\mathbf{V}_j\| \leq 1, j \neq i} \|\mathbf{Z}_i(\mathbf{V}_{i+1} \otimes \cdots \otimes \mathbf{V}_m \otimes \mathbf{V}_1 \otimes \cdots \otimes \mathbf{V}_{i-1})\| \leq C_m(\sqrt{\bar{d}\bar{r}} + \bar{r}^{\frac{m-1}{2}})\sigma_z \right\}.$$

And from (Zhang and Xia, 2018, Lemma 5), we have $\mathbb{P}(\mathcal{E}_4) \geq 1 - Cm \exp(-c\bar{d})$. For the following we denote

$$\begin{aligned} \mathbf{X}_1^t &= \mathbf{T}_1^*(\hat{\mathbf{U}}_2^t \otimes \cdots \otimes \hat{\mathbf{U}}_m^t) = \mathbf{T}_1^*(\mathcal{P}_{\mathbf{U}_2^*} \hat{\mathbf{U}}_2^t \otimes \cdots \otimes \mathcal{P}_{\mathbf{U}_m^*} \hat{\mathbf{U}}_m^t) \\ \mathbf{Z}_1^t &= \mathbf{Z}_1(\hat{\mathbf{U}}_2^t \otimes \cdots \otimes \hat{\mathbf{U}}_m^t) \\ \tilde{\mathbf{A}}_1^t &= \tilde{\mathbf{A}}_1(\hat{\mathbf{U}}_2^t \otimes \cdots \otimes \hat{\mathbf{U}}_m^t), \end{aligned}$$

where $\mathcal{P}_{\mathbf{U}} = \mathbf{U}\mathbf{U}^T$. We shall denote $L_t = \max_{i=1}^m d_c(\hat{\mathbf{U}}_i^t, \mathbf{U}_i^*)$. For the base case, from (12.41) and condition (b), we see $L_0 \leq \frac{1}{2}$. Now suppose we have $L_t \leq \frac{1}{2}$.

From the process of HOOI, we have $\hat{\mathbf{U}}_1^{t+1} = \text{SVD}_{r_1}(\tilde{\mathbf{A}}_1(\hat{\mathbf{U}}_2^t \otimes \cdots \otimes \hat{\mathbf{U}}_m^t))$. And thus we obtain

$$\begin{aligned} \sigma_{r_1}(\mathbf{X}_1^t) &\geq \sigma_{r_1}(\mathbf{U}_2^* \otimes \cdots \otimes \mathbf{U}_m^*) \cdot \prod_{i=2}^m \sigma_{\min}(\mathbf{U}_i^{*T} \hat{\mathbf{U}}_i^t) \\ &\geq \sigma_{r_1}(\mathbf{U}_2^* \otimes \cdots \otimes \mathbf{U}_m^*) (1 - L_t^2)^{(m-1)/2} \\ &\geq c_m (1 - L_t)^2 \underline{\lambda}, \end{aligned} \tag{12.42}$$

for some small constant $c_m > 0$ depending only on m , and the last inequality holds since $1 - L_t^2 \geq \frac{3}{4}$. We bound $\|\mathbf{Z}_1^t\|$ under the event \mathcal{E}_4 .

$$\begin{aligned} \|\mathbf{Z}_1^t\| &= \|\mathbf{Z}_1(\hat{\mathbf{U}}_2^t \otimes \cdots \otimes \hat{\mathbf{U}}_m^t)\| \\ &= \|\mathbf{Z}_1((\mathcal{P}_{\mathbf{U}_2^*} + \mathcal{P}_{\mathbf{U}_2^*}^\perp) \otimes \cdots \otimes (\mathcal{P}_{\mathbf{U}_m^*} + \mathcal{P}_{\mathbf{U}_m^*}^\perp))(\hat{\mathbf{U}}_2^t \otimes \cdots \otimes \hat{\mathbf{U}}_m^t)\| \\ &\leq C_m[(\bar{d})^{1/2} + \bar{r}^{(m-1)/2}]\sigma_z + C_m[(\bar{d}\bar{r})^{1/2} + \bar{r}^{(m-1)/2}]\sigma_z L_t, \end{aligned} \tag{12.43}$$

where the last inequality holds since \mathcal{E}_4 holds and $\|\hat{\mathbf{U}}_i^{tT} \mathbf{U}_{i\perp}^*\| \leq L_t$. Now since $\hat{\mathbf{U}}_1^{t+1}$ is the top r_1 left singular vectors of $\tilde{\mathbf{A}}_1^t$ and \mathbf{U}_1 is the top r_1 left singular vectors of \mathbf{X}_1^t , from Wedin's $\sin\Theta$ Theorem, we have

$$\begin{aligned} d_c(\hat{\mathbf{U}}_1^{t+1}, \mathbf{U}_1) &\leq \frac{C\|\tilde{\mathbf{A}}_1^t - \mathbf{X}_1^t\|}{\underline{\lambda}} \leq \frac{C(\|\mathbf{E}_1\|_F + \|\mathbf{Z}_1^t\|)}{\underline{\lambda}} \\ &\stackrel{(12.43)}{\leq} \frac{C|\Omega^*|^{1/2}\tau_u + C_m[(\bar{d})^{1/2} + \bar{r}^{(m-1)/2}]\sigma_z + C_m[(\bar{d}\bar{r})^{1/2} + \bar{r}^{(m-1)/2}]\sigma_z L_t}{\underline{\lambda}}. \end{aligned}$$

The derivation for $d_c(\hat{\mathbf{U}}_i^{t+1}, \mathbf{U}_i)$ when $i \geq 2$ is similar to this case and hence

$$L_{t+1} \leq \frac{C|\Omega^*|^{1/2}\tau_u + C_m[(\bar{d})^{1/2} + \bar{r}^{(m-1)/2}]\sigma_z}{\underline{\lambda}} + \frac{C_m[(\bar{d}\bar{r})^{1/2} + \bar{r}^{(m-1)/2}]\sigma_z}{\underline{\lambda}} L_t.$$

From condition (b), we have $C_m[(\bar{d}\bar{r})^{1/2} + \bar{r}^{(m-1)/2}]\sigma_z/\underline{\lambda} \leq 1/2$, so the above inequality implies

$$L_{t_{\max}} \leq \left(\frac{1}{2}\right)^{t_{\max}} \cdot L_0 + \frac{C|\Omega^*|^{1/2}\tau_u + C_m[(\bar{d})^{1/2} + \bar{r}^{(m-1)/2}]\sigma_z}{\underline{\lambda}}.$$

If we choose $t_{\max} \geq (C_m \log(\bar{d}\kappa_0) \vee 1)$, then

$$L_{t_{\max}} \leq \frac{C|\Omega^*|^{1/2}\tau_u}{\underline{\lambda}} + \frac{C_m[(\bar{d})^{1/2} + \bar{r}^{(m-1)/2}]\sigma_z}{\underline{\lambda}}. \quad (12.44)$$

Set the event $\mathcal{E}_5 = \{\|\mathcal{Z} \times_{i=1}^m \mathcal{P}_{\hat{\mathbf{U}}_i}\|_{\text{F}} \leq C(r^* + \sum_{i=1}^m d_i r_i) \sigma_z^2\}$. Then from (Zhang and Xia, 2018, Lemma 5), $\mathbb{P}(\mathcal{E}_5) \geq 1 - \exp(-C\bar{d}\bar{r})$. And we also consider $\|\mathcal{T}^* \times_i \hat{\mathbf{U}}_{i\perp}^T\|_{\text{F}}$, we consider $i = 1$ for simplicity.

$$\begin{aligned} \|\mathcal{T}^* \times_1 \hat{\mathbf{U}}_{1\perp}^T\|_{\text{F}} &= \|\hat{\mathbf{U}}_{1\perp}^T \mathbf{T}_1^*\|_{\text{F}} \leq \|\mathcal{P}_{\hat{\mathbf{U}}_{1\perp}} \mathbf{T}_1^*(\hat{\mathbf{U}}_2^{t_{\max}-1} \otimes \dots \otimes \hat{\mathbf{U}}_m^{t_{\max}-1})\|_{\text{F}} \cdot \prod_{i=2}^m \sigma_{\min}^{-1}(\mathbf{U}_i^{*T} \hat{\mathbf{U}}_i^{t_{\max}-1}) \\ &\leq C_m(\|\mathcal{E}\|_{\text{F}} + \sqrt{r_1} \|\mathbf{Z}_1^{t_{\max}-1}\|) \\ &\leq C_m|\Omega^*|^{1/2}\tau_u + C_m(\sqrt{d_1 r_1} + \sqrt{r^*})\sigma_z, \end{aligned} \quad (12.45)$$

where the second inequality holds from (Zhang and Xia, 2018, Lemma 6) and the last inequality holds from (12.43).

Now we are in the right position to bound $\|\hat{\mathcal{T}} - \mathcal{T}^*\|_{\text{F}}$ under \mathcal{E}_5 .

$$\begin{aligned} \|\hat{\mathcal{T}} - \mathcal{T}^*\|_{\text{F}} &= \|\tilde{\mathcal{A}} \times_{i=1}^m \mathcal{P}_{\hat{\mathbf{U}}_i} - \mathcal{T}^*\|_{\text{F}} \\ &\leq \|(\tilde{\mathcal{A}} - \mathcal{T}^*) \times_{i=1}^m \mathcal{P}_{\hat{\mathbf{U}}_i}\|_{\text{F}} + \|\mathcal{T}^* - \mathcal{T}^* \times_{i=1}^m \mathcal{P}_{\hat{\mathbf{U}}_i}\|_{\text{F}} \\ &\leq \|\mathcal{E}\|_{\text{F}} + \|\mathcal{Z} \times_{i=1}^m \mathcal{P}_{\hat{\mathbf{U}}_i}\|_{\text{F}} + \sum_{i=1}^m \|\mathcal{T}^* \times_i \hat{\mathbf{U}}_{i\perp}^T\|_{\text{F}} \\ &\leq C_m|\Omega^*|^{1/2}\tau_u + C_m(\sqrt{r^*} + \sqrt{\bar{d}\bar{r}})\sigma_z, \end{aligned} \quad (12.46)$$

where the last inequality follows from (12.45). Finally applying Lemma 13.6 and we get $\hat{\mathcal{T}}_0$ is $(2\mu_1\kappa_0)^2$ -incoherent and $\|\hat{\mathcal{T}}_0 - \mathcal{T}^*\|_{\text{F}} \leq 2\|\hat{\mathcal{T}} - \mathcal{T}^*\|_{\text{F}}$. Therefore from condition (a), (b) in Lemma 5.2, the initialization condition (a) in Theorem 5.1 holds.

12.5 Proof of Lemma 5.3

For each $j \in [m]$ and $i \in [d_j]$, we have

$$\|\mathbf{e}_i^\top \mathcal{M}_j(\mathcal{S}_\alpha)\|_{\ell_0} = \sum_{\omega: \omega_j=i} \mathbb{1}(|[\mathcal{Z}]_\omega| > \alpha\sigma_z) = \sum_{\omega: \omega_j=i} [\mathcal{Y}]_\omega$$

where $\mathcal{Y} \in \{0, 1\}^{d_1 \times \dots \times d_m}$ having *i.i.d.* Bernoulli entries and $q := \mathbb{P}([\mathcal{Y}]_\omega = 1) = \mathbb{P}(|[\mathcal{Z}]_\omega| > \alpha\sigma_z) \leq \alpha^{-\theta}$.

Denote $X_{ij} = \sum_{\omega: \omega_j=i} [\mathfrak{Y}]_{\omega}$. By Chernoff bound, if $d_j^- q \geq 3 \log(m\bar{d}^3)$, we get

$$\mathbb{P}(X_{ij} - d_j^- q \geq d_j^- q) \leq \exp\{-d_j^{-1} q/3\} \leq (m\bar{d}^3)^{-1}$$

implying that

$$\mathbb{P}\left(\bigcap_{i,j} \{X_{ij} \leq 2d_j^- q\}\right) \geq 1 - m\bar{d}(m\bar{d}^3)^{-1} = 1 - \bar{d}^{-2}. \quad (12.47)$$

On the other hand, if $d_j^- q \leq 3 \log(m\bar{d}^3)$, by Chernoff bound, we get

$$\mathbb{P}(X_{ij} \geq 10 \log(m\bar{d}^3)) \leq (m\bar{d}^3)^{-1}$$

implying that

$$\mathbb{P}\left(\bigcap_{i,j} \{X_{ij} \leq 10 \log(m\bar{d}^3)\}\right) \geq 1 - m\bar{d}(m\bar{d}^3)^{-1} = 1 - \bar{d}^{-2}. \quad (12.48)$$

Putting (12.47) and (12.48), since $q \leq \alpha^{-\theta}$, we get

$$\mathbb{P}\left(\bigcap_{i,j} \left\{X_{ij} \leq \max\{10 \log(m\bar{d}^3), 2d_j^- \alpha^{-\theta}\}\right\}\right) \geq 1 - \bar{d}^{-2},$$

which completes the proof.

12.6 Proof of Theorem 5.4

Conditioned on \mathfrak{E}_1 defined in Lemma 5.3, Theorem 5.4 is a special case of Theorem 5.1. Indeed, in Theorem 5.1, we replace σ_z with $\alpha\sigma_z$, and $|\Omega^*| \log \bar{d}$ with $\alpha' d^* \asymp \bar{d} \log(m\bar{d})$, then we get Theorem 5.4.

12.7 Proof of Lemma 5.5

From the choice of α in Theorem 5.4, we see that the sparsity of \mathcal{S}_{α} is bounded by $\alpha' \asymp \frac{\bar{d}}{d^*} \log(m\bar{d}^3)$. Therefore the condition (a) in Lemma 5.2 is satisfied. Now applying Lemma 5.2 and we get the desired result.

12.8 Proof of Lemma 5.6

From Lemma 13.6, we have $\text{Trim}_{\eta, \mathbf{r}}(\mathcal{W})$ is $2\mu_1\kappa_0$ -incoherent. Now for all $j \in [m]$,

$$\|\mathcal{M}_j(\mathcal{H}_{\mathbf{r}}^{\text{HO}}(\widetilde{\mathcal{W}}))\| \leq \|\mathcal{M}_j(\widetilde{\mathcal{W}})\| \leq \|\mathcal{M}_j(\mathcal{T}^*)\| + \|\mathcal{W} - \mathcal{T}^*\|_{\text{F}} \leq \frac{9}{8}\bar{\lambda}.$$

So we conclude

$$\|\text{Trim}_{\eta, \mathbf{r}}(\mathcal{W})\|_{\ell_{\infty}} \leq \frac{9}{8}\bar{\lambda} \prod_{i=1}^m (2\mu_1\kappa_0) \sqrt{\frac{r_j}{d_j}} \leq (9\zeta/16) \cdot (\mu_1\kappa_0)^m.$$

where the last inequality follows from the upper bound for $\bar{\lambda}$. This finishes the proof of the lemma.

12.9 Proof of Theorem 5.7

From the choice of ζ' and Lemma 5.6, we know Assumption 2 and 3 hold with parameters $b_{l,\zeta'}$ and $b_{u,\zeta'}$ with respect to the set $\mathbb{B}_2^* = \mathbb{B}_\infty^* = \{\mathcal{T} + \mathcal{S} : \|\mathcal{T} + \mathcal{S}\|_{\ell_\infty} \leq \zeta', \mathcal{T} \in \mathbb{M}_r, \mathcal{S} \in \mathbb{S}_{\gamma\alpha}\}$. Now the proof follows the proof of Theorem 4.1 with slight modification. Since we can now guarantee in each iteration $\widehat{\mathcal{T}}_l + \widehat{\mathcal{S}}_l \in \mathbb{B}_2^* = \mathbb{B}_\infty^*$ from Lemma 5.6 and the choice of k_{pr} , we can use Assumption 3 instead of Assumption 2 when estimating the low rank part. So we only need to estimate Err_∞ and Err_{2r} . From (5.8), we have $\text{Err}_\infty \leq L_\zeta$. Now we estimate Err_{2r} . In fact, from the definition of Err_{2r} , we have

$$\text{Err}_{2r} = \sup_{\mathcal{M} \in \mathbb{M}_{2r}, \|\mathcal{M}\|_F \leq 1} \langle \nabla \mathcal{L}(\mathcal{T}^* + \mathcal{S}^*), \mathcal{M} \rangle.$$

Since for all $\omega \in [d_1] \times \dots \times [d_m]$, we have $[\nabla \mathcal{L}(\mathcal{T}^* + \mathcal{S}^*)]_\omega$ is bounded random variable with the upper bound given by L_ζ . So apply Lemma 13.3, we have $\text{Err}_{2r} \leq CL_\zeta \cdot (\bar{d}r + r^*)^{1/2}$ with probability at least $1 - \bar{d}^{-2}$. Now we plug in the bounds for Err_∞ and Err_{2r} to Theorem 4.1 and we get the first part of the theorem. For the ℓ_∞ bound, we apply Theorem 4.3 and Lemma 13.7. And we finish the proof of the theorem.

12.10 Proof of Lemma 5.8

Algorithm 7 Initialization for binary tensor

Let $\mathbf{A} = \mathcal{A}^{(m_0)} := \text{reshape}(\mathcal{A}, [d_1 \dots d_{m_0}, d_{m_0+1} \dots d_m])$ with $m_0 = \lfloor \frac{m}{2} \rfloor$ and let $\widehat{\mathbf{M}}$ be the minimizer to (12.49).

$\widehat{\mathcal{T}} = \text{reshape}(\widehat{\mathbf{M}}, [d_1, \dots, d_m])$.

$\widehat{\mathcal{T}}_0 = \text{Trim}_{\eta, r}(\widehat{\mathcal{T}})$ with $\eta = 16\mu_1 \|\widehat{\mathcal{T}}\|_F / (7\sqrt{d^*})$.

Output: $\widehat{\mathcal{T}}_0$.

We first introduce some notations. Let $m_0 = \lfloor \frac{m}{2} \rfloor$, and denote $\mathbf{T}^* = (\mathcal{T}^*)^{(m_0)}$, $\mathbf{S}^* = (\mathcal{S}^*)^{(m_0)}$ and $\mathbf{A} = \mathcal{A}^{(m_0)}$, then $\mathbf{T}^*, \mathbf{S}^*, \mathbf{A}$ are matrices of size $d_1 \dots d_{m_0} \times d_{m_0+1} \dots d_m =: d_1^* \times d_2^*$. Since \mathcal{T}^* admits the decomposition $\mathcal{T}^* = \mathcal{C}^* \cdot \llbracket \mathbf{U}_1^*, \dots, \mathbf{U}_m^* \rrbracket$, we have $\mathcal{T}^* = (\mathbf{U}_{m_0} \otimes \dots \otimes \mathbf{U}_1) \mathcal{C}^{(m_0)} (\mathbf{U}_m \otimes \dots \otimes \mathbf{U}_{m_0+1})^T$ and hence the rank of \mathbf{T}^* is $r = \min\{r_1 \dots r_{m_0}, r_{m_0+1} \dots r_m\}$. We denote $\mathbf{M} = \mathbf{T}^* + \mathbf{S}^*$.

Under Assumption 5, we have $\|\mathbf{T}^*\|_{\ell_\infty}, \|\mathbf{S}^*\|_{\ell_\infty} \leq \frac{\zeta}{2}$ and thus $\|\mathbf{M}\|_{\ell_\infty} \leq \zeta$. Now we bound the

nuclear norm of \mathbf{M} . Using triangle inequality and we have

$$\begin{aligned}
\|\mathbf{M}\|_* &\leq \|\mathbf{T}^*\|_* + \|\mathbf{S}^*\|_* \\
&\leq \frac{\zeta}{2}(rd^*)^{1/2} + \frac{\zeta}{2}|\Omega^*|^{1/2} \min(d_1^*, d_2^*)^{1/2} \\
&= \left(\frac{\zeta}{2} + \frac{\zeta}{2} \cdot \frac{\min(d_1^*, d_2^*)^{1/2}}{(rd^*)^{1/2}} |\Omega^*|^{1/2}\right) (rd^*)^{1/2} \\
&\leq \zeta (rd^*)^{1/2},
\end{aligned}$$

where the last inequality holds since condition (a) holds. Now with a little bit abuse of notation, we consider the following convex program,

$$\min \mathcal{L}(\mathbf{X}) = -\langle \mathbf{A}, \log(p(\mathbf{X})) \rangle - \langle 1 - \mathbf{A}, \log(1 - p(\mathbf{X})) \rangle, \text{ s.t. } \|\mathbf{X}\|_* \leq \zeta \sqrt{d^* r} \text{ and } \|\mathbf{X}\|_{\ell_\infty} \leq \zeta, \quad (12.49)$$

where the notation $1 - \mathbf{A}$ is the entrywise subtraction, and $p(\mathbf{X})$ is applying p entrywisely to \mathbf{X} . Denote $\widehat{\mathbf{M}}$ be the minimizer to (12.49) and apply the Theorem 1 in [Davenport et al. \(2014\)](#) with the sample size d^* and we get with probability at least $1 - \frac{C}{d_1^* + d_2^*}$,

$$\|\widehat{\mathbf{M}} - \mathbf{M}\|_{\text{F}}^2 \leq C_\zeta [r(d_1^* + d_2^*)d^*]^{1/2}$$

with $C_\zeta = C \cdot \zeta L_\zeta \beta_\zeta$ and $\beta_\zeta = \sup_{|x| \leq \zeta} \frac{p(x)(1-p(x))}{(p'(x))^2}$.

Now we reshape $\widehat{\mathbf{M}}$ back to a tensor, and denote $\widehat{\mathcal{T}} = \text{reshape}(\widehat{\mathbf{M}}, [d_1, \dots, d_m])$. Since reshape keeps the Frobenius norm unchanged, we have

$$\|\widehat{\mathcal{T}} - \mathcal{T}^*\|_{\text{F}} = \|\widehat{\mathbf{T}} - \mathbf{T}^*\|_{\text{F}} \leq \|\widehat{\mathbf{M}} - \mathbf{M}\|_{\text{F}} + \|\mathbf{S}^*\|_{\text{F}} \leq C_\zeta^{1/2} [r(d_1^* + d_2^*)d^*]^{1/4} + |\Omega^*|^{1/2} \frac{\zeta}{2}.$$

Finally we output $\mathcal{T}_0 = \text{Trim}_{\eta, \mathbf{r}}(\widehat{\mathcal{T}})$ with $\eta = 16\mu_1 \|\widehat{\mathcal{T}}\|_{\text{F}} / (7\sqrt{d^*})$, and from Lemma 5.6 and Lemma 13.6, since condition (b) and (c) hold, we get

$$(1) \mu(\widehat{\mathcal{T}}_0) \leq 2\kappa_0\mu_1; (2) \|\widehat{\mathcal{T}}_0 - \mathcal{T}^*\|_{\text{F}} \leq 2\|\widehat{\mathcal{T}} - \mathcal{T}^*\|_{\text{F}}; (3) \|\widehat{\mathcal{T}}\|_{\ell_\infty} \leq C_m(\mu_1\kappa_0)^m \frac{\sqrt{r^*}}{\sqrt{d^*}} \bar{\lambda}.$$

And together with the upper bound for $\underline{\lambda}$ in Assumption 5, the initialization condition in Theorem 5.7 is satisfied.

12.11 Proof of Theorem 5.9

The proof of this theorem is similar to that of Theorem 5.7. From the choice of ζ' and Lemma 5.6, we know Assumption 2 and 3 hold with parameters $b_{l, \zeta'} = e^{-\zeta'}$ and $b_{u, \zeta'} = e^{\zeta'}$ with respect to the set $\mathbb{B}_2^* = \mathbb{B}_\infty^* = \{\mathcal{T} + \mathcal{S} : \|\mathcal{T} + \mathcal{S}\|_{\ell_\infty} \leq \zeta', \mathcal{T} \in \mathbb{M}_{\mathbf{r}}, \mathcal{S} \in \mathbb{S}_{\gamma\alpha}\}$. Now the proof follows

the proof of Theorem 4.1 with slight modification. Since we can now guarantee in each iteration $\widehat{\mathcal{T}}_l + \widehat{\mathcal{S}}_l \in \mathbb{B}_2^* = \mathbb{B}_\infty^*$ from Lemma 5.6 and the choice of \mathbf{k}_{pr} , we can use Assumption 3 instead of Assumption 2 when estimating the low rank part. So we only need to estimate Err_∞ and $\text{Err}_{2\mathbf{r}}$. From (5.8), we have $\text{Err}_\infty \leq \|\nabla \mathcal{L}(\mathcal{T}^* + \mathcal{S}^*)\|_{\ell_\infty}$. Simple calculation shows

$$\nabla \mathcal{L}(\mathcal{T}^* + \mathcal{S}^*) = -\frac{1}{I} \mathcal{Y} + \exp(\mathcal{T}^* + \mathcal{S}^*),$$

and notice using a union bound and Poisson's tail bound, when $I \geq Ce^\zeta \log(d^*)$, we have with probability exceeding $1 - \frac{1}{d^*}$, $\|\mathcal{Y}\|_{\ell_\infty} \leq 10Ie^\zeta$. Therefore we have $\text{Err}_\infty \leq 11e^\zeta$.

The estimation for $\text{Err}_{2\mathbf{r}}$ is given in Theorem 4.3 Han et al. (2020), which states

$$\text{Err}_{2\mathbf{r}} \leq C \sqrt{\frac{r^* + m\bar{d}\bar{r}}{I/e^\zeta}}$$

with probability exceeding $1 - \frac{1}{d^*}$.

Now we plug in the bounds for Err_∞ and $\text{Err}_{2\mathbf{r}}$ to Theorem 4.1 and we get the first part of the theorem. For the ℓ_∞ bound, we apply Theorem 4.3 and Lemma 13.7. And we finish the proof of the theorem.

12.12 Proof of Lemma 5.10

With slight modification of the proof of Theorem 4.3 in Han et al. (2020), we have

$$\|\tilde{\mathcal{T}}_0 - \mathcal{T}^*\|_{\text{F}} \leq C \sqrt{\frac{e^\zeta}{I}} \left(\sum_{i=1}^m \sqrt{d_i r_i} + \sqrt{d_i^- r_i} \right) + \|\mathcal{S}^*\|_{\text{F}}$$

under the condition $I \geq Ce^\zeta \bar{d}$ with probability exceeding $1 - 1/d^*$. Therefore since we assume $I \geq C_1 \sum_{i=1}^m (d_i r_i + d_i^- r_i) \bar{r} \underline{\lambda}^{-2}$ and $|\Omega^*| \leq C\zeta^{-2} \underline{\lambda}^2 \bar{r}^{-1}$, we have $\|\tilde{\mathcal{T}}_0 - \mathcal{T}^*\|_{\text{F}} \leq c_{1,m} \underline{\lambda} \cdot \min \{ \delta^2 \bar{r}^{-1/2}, (\kappa_0^2 m \bar{r}^{1/2})^{-1} \} \leq \underline{\lambda}/8$. Now we apply Lemma 5.6 and Lemma 13.6 we see

$$(1) \mu(\widehat{\mathcal{T}}_0) \leq 2\kappa_0 \mu_1; (2) \|\widehat{\mathcal{T}}_0 - \mathcal{T}^*\|_{\text{F}} \leq 2\|\widehat{\mathcal{T}} - \mathcal{T}^*\|_{\text{F}}; (3) \|\widehat{\mathcal{T}}\|_{\ell_\infty} \leq C_m (\mu_1 \kappa_0)^m \frac{\sqrt{r^*}}{\sqrt{d^*}} \bar{\lambda}.$$

From Assumption 6, we see the initialization requirements in 5.9 is satisfied.

12.13 Proof of Theorem 6.1

We use induction to prove this theorem.

Step 0: Base case. From the initialization, we have $\|\widehat{\mathcal{T}}_0 - \mathcal{T}^*\|_{\text{F}} \leq c_{1,m} \delta \bar{r}^{-1/2} \cdot \underline{\lambda}$.

Step 1: Estimating $\|\widehat{\mathcal{T}}_{l+1} - \mathcal{T}^*\|_F$. We prove this case assuming

$$\|\widehat{\mathcal{T}}_l - \mathcal{T}^*\|_F \leq c_{1,m} \delta \bar{r}^{-1/2} \cdot \underline{\lambda}. \quad (12.50)$$

We point out that this also implies $\|\widehat{\mathcal{T}}_l - \mathcal{T}^*\|_F \leq c_{1,m} b_l b_u^{-1} \bar{r}^{-1/2} \cdot \underline{\lambda}$ since $\delta \lesssim b_l^2 b_u^{-2}$. In order to use Lemma 13.2, we need to derive an upper bound for $\|\widehat{\mathcal{T}}_l - \mathcal{T}^* - \beta \mathcal{P}_{\mathbb{T}_l} \mathcal{G}_l\|_F$.

Step 1.1: Estimating $\|\widehat{\mathcal{T}}_l - \mathcal{T}^* - \beta \mathcal{P}_{\mathbb{T}_l} \mathcal{G}_l\|_F$. For arbitrary $1 \geq \delta > 0$, we have,

$$\|\widehat{\mathcal{T}}_l - \mathcal{T}^* - \beta \mathcal{P}_{\mathbb{T}_l} \mathcal{G}_l\|_F^2 \leq (1 + \delta/2) \|\widehat{\mathcal{T}}_l - \mathcal{T}^* - \beta \mathcal{P}_{\mathbb{T}_l} (\mathcal{G}_l - \mathcal{G}^*)\|_F^2 + (1 + 2/\delta) \beta^2 \|\mathcal{P}_{\mathbb{T}_l} \mathcal{G}^*\|_F^2 \quad (12.51)$$

Now we consider the bound for $\|\widehat{\mathcal{T}}_l - \mathcal{T}^* - \beta \mathcal{P}_{\mathbb{T}_l} (\mathcal{G}_l - \mathcal{G}^*)\|_F^2$.

$$\begin{aligned} \|\widehat{\mathcal{T}}_l - \mathcal{T}^* - \beta \mathcal{P}_{\mathbb{T}_l} (\mathcal{G}_l - \mathcal{G}^*)\|_F^2 &= \|\widehat{\mathcal{T}}_l - \mathcal{T}^*\|_F^2 - 2\beta \langle \widehat{\mathcal{T}}_l - \mathcal{T}^*, \mathcal{P}_{\mathbb{T}_l} (\mathcal{G}_l - \mathcal{G}^*) \rangle + \beta^2 \|\mathcal{P}_{\mathbb{T}_l} (\mathcal{G}_l - \mathcal{G}^*)\|_F^2 \\ &\leq (1 + \beta^2 b_u^2) \|\widehat{\mathcal{T}}_l - \mathcal{T}^*\|_F^2 - 2\beta \langle \widehat{\mathcal{T}}_l - \mathcal{T}^*, \mathcal{P}_{\mathbb{T}_l} (\mathcal{G}_l - \mathcal{G}^*) \rangle \end{aligned} \quad (12.52)$$

where the last inequality holds from the Assumption 2 since $\widehat{\mathcal{T}}_l \in \mathbb{B}_2^*$ from (12.50). Also,

$$\begin{aligned} \langle \widehat{\mathcal{T}}_l - \mathcal{T}^*, \mathcal{P}_{\mathbb{T}_l} (\mathcal{G}_l - \mathcal{G}^*) \rangle &= \langle \widehat{\mathcal{T}}_l - \mathcal{T}^*, \mathcal{G}_l - \mathcal{G}^* \rangle - \langle \mathcal{P}_{\mathbb{T}_l}^\perp (\widehat{\mathcal{T}}_l - \mathcal{T}^*), \mathcal{G}_l - \mathcal{G}^* \rangle \\ &\geq b_l \|\widehat{\mathcal{T}}_l - \mathcal{T}^*\|_F^2 - \frac{C_{1,m} b_u}{\underline{\lambda}} \|\widehat{\mathcal{T}}_l - \mathcal{T}^*\|_F^3 \end{aligned} \quad (12.53)$$

where the last inequality is from Assumption 2, Lemma 13.1 and Cauchy-Schwartz inequality and $C_{1,m} = 2^m - 1$. Together with (12.52) and (12.53), and since we have $\|\widehat{\mathcal{T}}_l - \mathcal{T}^*\|_F \leq \frac{0.1 b_l}{2 b_u C_{1,m}} \cdot \underline{\lambda}$, we get,

$$\begin{aligned} \|\widehat{\mathcal{T}}_l - \mathcal{T}^* - \beta \mathcal{P}_{\mathbb{T}_l} (\mathcal{G}_l - \mathcal{G}^*)\|_F^2 &\leq (1 - 2\beta b_l + \beta^2 b_u^2) \|\widehat{\mathcal{T}}_l - \mathcal{T}^*\|_F^2 + \frac{2\beta C_{1,m} b_u}{\underline{\lambda}} \|\widehat{\mathcal{T}}_l - \mathcal{T}^*\|_F^3 \\ &\leq (1 - 1.9\beta b_l + \beta^2 b_u^2) \|\widehat{\mathcal{T}}_l - \mathcal{T}^*\|_F^2. \end{aligned} \quad (12.54)$$

Since we have $0.75 b_l b_u^{-1} \geq \delta^{1/2}$, if we choose $\beta \in [0.4 b_l b_u^{-2}, 1.5 b_l b_u^{-2}]$, we have $1 - 1.9\beta b_l + \beta^2 b_u^2 \leq 1 - \delta$.

So from (12.51) and (12.54), we get

$$\|\widehat{\mathcal{T}}_l - \mathcal{T}^* - \beta \mathcal{P}_{\mathbb{T}_l} \mathcal{G}_l\|_F^2 \leq (1 + \frac{\delta}{2})(1 - \delta) \|\widehat{\mathcal{T}}_l - \mathcal{T}^*\|_F^2 + (1 + \frac{2}{\delta}) \text{Err}_{2\mathbf{r}}^2 \quad (12.55)$$

where in the inequality we use the definition of $\text{Err}_{2\mathbf{r}}$ and that $\beta \leq 1$. Now from the upper bound for $\|\widehat{\mathcal{T}}_l - \mathcal{T}^*\|_F$ and the signal-to-noise ratio, we verified that $\|\widehat{\mathcal{T}}_l - \mathcal{T}^* - \beta \mathcal{P}_{\mathbb{T}_l} \mathcal{G}_l\|_F \leq \underline{\lambda}/8$ and thus $\sigma_{\max}(\widehat{\mathcal{T}}_l - \mathcal{T}^* - \beta \mathcal{P}_{\mathbb{T}_l} \mathcal{G}_l) \leq \underline{\lambda}/8$.

Step 1.2: Estimating $\|\widehat{\mathcal{T}}_{l+1} - \mathcal{T}^*\|_F$. Now that we verified the condition of Lemma 13.2, from the Algorithm 5, we have,

$$\|\widehat{\mathcal{T}}_{l+1} - \mathcal{T}^*\|_F^2 \leq \|\widehat{\mathcal{T}}_l - \mathcal{T}^* - \beta \mathcal{P}_{\mathbb{T}_l} \mathcal{G}_l\|_F^2 + C_m \frac{\sqrt{r}}{\underline{\lambda}} \|\widehat{\mathcal{T}}_l - \mathcal{T}^* - \beta \mathcal{P}_{\mathbb{T}_l} \mathcal{G}_l\|_F^3 \quad (12.56)$$

where $C_m > 0$ is the constant depending only on m as in Lemma 13.2. From (12.55) and the assumption that $\|\widehat{\mathcal{T}}_l - \mathcal{T}^*\|_F \lesssim_m \frac{\delta}{\sqrt{r}} \cdot \underline{\lambda}$ and $\text{Err}_{2r} \lesssim_m \frac{\delta^2}{\sqrt{r}} \cdot \underline{\lambda}$, we get

$$C_m \frac{\sqrt{r}}{\underline{\lambda}} \|\widehat{\mathcal{T}}_l - \mathcal{T}^* - \beta \mathcal{P}_{\mathbb{T}_l} \mathcal{G}_l\|_F \leq \frac{\delta}{4} \quad (12.57)$$

From (12.56), (12.55) and (12.57), we get

$$\|\widehat{\mathcal{T}}_{l+1} - \mathcal{T}^*\|_F^2 \leq (1 + \frac{\delta}{4}) \|\widehat{\mathcal{T}}_l - \mathcal{T}^* - \beta \mathcal{P}_{\mathbb{T}_l} \mathcal{G}_l\|_F^2 \leq (1 - \delta^2) \|\widehat{\mathcal{T}}_l - \mathcal{T}^*\|_F^2 + \frac{4}{\delta} \text{Err}_{2r}^2 \quad (12.58)$$

Together with the assumption $\|\widehat{\mathcal{T}}_l - \mathcal{T}^*\|_F \lesssim_m \frac{\delta}{\sqrt{r}} \cdot \underline{\lambda}$ and $\text{Err}_{2r} \lesssim_m \frac{\delta^2}{\sqrt{r}} \cdot \underline{\lambda}$, we get

$$\|\widehat{\mathcal{T}}_{l+1} - \mathcal{T}^*\|_F \leq c_{1,m} \frac{\delta}{\sqrt{r}} \cdot \underline{\lambda}, \quad (12.59)$$

which completes the induction and completes the proof.

13 Technical Lemmas

Lemma 13.1. Suppose \mathbb{T}_l is the tangent space at the point $\widehat{\mathcal{T}}_l$, then we have

$$\|\mathcal{P}_{\mathbb{T}_l}^\perp \mathcal{T}^*\|_F \leq \frac{2^m - 1}{\underline{\lambda}} \|\mathcal{T}^* - \widehat{\mathcal{T}}_l\|_F^2.$$

Proof. See (Cai et al. (2020), Lemma 5.2). □

Lemma 13.2. Let $\mathcal{T}^* = \mathcal{S}^* \cdot (\mathbf{V}_1^*, \dots, \mathbf{V}_m^*)$ be the tensor with Tucker rank $\mathbf{r} = (r_1, \dots, r_m)$. Let $\mathcal{D} \in \mathbb{R}^{d_1 \times \dots \times d_m}$ be a perturbation tensor such that $\underline{\lambda} \geq 8\sigma_{\max}(\mathcal{D})$, where $\sigma_{\max}(\mathcal{D}) = \max_{i=1}^m \|\mathcal{M}_i(\mathcal{D})\|$.

Then we have

$$\|\mathcal{H}_{\mathbf{r}}^{\text{HO}}(\mathcal{T}^* + \mathcal{D}) - \mathcal{T}^*\|_F \leq \|\mathcal{D}\|_F + C_m \frac{\sqrt{r} \|\mathcal{D}\|_F^2}{\underline{\lambda}}$$

where $C_m > 0$ is an absolute constant depending only on m .

Proof. Without loss of generality, we only prove the Lemma in the case $m = 3$. First notice that

$$\mathcal{H}_{\mathbf{r}}^{\text{HO}}(\mathcal{T}^* + \mathcal{D}) = (\mathcal{T}^* + \mathcal{D}) \cdot \llbracket \mathcal{P}_{\mathbf{U}_1}, \mathcal{P}_{\mathbf{U}_2}, \mathcal{P}_{\mathbf{U}_3} \rrbracket,$$

where \mathbf{U}_i are leading r_i left singular vectors of $\mathcal{M}_i(\mathcal{T}^* + \mathcal{D})$ and $\mathcal{P}_{\mathbf{U}_i} = \mathbf{U}_i \mathbf{U}_i^\top$.

First from (Xia (2019), Theorem 1), we have for all $i \in [m]$

$$\mathcal{P}_{\mathbf{U}_i} - \mathcal{P}_{\mathbf{V}_i^*} = \mathcal{S}_{i,1} + \sum_{j \geq 2} \mathcal{S}_{i,j},$$

where $\mathcal{S}_{i,j} = \mathcal{S}_{\mathcal{M}_i(\mathcal{T}^*),j}(\mathcal{M}_i(\mathcal{D}))$ and specially $\mathcal{S}_{i,1} = (\mathcal{M}_i(\mathcal{T}^*)^\top)^\dagger (\mathcal{M}_i(\mathcal{D}))^\top \mathcal{P}_{\mathbf{V}_i^*}^\perp + \mathcal{P}_{\mathbf{V}_i^*}^\perp \mathcal{M}_i(\mathcal{D})(\mathcal{M}_i(\mathcal{T}^*))^\dagger$. The explicit form of $\mathcal{S}_{i,j}$ can be found in (Xia, 2019, Theorem 1). Here, we denote \mathbf{A}^\dagger the pseudo-inverse of \mathbf{A} , i.e., $\mathbf{A}^\dagger = \mathbf{R}\mathbf{\Sigma}^{-1}\mathbf{L}^\top$ if \mathbf{A} has a thin-SVD as $\mathbf{A} = \mathbf{L}\mathbf{\Sigma}\mathbf{R}^\top$. With a little abuse of notations, we write $(\mathbf{A}^\dagger)^k = \mathbf{R}\mathbf{\Sigma}^{-k}\mathbf{L}^\top$ for any positive integer $k \geq 1$.

For the sake of brevity, we denote $\mathbf{S}_i = \sum_{j \geq 1} \mathcal{S}_{i,j}$. By the definition of $\mathcal{S}_{i,j}$, we have the bound $\|\mathcal{S}_{i,j}\| \leq \left(\frac{4\sigma_{\max}(\mathcal{D})}{\lambda}\right)^j$. We get the upper bound for $\|\mathbf{S}_i\|$ as follows,

$$\|\mathbf{S}_i\| = \left\| \sum_{j \geq 1} \mathcal{S}_{i,j} \right\| \leq \frac{4\sigma_{\max}(\mathcal{D})}{\lambda - 4\sigma_{\max}(\mathcal{D})} \leq \frac{8\sigma_{\max}(\mathcal{D})}{\lambda} \quad (13.1)$$

So we have,

$$\begin{aligned} \mathcal{T}^* \cdot [\mathcal{P}_{\mathbf{U}_1}, \mathcal{P}_{\mathbf{U}_2}, \mathcal{P}_{\mathbf{U}_3}] &= \mathcal{T}^* \cdot [\mathcal{P}_{\mathbf{V}_1^*} + \mathbf{S}_1, \mathcal{P}_{\mathbf{V}_2^*} + \mathbf{S}_2, \mathcal{P}_{\mathbf{V}_3^*} + \mathbf{S}_3] \\ &= \mathcal{T}^* \cdot [\mathcal{P}_{\mathbf{V}_1^*}, \mathcal{P}_{\mathbf{V}_2^*}, \mathcal{P}_{\mathbf{V}_3^*}] \end{aligned} \quad (13.2)$$

$$\begin{aligned} &+ \mathcal{T}^* \cdot [\mathbf{S}_1, \mathcal{P}_{\mathbf{V}_2^*}, \mathcal{P}_{\mathbf{V}_3^*}] + \mathcal{T}^* \cdot [\mathcal{P}_{\mathbf{V}_1^*}, \mathbf{S}_2, \mathcal{P}_{\mathbf{V}_3^*}] + \mathcal{T}^* \cdot [\mathcal{P}_{\mathbf{V}_1^*}, \mathcal{P}_{\mathbf{V}_2^*}, \mathbf{S}_3] \\ &+ \mathcal{T}^* \cdot [\mathbf{S}_1, \mathbf{S}_2, \mathcal{P}_{\mathbf{V}_3^*}] + \mathcal{T}^* \cdot [\mathcal{P}_{\mathbf{V}_1^*}, \mathbf{S}_2, \mathbf{S}_3] + \mathcal{T}^* \cdot [\mathbf{S}_1, \mathcal{P}_{\mathbf{V}_2^*}, \mathbf{S}_3] \\ &+ \mathcal{T}^* \cdot [\mathbf{S}_1, \mathbf{S}_2, \mathbf{S}_3] \end{aligned} \quad (13.3)$$

We now bound each of $\|\mathcal{T}^* \cdot [\mathbf{S}_1, \mathbf{S}_2, \mathcal{P}_{\mathbf{V}_3^*}]\|_{\text{F}}$, $\|\mathcal{T}^* \cdot [\mathcal{P}_{\mathbf{V}_1^*}, \mathbf{S}_2, \mathbf{S}_3]\|_{\text{F}}$ and $\|\mathcal{T}^* \cdot [\mathbf{S}_1, \mathcal{P}_{\mathbf{V}_2^*}, \mathbf{S}_3]\|_{\text{F}}$. Without loss of generality, we only prove the bound of the first term.

$$\mathcal{M}_1(\mathcal{T}^* \cdot [\mathbf{S}_1, \mathbf{S}_2, \mathcal{P}_{\mathbf{V}_3^*}]) = \mathbf{S}_1 \mathcal{M}_1(\mathcal{T}^*) (\mathcal{P}_{\mathbf{V}_3^*}^* \otimes \mathbf{S}_2)^\top \quad (13.4)$$

Write

$$\begin{aligned} \mathbf{S}_1 \mathcal{M}_1(\mathcal{T}^*) &= \left(\mathcal{S}_{1,1} + \sum_{j \geq 2} \mathcal{S}_{1,j} \right) \mathcal{M}_1(\mathcal{T}^*) \\ &= \mathcal{P}_{\mathbf{V}_1^*}^\perp \mathcal{M}_1(\mathcal{D}) (\mathcal{M}_1(\mathcal{T}^*))^\dagger \mathcal{M}_1(\mathcal{T}^*) + \sum_{j \geq 2} \mathcal{S}_{1,j} \mathcal{M}_1(\mathcal{T}^*) \\ &= \mathcal{M}_1(\mathcal{D} \cdot [\mathcal{P}_{\mathbf{V}_1^*}^\perp, \mathcal{P}_{\mathbf{V}_2^*}, \mathcal{P}_{\mathbf{V}_3^*}]) + \sum_{j \geq 2} \mathcal{S}_{1,j} \mathcal{M}_1(\mathcal{T}^*) \end{aligned} \quad (13.5)$$

where we used the fact $\mathcal{P}_{\mathbf{V}_1^*}^\perp \mathcal{M}_1(\mathcal{T}^*) = \mathbf{0}$.

Thus we obtain an upper bound for $\|\mathbf{S}_1 \mathcal{M}_1(\mathcal{T}^*)\|$ as follows

$$\|\mathbf{S}_1 \mathcal{M}_1(\mathcal{T}^*)\| \leq \sigma_{\max}(\mathcal{D}) + \lambda \sum_{j \geq 2} \left(\frac{4\sigma_{\max}(\mathcal{D})}{\lambda} \right)^j \leq 4\sigma_{\max}(\mathcal{D}), \quad (13.6)$$

where the first inequality is due to the explicit form of $\mathcal{S}_{1,j}$. See (Xia, 2019, Theorem 1).

So from (13.4) and (13.6), we get

$$\|\mathcal{T}^* \cdot \llbracket \mathbf{S}_1, \mathbf{S}_2, \mathcal{P}_{\mathbf{V}_3^*} \rrbracket\|_{\mathbf{F}} \leq \|\mathbf{S}_1 \mathcal{M}_1(\mathcal{T}^*)\|_{\mathbf{F}} \cdot \|\mathcal{P}_{\mathbf{V}_3^*} \otimes \mathbf{S}_2\| \leq C_1 \sqrt{\bar{r}} \frac{\sigma_{\max}(\mathcal{D})^2}{\lambda} \quad (13.7)$$

where $C_1 > 0$ is an absolute constant.

Now we consider the linear terms $\mathcal{T}^* \cdot \llbracket \mathbf{S}_1, \mathcal{P}_{\mathbf{V}_2^*}, \mathcal{P}_{\mathbf{V}_3^*} \rrbracket$, $\mathcal{T}^* \cdot \llbracket \mathcal{P}_{\mathbf{V}_1^*}, \mathbf{S}_2, \mathcal{P}_{\mathbf{V}_3^*} \rrbracket$ and $\mathcal{T}^* \cdot \llbracket \mathcal{P}_{\mathbf{V}_1^*}, \mathcal{P}_{\mathbf{V}_2^*}, \mathbf{S}_3 \rrbracket$. Clearly, we have

$$\begin{aligned} \mathcal{M}_1(\mathcal{T}^* \cdot \llbracket \mathbf{S}_1, \mathcal{P}_{\mathbf{V}_2^*}, \mathcal{P}_{\mathbf{V}_3^*} \rrbracket) &= \mathbf{S}_1 \mathcal{M}_1(\mathcal{T}^*) \\ \mathcal{M}_2(\mathcal{T}^* \cdot \llbracket \mathcal{P}_{\mathbf{V}_1^*}, \mathbf{S}_2, \mathcal{P}_{\mathbf{V}_3^*} \rrbracket) &= \mathbf{S}_2 \mathcal{M}_2(\mathcal{T}^*) \\ \mathcal{M}_3(\mathcal{T}^* \cdot \llbracket \mathcal{P}_{\mathbf{V}_1^*}, \mathcal{P}_{\mathbf{V}_2^*}, \mathbf{S}_3 \rrbracket) &= \mathbf{S}_3 \mathcal{M}_3(\mathcal{T}^*), \end{aligned} \quad (13.8)$$

whose explicit representations are already studied in eq. (13.5). As a result, we can write

$$\begin{aligned} &\mathcal{T}^* \cdot \llbracket \mathbf{S}_1, \mathcal{P}_{\mathbf{V}_2^*}, \mathcal{P}_{\mathbf{V}_3^*} \rrbracket + \mathcal{T}^* \cdot \llbracket \mathcal{P}_{\mathbf{V}_1^*}, \mathbf{S}_2, \mathcal{P}_{\mathbf{V}_3^*} \rrbracket + \mathcal{T}^* \cdot \llbracket \mathcal{P}_{\mathbf{V}_1^*}, \mathcal{P}_{\mathbf{V}_2^*}, \mathbf{S}_3 \rrbracket \\ &= \mathcal{D} \cdot \llbracket \mathcal{P}_{\mathbf{V}_1^*}^\perp, \mathcal{P}_{\mathbf{V}_2^*}, \mathcal{P}_{\mathbf{V}_3^*} \rrbracket + \mathcal{D} \cdot \llbracket \mathcal{P}_{\mathbf{V}_1^*}, \mathcal{P}_{\mathbf{V}_2^*}^\perp, \mathcal{P}_{\mathbf{V}_3^*} \rrbracket + \mathcal{D} \cdot \llbracket \mathcal{P}_{\mathbf{V}_1^*}, \mathcal{P}_{\mathbf{V}_2^*}, \mathcal{P}_{\mathbf{V}_3^*}^\perp \rrbracket \\ &\quad + \sum_{j \geq 2} \left(\mathcal{M}_1(\mathcal{T}^*) \cdot \llbracket \mathbf{S}_{1,j}, \mathcal{P}_{\mathbf{V}_2^*}, \mathcal{P}_{\mathbf{V}_3^*} \rrbracket + \mathcal{M}_2(\mathcal{T}^*) \cdot \llbracket \mathcal{P}_{\mathbf{V}_1^*}, \mathbf{S}_{2,j}, \mathcal{P}_{\mathbf{V}_3^*} \rrbracket + \mathcal{M}_3(\mathcal{T}^*) \cdot \llbracket \mathcal{P}_{\mathbf{V}_1^*}, \mathcal{P}_{\mathbf{V}_2^*}, \mathbf{S}_{3,j} \rrbracket \right). \end{aligned} \quad (13.9)$$

Now we bound $\mathcal{D} \cdot \llbracket \mathcal{P}_{\mathbf{U}_1}, \mathcal{P}_{\mathbf{U}_2}, \mathcal{P}_{\mathbf{U}_3} \rrbracket$ as follows

$$\begin{aligned} \mathcal{D} \cdot \llbracket \mathcal{P}_{\mathbf{U}_1}, \mathcal{P}_{\mathbf{U}_2}, \mathcal{P}_{\mathbf{U}_3} \rrbracket &= \mathcal{D} \cdot \llbracket \mathcal{P}_{\mathbf{V}_1^*} + \mathbf{S}_1, \mathcal{P}_{\mathbf{V}_2^*} + \mathbf{S}_2, \mathcal{P}_{\mathbf{V}_3^*} + \mathbf{S}_3 \rrbracket \\ &= \mathcal{D} \cdot \llbracket \mathcal{P}_{\mathbf{V}_1^*}, \mathcal{P}_{\mathbf{V}_2^*}, \mathcal{P}_{\mathbf{V}_3^*} \rrbracket \\ &\quad + \mathcal{D} \cdot \llbracket \mathbf{S}_1, \mathcal{P}_{\mathbf{V}_2^*}, \mathcal{P}_{\mathbf{V}_3^*} \rrbracket + \mathcal{D} \cdot \llbracket \mathcal{P}_{\mathbf{V}_1^*}, \mathbf{S}_2, \mathcal{P}_{\mathbf{V}_3^*} \rrbracket + \mathcal{D} \cdot \llbracket \mathcal{P}_{\mathbf{V}_1^*}, \mathcal{P}_{\mathbf{V}_2^*}, \mathbf{S}_3 \rrbracket \\ &\quad + \mathcal{D} \cdot \llbracket \mathbf{S}_1, \mathbf{S}_2, \mathcal{P}_{\mathbf{V}_3^*} \rrbracket + \mathcal{D} \cdot \llbracket \mathcal{P}_{\mathbf{V}_1^*}, \mathbf{S}_2, \mathbf{S}_3 \rrbracket + \mathcal{D} \cdot \llbracket \mathbf{S}_1, \mathcal{P}_{\mathbf{V}_2^*}, \mathbf{S}_3 \rrbracket \\ &\quad + \mathcal{D} \cdot \llbracket \mathbf{S}_1, \mathbf{S}_2, \mathbf{S}_3 \rrbracket \end{aligned} \quad (13.10)$$

Similarly as proving the bound (13.7), we can show

$$\max \left\{ \|\mathcal{D} \cdot \llbracket \mathbf{S}_1, \mathcal{P}_{\mathbf{V}_2^*}, \mathcal{P}_{\mathbf{V}_3^*} \rrbracket\|_{\mathbf{F}}, \|\mathcal{D} \cdot \llbracket \mathbf{S}_1, \mathbf{S}_2, \mathcal{P}_{\mathbf{V}_3^*} \rrbracket\|_{\mathbf{F}}, \|\mathcal{D} \cdot \llbracket \mathbf{S}_1, \mathbf{S}_2, \mathbf{S}_3 \rrbracket\|_{\mathbf{F}} \right\} \leq C_1 \sqrt{\bar{r}} \frac{\sigma_{\max}(\mathcal{D})^2}{\lambda} \quad (13.11)$$

where $C_1 > 0$ is an absolute constant.

Finally, by (13.5), (13.7), (13.9) and (13.11), we have

$$\begin{aligned}
& \|(\mathcal{T}^* + \mathcal{D}) \cdot [\mathcal{P}_{\mathbf{U}_1}, \mathcal{P}_{\mathbf{U}_2}, \mathcal{P}_{\mathbf{U}_3}] - \mathcal{T}^*\|_{\text{F}} \\
& \leq \left\| \mathcal{D} \cdot [\mathcal{P}_{\mathbf{V}_1^*}^\perp, \mathcal{P}_{\mathbf{V}_2^*}, \mathcal{P}_{\mathbf{V}_3^*}] + \mathcal{D} \cdot [\mathcal{P}_{\mathbf{V}_1^*}, \mathcal{P}_{\mathbf{V}_2^*}^\perp, \mathcal{P}_{\mathbf{V}_3^*}] + \mathcal{D} \cdot [\mathcal{P}_{\mathbf{V}_1^*}, \mathcal{P}_{\mathbf{V}_2^*}, \mathcal{P}_{\mathbf{V}_3^*}^\perp] + \mathcal{D} \cdot [\mathcal{P}_{\mathbf{V}_1^*}, \mathcal{P}_{\mathbf{V}_2^*}, \mathcal{P}_{\mathbf{V}_3^*}] \right\|_{\text{F}} \\
& \quad + C_1 \frac{\sqrt{\bar{r}} \sigma_{\max}(\mathcal{D})^2}{\lambda} \\
& \leq \|\mathcal{D}\|_{\text{F}} + C_2 \frac{\sqrt{\bar{r}} \sigma_{\max}(\mathcal{D})^2}{\lambda}
\end{aligned} \tag{13.12}$$

where $C_1, C_2 > 0$ are absolute constants ($C_{2,m} = 16m + 2^{m+1}$ in the case of general m). This finishes the proof of the lemma. \square

Lemma 13.3. *Assume all the entries of $\mathcal{Z} \in \mathbb{R}^{d_1 \times \dots \times d_m}$ are independent mean-zero random variables with bounded Orlicz- ψ_2 norm:*

$$\|[\mathcal{Z}]_\omega\|_{\psi_2} = \sup_{q \geq 1} (\mathbb{E}|[\mathcal{Z}]_\omega|^q)^{1/q} / q^{1/2} \leq \sigma_z$$

Then there exists some constants $C_m, c_m > 0$ depending only on m such that

$$\sup_{\mathcal{M} \in \mathbb{M}_{2\mathbf{r}}, \|\mathcal{M}\|_{\text{F}} \leq 1} \langle \mathcal{Z}, \mathcal{M} \rangle \leq C_m \sigma_z \left(r^* + \sum_{i=1}^m d_i r_i \right)^{1/2}$$

with probability at least $1 - \exp(-c_m \sum_{i=1}^m d_i r_i)$, where $r^* = r_1 \dots r_m$.

Proof. See the proof of (Han et al. (2020), Lemma D.5). \square

Lemma 13.4 (Maximum of sub-Gaussian). *Let Z_1, \dots, Z_N be N random variables such that $\mathbb{E} \exp\{tZ_i\} \leq \exp\{t^2 \sigma_z^2/2\}$ for all $i \in [N]$. Then*

$$\mathbb{P}(\max_{1 \leq i \leq N} |Z_i| > t) \leq 2N \exp(-\frac{t^2}{2\sigma_z^2}).$$

Proof. The claim follows from the following two facts:

$$\mathbb{P}(\max_{1 \leq i \leq N} Z_i > t) \leq \mathbb{P}(\cup_{1 \leq i \leq N} \{Z_i > t\}) \leq N \mathbb{P}(Z_i > t) \leq N \exp(-\frac{t^2}{2\sigma_z^2}),$$

and

$$\max_{1 \leq i \leq N} |Z_i| = \max_{1 \leq i \leq 2N} Z_i$$

with $Z_{N+i} = -Z_i$ for $i \in [N]$. \square

Lemma 13.5 (Spikiness implies incoherence). *Let $\mathcal{T}^* \in \mathbb{M}_{\mathbf{r}}$ satisfies Assumption 1 with parameter μ_1 . Then we have:*

$$\mu(\mathcal{T}^*) \leq \mu_1 \kappa_0.$$

where $\mu(\mathcal{T}^*)$ is the incoherence parameter of \mathcal{T}^* and κ_0 is the condition number of \mathcal{T}^* .

Proof. Denote $\mathcal{T}^* = \mathcal{C}^* \cdot [\mathbf{U}_1, \dots, \mathbf{U}_m]$. Now we check the incoherence condition of \mathcal{T}^* . For all $i \in [d_j]$ and $j \in [m]$,

$$\|\mathbf{e}_i^\top \mathcal{M}_j(\mathcal{T}^*)\|_{\ell_2} = \|\mathbf{e}_i^\top \mathbf{U}_j \mathcal{M}_j(\mathcal{C}^*)\|_{\ell_2} \geq \|\mathbf{e}_i^\top \mathbf{U}_j\|_{\ell_2} \cdot \lambda \geq \|\mathbf{e}_i^\top \mathbf{U}_j\|_{\ell_2} \frac{\|\mathcal{T}^*\|_{\text{F}}}{\sqrt{r_j} \kappa_0}.$$

On the other hand, we have

$$\|\mathbf{e}_i^\top \mathcal{M}_j(\mathcal{T}^*)\|_{\ell_2} \leq \sqrt{d_j^-} \|\mathcal{T}^*\|_{\ell_\infty} \leq \mu_1 \|\mathcal{T}^*\|_{\text{F}} \frac{1}{\sqrt{d_j}},$$

where the last inequality is due to the spikiness condition \mathcal{T}^* satisfies. Together with these two inequalities, we have

$$\|\mathbf{e}_i^\top \mathbf{U}_j\|_{\ell_2} \leq \sqrt{\frac{r_j}{d_j}} \mu_1 \kappa_0.$$

And this finishes the proof of the lemma. \square

Lemma 13.6. *Let $\mathcal{T}^* \in \mathbb{M}_{\mathbf{r}}$ satisfies Assumption 1 with parameter μ_1 . Suppose that \mathcal{W} satisfies $\|\mathcal{W} - \mathcal{T}^*\|_{\text{F}} \leq \frac{\lambda}{8}$, then we have $\text{Trim}_{\zeta, \mathbf{r}}(\mathcal{W})$ is $(2\mu_1 \kappa_0)^2$ -incoherent if we choose $\zeta = \frac{16}{7} \mu_1 \frac{\|\mathcal{W}\|_{\text{F}}}{\sqrt{d^*}}$. Also, it satisfies*

$$\|\text{Trim}_{\zeta, \mathbf{r}}(\mathcal{W}) - \mathcal{T}^*\|_{\text{F}} \leq \|\mathcal{W} - \mathcal{T}^*\|_{\text{F}} + \frac{C_m \sqrt{\bar{r}} \|\mathcal{W} - \mathcal{T}^*\|_{\text{F}}^2}{\lambda},$$

where $C_m > 0$ depends only on m .

Proof. Notice $\text{Trim}_{\zeta, \mathbf{r}}(\mathcal{W}) = \mathcal{H}_{\mathbf{r}}^{\text{HO}}(\widetilde{\mathcal{W}})$, where $\widetilde{\mathcal{W}}$ is the entrywise truncation of \mathcal{W} with the thresholding $\zeta/2$. To check the incoherence of $\mathcal{H}_{\mathbf{r}}^{\text{HO}}(\widetilde{\mathcal{W}})$, denote $\widetilde{\mathbf{U}}_j$ the top- r_j left singular vectors of $\mathcal{M}_j(\widetilde{\mathcal{W}})$, and $\widetilde{\mathbf{\Lambda}}_j$ the $r_j \times r_j$ diagonal matrix containing the top- r_j singular values of $\mathcal{M}_j(\widetilde{\mathcal{W}})$. Then, there exist a $\widetilde{\mathbf{V}}_j \in \mathbb{R}^{d_j^- \times r_j}$ satisfying $\widetilde{\mathbf{V}}_j^\top \widetilde{\mathbf{V}}_j = \mathbf{I}_{r_j}$ such that

$$\widetilde{\mathbf{U}}_j \widetilde{\mathbf{\Lambda}}_j = \mathcal{M}_j(\widetilde{\mathcal{W}}) \widetilde{\mathbf{V}}_j.$$

Now we can also bound the ℓ_∞ -norm of \mathcal{T}^* :

$$\|\mathcal{T}^*\|_{\ell_\infty} \leq \mu_1 \frac{\|\mathcal{T}^*\|_{\text{F}}}{\sqrt{d^*}} \leq \mu_1 \frac{\|\mathcal{W}\|_{\text{F}} + \|\mathcal{T}^* - \mathcal{W}\|_{\text{F}}}{\sqrt{d^*}} \leq \mu_1 \frac{\|\mathcal{W}\|_{\text{F}} + \|\mathcal{T}^*\|_{\text{F}}/8}{\sqrt{d^*}}.$$

This together with the definition of ζ , we have:

$$\mu_1 \frac{\|\mathcal{T}^*\|_{\text{F}}}{\sqrt{d^*}} \leq 8/7 \cdot \mu_1 \frac{\|\mathcal{W}\|_{\text{F}}}{\sqrt{d^*}} = \zeta/2.$$

And thus $\|\mathcal{T}^*\|_{\ell_\infty} \leq \zeta/2$. Then for all $i \in [d_j]$,

$$\|\mathbf{e}_i^\top \widetilde{\mathbf{U}}_j\|_{\ell_2} = \|\mathbf{e}_i^\top \mathcal{M}_j(\widetilde{\mathcal{W}}) \widetilde{\mathbf{V}}_j \widetilde{\mathbf{\Lambda}}_j^{-1}\|_{\ell_2} \leq \frac{\|\mathbf{e}_i^\top \mathcal{M}_j(\widetilde{\mathcal{W}})\|_{\ell_2}}{\lambda_{r_j}(\widetilde{\mathbf{\Lambda}}_j)} \leq \frac{\zeta/2 \cdot (d_j^-)^{1/2}}{7/8 \cdot \lambda_{r_j}(\mathcal{M}_j(\mathcal{T}^*))}.$$

where the last inequality is due to $\|\widetilde{\mathbf{W}} - \mathcal{T}^*\|_F \leq \|\mathbf{W} - \mathcal{T}^*\|_F \leq \underline{\lambda}/8$ since $\|\mathcal{T}^*\|_{\ell_\infty} \leq \zeta/2$ and $\|\widetilde{\mathbf{W}}\|_{\ell_\infty} \leq \zeta/2$. Meanwhile,

$$\|\mathcal{T}^*\|_F \leq \sqrt{r_j} \kappa_0 \lambda_{r_j}(\mathcal{M}_j(\mathcal{T}^*)).$$

There for the $\zeta = \frac{16}{7} \mu_1 \frac{\|\mathbf{W}\|_F}{\sqrt{d^*}}$, we have for all $j \in [m]$

$$\max_{i \in [d_j]} \|\mathbf{e}_i \widetilde{\mathbf{U}}_j\|_{\ell_2} \leq \frac{64}{49} \mu_1 \kappa_0 \frac{\|\mathcal{T}^*\|_F + \underline{\lambda}/8}{\|\mathcal{T}^*\|_F} \sqrt{\frac{r_j}{d_j}} \leq 2\mu_1 \kappa_0 \sqrt{\frac{r_j}{d_j}}.$$

where the second last inequality is from $\|\mathbf{W}\|_F \leq \|\mathcal{T}^*\|_F + \|\mathbf{W} - \mathcal{T}^*\|_F$ and the last inequality is from $\|\mathcal{T}^*\|_F \geq \underline{\lambda}$.

The second claim follows from the fact that $\|\widetilde{\mathbf{W}} - \mathcal{T}^*\|_F \leq \|\mathbf{W} - \mathcal{T}^*\|_F \leq \underline{\lambda}/8$, and from Lemma 13.2,

$$\begin{aligned} \|\text{Trim}_{\zeta, \mathbf{r}}(\mathbf{W}) - \mathcal{T}^*\|_F &= \|\widetilde{\mathbf{W}} - \mathcal{T}^*\|_F \leq \|\widetilde{\mathbf{W}} - \mathcal{T}^*\|_F + C_m \frac{\sqrt{\bar{r}} \|\widetilde{\mathbf{W}} - \mathcal{T}^*\|_F^2}{\underline{\lambda}} \\ &\leq \|\mathbf{W} - \mathcal{T}^*\|_F + C_m \frac{\sqrt{\bar{r}} \|\mathbf{W} - \mathcal{T}^*\|_F^2}{\underline{\lambda}} \end{aligned}$$

This finishes the proof of the lemma. \square

We introduce some notations for the following lemmas. Denote by $\widehat{\mathcal{T}}_l = \mathcal{C}_l \cdot (\mathbf{U}_1, \dots, \mathbf{U}_m)$, $\mathcal{T}^* = \mathcal{C}^* \cdot (\mathbf{U}_1^*, \dots, \mathbf{U}_m^*)$.

$$\mathbf{R}_i = \arg \min_{\mathbf{R} \in \mathbb{O}_{r_i}} \|\mathbf{U}_i - \mathbf{U}_i^* \mathbf{R}\|_F, i \in [m] \quad (13.13)$$

If we let $\mathbf{U}_i^{*T} \mathbf{U}_i = \mathbf{L}_i \mathbf{S}_i \mathbf{W}_i^\top$ be the SVD of $\mathbf{U}_i^{*T} \mathbf{U}_i$, then the closed form of \mathbf{R}_i is given by $\mathbf{R}_i = \mathbf{L}_i \mathbf{W}_i^\top$. And we rewrite

$$\mathcal{T}^* = \mathcal{S}^* \cdot (\mathbf{V}_1^*, \dots, \mathbf{V}_m^*)$$

where $\mathcal{S}^* = \mathcal{C}^* \cdot (\mathbf{R}_1^\top, \dots, \mathbf{R}_m^\top)$ and $\mathbf{V}_i^* = \mathbf{U}_i^* \mathbf{R}_i, i \in [m]$. So \mathbf{V}_i^* is also μ_0 -incoherent.

Lemma 13.7 (Entry-wise estimation of $[\widehat{\mathcal{T}}_l - \mathcal{T}^*]_\omega$). *Suppose \mathcal{T}^* satisfies Assumption 1. Under the assumptions that $\widehat{\mathcal{T}}_l$ is $(2\mu_1 \kappa_0)^2$ -incoherent and $\|\widehat{\mathcal{T}}_l - \mathcal{T}^*\|_F \leq \frac{\underline{\lambda}}{16m\bar{r}^{1/2}\kappa_0}$, then we have*

$$|[\widehat{\mathcal{T}}_l - \mathcal{T}^*]_\omega|^2 \leq C_m \bar{r}^m \underline{d}^{-(m-1)} (\mu_1 \kappa_0)^{4m} \|\widehat{\mathcal{T}}_l - \mathcal{T}^*\|_F^2,$$

where $C_m = 2^{4m+1}(m+1)$.

Proof. First we have

$$\widehat{\mathcal{T}}_l - \mathcal{T}^* = (\mathcal{C}_l - \mathcal{S}^*) \cdot (\mathbf{U}_1, \dots, \mathbf{U}_m) + \sum_{i=1}^m \mathcal{S}^* \cdot (\mathbf{V}_1^*, \dots, \mathbf{V}_{i-1}^*, \mathbf{U}_i - \mathbf{V}_i^*, \mathbf{U}_{i+1}, \dots, \mathbf{U}_m) \quad (13.14)$$

From Lemma 13.5, we get \mathcal{T}^* is $\mu_1^2 \kappa_0^2$ -incoherent. So we have for all $\omega = (\omega_1, \dots, \omega_m) \in [d_1] \times \dots \times [d_m]$

$$\begin{aligned} |[\widehat{\mathcal{T}}_l - \mathcal{T}^*]_\omega| &\leq \|\mathcal{C}_l - \mathcal{S}^*\|_F \prod_{i=1}^m \|(\mathbf{U}_i)_{\omega_i}\| + \sum_{i=1}^m \|\mathcal{S}^*\|_F \|(\mathbf{U}_i - \mathbf{V}_i^*)_{\omega_i}\| \prod_{k=1}^{i-1} \|(\mathbf{V}_k^*)_{\omega_k}\| \prod_{k=i+1}^m \|(\mathbf{U}_k)_{\omega_k}\| \\ &\leq \sqrt{\frac{r^*}{d^*}} (2\mu_1 \kappa_0)^{2m} \|\mathcal{C}_l - \mathcal{S}^*\|_F + (2\mu_1 \kappa_0)^{2m-2} \sqrt{\frac{\bar{r}^{m-1}}{\underline{d}^{m-1}}} \|\mathcal{S}^*\|_F \sum_{i=1}^m \|(\mathbf{U}_i - \mathbf{V}_i^*)_{\omega_i}\| \end{aligned}$$

where $r^* = \prod_{i=1}^m r_i$, $d^* = \prod_{i=1}^m d_i$ and $\bar{r} = \max_{i=1}^m r_i$, $\underline{d} = \min_{i=1}^m d_i$. From AG-GM inequality, we have

$$\begin{aligned} |[\widehat{\mathcal{T}}_l - \mathcal{T}^*]_\omega|^2 &\leq (m+1)(2\mu_1 \kappa_0)^{4m} \frac{r^*}{d^*} \|\mathcal{C}_l - \mathcal{S}^*\|_F^2 + (m+1)(2\mu_1 \kappa_0)^{4m-4} \frac{\bar{r}^{m-1}}{\underline{d}^{m-1}} \|\mathcal{S}^*\|_F^2 \sum_{i=1}^m \|(\mathbf{U}_i - \mathbf{V}_i^*)_{\omega_i}\|^2 \\ &\leq (m+1) \bar{r}^m \underline{d}^{-(m-1)} (2\mu_1 \kappa_0)^{4m} \left(\|\mathcal{C}_l - \mathcal{S}^*\|_F^2 + \lambda^2 \sum_{i=1}^m \|\mathbf{U}_i - \mathbf{V}_i^*\|_F^2 \right) \\ &\leq 2(m+1) \bar{r}^m \underline{d}^{-(m-1)} (2\mu_1 \kappa_0)^{4m} \|\widehat{\mathcal{T}}_l - \mathcal{T}^*\|_F^2 \end{aligned} \tag{13.15}$$

where the last inequality is from Lemma 13.9, and this finishes the proof of the lemma. \square

Lemma 13.8 (Estimation of $\|\mathcal{P}_\Omega(\widehat{\mathcal{T}}_l - \mathcal{T}^*)\|_F^2$). *Let Ω be the α -fraction set. Suppose \mathcal{T}^* satisfies Assumption 1. Under the assumptions that $\widehat{\mathcal{T}}_l$ is $(2\mu_1 \kappa_0)^2$ -incoherent and $\|\widehat{\mathcal{T}}_l - \mathcal{T}^*\|_F \leq \frac{\lambda}{16m\bar{r}^{1/2}\kappa_0}$, we have*

$$\|\mathcal{P}_\Omega(\widehat{\mathcal{T}}_l - \mathcal{T}^*)\|_F^2 \leq C_m (\mu_1 \kappa_0)^{4m} \bar{r}^m \alpha \|\widehat{\mathcal{T}}_l - \mathcal{T}^*\|_F^2,$$

where $C_m = 2^{4m+1}(m+1)$.

Proof. First from (13.15) in Lemma 13.7, we have

$$|[\widehat{\mathcal{T}}_l - \mathcal{T}^*]_\omega|^2 \leq (m+1)(2\mu_1 \kappa_0)^{4m} \frac{r^*}{d^*} \|\mathcal{C}_l - \mathcal{S}^*\|_F^2 + (m+1)(2\mu_1 \kappa_0)^{4m-4} \frac{\bar{r}^{m-1}}{\underline{d}^{m-1}} \|\mathcal{S}^*\|_F^2 \sum_{i=1}^m \|(\mathbf{U}_i - \mathbf{V}_i^*)_{\omega_i}\|^2.$$

Since Ω is an α -fraction set, we have

$$\begin{aligned} \|\mathcal{P}_\Omega(\widehat{\mathcal{T}}_l - \mathcal{T}^*)\|_F^2 &= \sum_{\omega \in \Omega} |[\widehat{\mathcal{T}}_l - \mathcal{T}^*]_\omega|^2 \\ &\leq (m+1)(2\mu_1 \kappa_0)^{4m} \alpha r^* \|\mathcal{C}_l - \mathcal{S}^*\|_F^2 + (m+1)(2\mu_1 \kappa_0)^{4m-4} \alpha \bar{r}^{m-1} \|\mathcal{S}^*\|_F^2 \sum_{i=1}^m \|\mathbf{U}_i - \mathbf{V}_i^*\|_F^2 \\ &\leq (m+1)(2\mu_1 \kappa_0)^{4m} \alpha r^* \|\mathcal{C}_l - \mathcal{S}^*\|_F^2 + (m+1)(2\mu_1 \kappa_0)^{4m-4} \alpha \bar{r}^m \lambda^2 \sum_{i=1}^m \|\mathbf{U}_i - \mathbf{V}_i^*\|_F^2 \\ &\leq (m+1)(2\mu_1 \kappa_0)^{4m} \bar{r}^m \alpha \left(\|\mathcal{C}_l - \mathcal{S}^*\|_F^2 + \lambda^2 \sum_{i=1}^m \|\mathbf{U}_i - \mathbf{V}_i^*\|_F^2 \right) \end{aligned} \tag{13.16}$$

Now we invoke Lemma 13.9, and we get

$$\|\mathcal{P}_\Omega(\widehat{\mathcal{T}}_l - \mathcal{T}^*)\|_F^2 \leq 2(m+1)(2\mu_1\kappa_0)^{4m}\bar{r}^m\alpha\|\widehat{\mathcal{T}}_l - \mathcal{T}^*\|_F^2,$$

which finishes the proof of the lemma. \square

Lemma 13.9 (Estimation of $\|\widehat{\mathcal{T}}_l - \mathcal{T}^*\|_F^2$). *Let $\widehat{\mathcal{T}}_l = \mathcal{C}_l \cdot (\mathbf{U}_1, \dots, \mathbf{U}_m)$ be the l -th step value in Algorithm 2 and let $\mathcal{T}^* = \mathcal{S}^* \cdot (\mathbf{V}_1^*, \dots, \mathbf{V}_m^*)$. Suppose $\widehat{\mathcal{T}}_l$ satisfies $\|\widehat{\mathcal{T}}_l - \mathcal{T}^*\|_F \leq \frac{\lambda}{16m\bar{r}^{1/2}\kappa_0}$. Then we have the following estimation for $\|\widehat{\mathcal{T}}_l - \mathcal{T}^*\|_F^2$:*

$$\|\widehat{\mathcal{T}}_l - \mathcal{T}^*\|_F^2 \geq 0.5\|\mathcal{C}_l - \mathcal{S}^*\|_F^2 + 0.5\lambda^2 \sum_{i=1}^m \|\mathbf{U}_i - \mathbf{V}_i^*\|_F^2.$$

Proof. First we have

$$\widehat{\mathcal{T}}_l - \mathcal{T}^* = (\mathcal{C}_l - \mathcal{S}^*) \cdot (\mathbf{U}_1, \dots, \mathbf{U}_m) + \sum_{i=1}^m \mathcal{S}^* \cdot (\mathbf{V}_1^*, \dots, \mathbf{V}_{i-1}^*, \mathbf{U}_i - \mathbf{V}_i^*, \mathbf{U}_{i+1}, \dots, \mathbf{U}_m) \quad (13.17)$$

Notice that we have

$$\|\mathcal{S}^* \cdot (\mathbf{V}_1^*, \dots, \mathbf{V}_{i-1}^*, \mathbf{U}_i - \mathbf{V}_i^*, \mathbf{U}_{i+1}, \dots, \mathbf{U}_m)\|_F^2 = \|(\mathbf{U}_i - \mathbf{V}_i^*)\mathcal{M}_i(\mathcal{S}^*)\|_F^2 \quad (13.18)$$

Denote $\mathcal{X}_i = \mathcal{S}^* \cdot (\mathbf{V}_1^*, \dots, \mathbf{V}_{i-1}^*, \mathbf{U}_i - \mathbf{V}_i^*, \mathbf{U}_{i+1}, \dots, \mathbf{U}_m)$, then we have

$$\begin{aligned} \|\widehat{\mathcal{T}}_l - \mathcal{T}^*\|_F^2 &= \|\mathcal{C}_l - \mathcal{S}^*\|_F^2 + \sum_{i=1}^m \|(\mathbf{U}_i - \mathbf{V}_i^*)\mathcal{M}_i(\mathcal{S}^*)\|_F^2 + 2 \sum_{i < j} \langle \mathcal{X}_i, \mathcal{X}_j \rangle + 2 \sum_{i=1}^m \langle (\mathcal{C}_l - \mathcal{S}^*) \cdot (\mathbf{U}_1, \dots, \mathbf{U}_m), \mathcal{X}_i \rangle \\ &\geq \|\mathcal{C}_l - \mathcal{S}^*\|_F^2 + \sum_{i=1}^m \lambda^2 \|\mathbf{U}_i - \mathbf{V}_i^*\|_F^2 + 2 \sum_{i < j} \langle \mathcal{X}_i, \mathcal{X}_j \rangle + 2 \sum_{i=1}^m \langle (\mathcal{C}_l - \mathcal{S}^*) \cdot (\mathbf{U}_1, \dots, \mathbf{U}_m), \mathcal{X}_i \rangle \end{aligned} \quad (13.19)$$

Notice that $\mathcal{M}_i(\mathcal{X}_i) = (\mathbf{U}_i - \mathbf{V}_i^*)\mathcal{M}_i(\mathcal{S}^*)(\mathbf{U}_m \otimes \mathbf{U}_{i+1} \otimes \mathbf{V}_{i-1} \otimes \mathbf{V}_1)^\top$. So we have the estimation of $|\langle (\mathcal{C}_l - \mathcal{S}^*) \cdot (\mathbf{U}_1, \dots, \mathbf{U}_m), \mathcal{X}_i \rangle|$ is as follows:

$$\begin{aligned} |\langle (\mathcal{C}_l - \mathcal{S}^*) \cdot (\mathbf{U}_1, \dots, \mathbf{U}_m), \mathcal{X}_i \rangle| &= |\langle \mathcal{M}_i((\mathcal{C}_l - \mathcal{S}^*) \cdot (\mathbf{U}_1, \dots, \mathbf{U}_m)), \mathcal{M}_i(\mathcal{X}_i) \rangle| \\ &\leq \|(\mathbf{U}_i - \mathbf{V}_i^*)^\top \mathbf{U}_i\| \|\mathcal{C}_l - \mathcal{S}^*\|_F \|\mathcal{S}^*\|_F \\ &\leq \sqrt{\bar{r}}\bar{\lambda} \|\mathbf{U}_i^\top (\mathbf{U}_i - \mathbf{V}_i^*)\|_F \|\mathcal{C}_l - \mathcal{S}^*\|_F \end{aligned} \quad (13.20)$$

Now we estimate $\|\mathbf{U}_i^\top (\mathbf{U}_i - \mathbf{V}_i^*)\|_F$ by plugging in the closed form of \mathbf{V}_i^* as in (13.13)

$$\|\mathbf{U}_i^\top (\mathbf{U}_i - \mathbf{V}_i^*)\|_F = \|\mathbf{I} - \mathbf{S}_i\|_F \leq \|\mathbf{I} - \mathbf{S}_i^2\|_F = \|\mathbf{U}_{i\perp}^{*T} \mathbf{U}_i\|_F^2 \leq \|\mathbf{U}_i - \mathbf{U}_i^* \mathbf{R}_i\|_F^2 \quad (13.21)$$

From Wedin' sin Θ Theorem, we have for $i \in [m]$

$$\|\mathbf{U}_i - \mathbf{V}_i^*\|_F \leq \|\mathbf{U}_i - \mathbf{U}_i^*\|_F \leq \frac{\sqrt{2}\|\widehat{\mathcal{T}}_l - \mathcal{T}^*\|_F}{\underline{\lambda} - \|\widehat{\mathcal{T}}_l - \mathcal{T}^*\|_F} \leq \frac{2\sqrt{2}\|\widehat{\mathcal{T}}_l - \mathcal{T}^*\|_F}{\underline{\lambda}} \leq \frac{1}{4m\bar{r}^{1/2}\kappa_0} \quad (13.22)$$

where the second last inequality is from $\|\widehat{\mathcal{T}}_l - \mathcal{T}^*\|_F \leq \underline{\lambda}/2$ and the last inequality is from $\|\widehat{\mathcal{T}}_l - \mathcal{T}^*\|_F \leq \frac{\underline{\lambda}}{16m\bar{r}^{1/2}\kappa_0}$. Then from (13.20) and (13.22), we have

$$|\langle (\mathcal{C}_l - \mathcal{S}^*) \cdot (\mathbf{U}_1, \dots, \mathbf{U}_m), \mathcal{X}_i \rangle| \leq \frac{1}{8m^2} \|\mathcal{C}_l - \mathcal{S}^*\|_F^2 + \frac{1}{8}\underline{\lambda}^2 \|\mathbf{U}_i - \mathbf{V}_i^*\|_F^2 \quad (13.23)$$

The estimation of $|\langle \mathcal{X}_i, \mathcal{X}_j \rangle|$ ($i < j$) is as follows. From (13.22), we have

$$\begin{aligned} |\langle \mathcal{X}_i, \mathcal{X}_j \rangle| &= |\langle \mathcal{M}_i(\mathcal{S}^*)\mathbf{M}_{i,j}, (\mathbf{U}_i - \mathbf{V}_i^*)^\top \mathbf{V}_i^* \mathcal{M}_i(\mathcal{S}^*) \rangle| \\ &\leq \bar{\lambda} \|\mathcal{S}^*\|_F \|\mathbf{M}_{i,j}\| \|(\mathbf{U}_i - \mathbf{V}_i^*)^\top \mathbf{V}_i^*\|_F \\ &\leq \bar{\lambda} \|\mathcal{S}^*\|_F \|(\mathbf{U}_i - \mathbf{V}_i^*)^\top \mathbf{V}_i^*\|_F \|(\mathbf{U}_j - \mathbf{V}_j^*)^\top \mathbf{V}_j^*\|_F \\ &\stackrel{(a)}{\leq} \sqrt{\bar{r}} \bar{\lambda}^2 \|\mathbf{U}_i - \mathbf{V}_i^*\|_F^2 \|\mathbf{U}_j - \mathbf{V}_j^*\|_F^2 \\ &\stackrel{(b)}{\leq} \frac{1}{16m^2} \underline{\lambda}^2 \|\mathbf{U}_i - \mathbf{V}_i^*\|_F \|\mathbf{U}_j - \mathbf{V}_j^*\|_F \\ &\leq \frac{1}{32m^2} \underline{\lambda}^2 \|\mathbf{U}_i - \mathbf{V}_i^*\|_F^2 + \frac{1}{32m^2} \underline{\lambda}^2 \|\mathbf{U}_j - \mathbf{V}_j^*\|_F^2 \end{aligned} \quad (13.24)$$

where $\mathbf{M}_{i,j} = \mathbf{I} \otimes \dots \otimes \mathbf{I} \otimes \mathbf{U}_j^\top (\mathbf{U}_j - \mathbf{V}_j^*) \otimes \mathbf{U}_{j-1}^\top \mathbf{V}_{j-1}^* \otimes \dots \otimes \mathbf{U}_{i+1}^\top \mathbf{V}_{i+1}^* \otimes \mathbf{I} \otimes \dots \otimes \mathbf{I}$, (a) holds because of (13.21), (b) holds because of (13.22).

As a result of (13.19), (13.23) and (13.24), we have

$$\|\widehat{\mathcal{T}}_l - \mathcal{T}^*\|_F^2 \geq 0.5 \|\mathcal{C}_l - \mathcal{S}^*\|_F^2 + 0.5 \underline{\lambda}^2 \sum_{i=1}^m \|\mathbf{U}_i - \mathbf{V}_i^*\|_F^2$$

which finishes the proof of the lemma. \square